Climate, vegetation cover and dust storm events in arid and semi-arid regions of Australia - relationships, models and predictions

Christa Pudmenzky

BSc (AES) (Hons)

A Thesis submitted for the award of

Doctor of Philosophy

International Centre for Applied Climate Sciences

University of Southern Queensland

Toowoomba, Australia

2016

Abstract

Wind erosion is a land degradation process in arid, semi-arid and agricultural regions of Australia. The loss of soil as a result of this process affects human health, environment and the economy. Climate variables such as rainfall and temperature play a major role in wind erosion activity. In particular, the quantity and distribution of rainfall influences the growth of vegetation cover which protects the soil surface from erosion (both wind and water erosion). Hence, climate variability is of great concern due to the pressure on agricultural land to produce more food for a growing population and the subsequent pressure to grow crops on drier more marginal lands that are more susceptible to wind erosion.

This research investigates the historic relationship between climatic conditions and recorded dust storm events based on more than 16 decades of collated dust storm event data from a wide number of sources (e.g. personal experiences, diaries, book excerpts, newspaper clippings, journal articles, reports and others). The 587 dust storm event records have been collated into a Historical Dust Event Database (HDED). The HDED indicated an increased number of dust storm events occurred in the 1900s, 1940s, 1960s and 2000s. This is due to the close link of rainfall and temperature to the ENSO cycle which directly impacts on the vegetation cover, a key factor driving the frequency, intensity and spatial distribution of dust events.

Broad scale estimation of spatial changes in vegetation cover would be useful in a wide range of applications and is of particular interest and value in areas of environmental, ecological and land-use modelling. Currently, broadly applicable modelling methods or indices are not available to realistically estimate vegetation cover levels for periods before the early 1990s when satellite remote sensing first became readily available. This includes any historical or future forecasting periods. As wind erosion/dust events are strongly dependent on vegetation cover, to analyse past or future dust events a means of estimating broad scale cover across Australia is required.

The newly developed Climate Aridity Vegetation Index (*CAVI*) is a simple broad scale vegetation index across Australia, based on rainfall and temperature data. The *CAVI* is calculated using 12 months weighted rainfall and temperature data to produce

vegetation cover maps without modelling individual vegetation type responses, seasonality and land-use. The *CAVI* produced particularly good estimation of vegetation cover during the Spring - Summer season but can over emphasise the relationship between rainfall, temperature and vegetation/green cover when increased rainfall occurs close to the month of interest. Nevertheless, the index produces good representative estimates and spatial maps of vegetation cover levels during the spring – summer seasons in Australia.

Wind erosion modelling occurs at a variety of spatial and temporal scales to determine the extent and severity of wind erosion across Australia. With the development of *CAVI*, historical and future wind erosion rates can be modelled, dust source areas can be estimated and identified, and the severity of these early dust storm events can be compared to modern events before land management changes were adopted. This has previously never been possible since reliable satellite derived photosynthetically active fractional vegetation cover (f_{PV}) data is not available prior to February 2000. To test the validity of such models, *CAVI* estimates of vegetation cover have been tested as a surrogate for remote sensed f_{PV} in the Computational Environmental Management System (CEMSYS) for two large scale dust storm events in September 2009 and October 2002. The CEMSYS estimated daily dust loads based on *CAVI* and f_{PV} were compared in regards to the spatial patterns of the eroded areas and the dust load intensity of the modelled wind erosion days. The use of *CAVI* as a surrogate for f_{PV} in September 2009 and October 2002 CEMSYS modelling results were encouraging. Similar spatial erosion characteristics were observed in the simulations but the dust concentration based the *CAVI* was on occasions lower than based on f_{PV} data. The *CAVI* was also applied to model the historical dust storm periods in November 1965. The modelling results from the study indicate~~s~~ that there is potential for *CAVI* to be used as a surrogate for f_{PV} and gives us for the first time some estimates of the extent and severity of historical dust storm events.

Certification of Thesis

This thesis is entirely the work of Christa Pudmenzky except where otherwise acknowledged. The work is original and has not previously been submitted for any other award, except where acknowledged.

Student and supervisors signatures of endorsement are held at USQ.

Dr Harry Butler

Principal Supervisor

Dr Rachel King

Associate Supervisor

Acknowledgements

My heartfelt thank you go to the many people who have shared my life as a PhD student.

To Prof. Roger Stone who encouraged me to take on the challenge so many years ago. I enjoyed the journey and would not hesitate to do it again.

To my team of supervisors Dr Harry Butler and Dr Rachel King at USQ and Dr Rob Allan from the UK Met Office, Exeter, UK for the continuous support, motivation, and immense knowledge.

To the members of the International Centre for Applied Climate Sciences for companionship and inspiration, especially Roger Stone, Shahbaz Mushtaq, Torben Marcussen, Joachim Ribbe, Kate Reardon-Smith, Daniel Brieva, and so many more.

A special thank you goes to Dr Rob Allan from ACRE, UK Met Office who introduced me to historical weather data rescue and the importance of preserving the past. To Dr Gil Compo from NOAA – 20CR for your 'contiguous' enthusiasm and to Kylie Andrews from ABC Science for making the Weather Detective Citizen Science Project possible.

To the University of Southern Queensland Faculty of Health, Engineering and Sciences, and Office of Research and Higher Degrees for support and encouragement throughout my candidature.

Last but not the least, I would like to thank my family and friends: in particular my sons Marcel and Andy, my family in Germany who believed in me, and of course my cat Mischka who kept me company during the long hours.

Published Works by the Author Incorporated into the Thesis

Publication 1: Included in Chapter 4

Pudmenzky, C, King, R & Butler, H 2015, 'Broad scale mapping of vegetation cover across Australia from rainfall and temperature data', *Journal of Arid Environments,* vol. 120, pp. 55-62.

Conference Presentations by the Author Relevant to the Thesis

This section lists conference presentations and posters by the author relevant to the thesis:

Pudmenzky, C, Stone, R, Butler, H, Allan, R, 2011, 'El Niño-Southern Oscillation Influence on the Dust Storm Activity in Australia: Can the Past Provide a Key to the Future?', 4th ACRE Workshop, 21st – 23rd September 2011, De Bilt, The Netherlands. (Poster).

Pudmenzky, C, Stone, R, Butler, H, Allan, R, 2011, 'El Niño-Southern Oscillation Influence on the Dust Storm Activity in Australia: Can the Past Provide a Key to the Future?', AGU Fall Meeting, 5th – 9th December 2011, San Francisco, USA. (Poster).

Pudmenzky, C, 2012, '20CR and Historical Dust Storms in Australia', 28th – 30th November 2012, Toulouse, France. (Oral Presentation).

Pudmenzky, C, 2012, 'Clement Wragge's Ship Logbook Compilations, 5th ACRE Workshop, 28th – 30th November 2012, Toulouse, France. (Oral Presentation).

Pudmenzky, C, Butler, H, 2013, 'Links between Climate Variability, Vegetation Cover and Dust Storm Frequency in Australia', NCCARF Climate Adaptation 2013: Knowledge & Partnerships Conference, 24th – 27th June 2013, Sydney, Australia. (Poster).

Pudmenzky, C, Stone, R, 2013, 'Historical Data Rescue & 20th Century Reanalysis Applications', 6th ACRE Workshop, 18th – 20th November 2013, Lisbon, Portugal. (Oral Presentation).

Pudmenzky, C, 2014, 'The ABC Citizen Science Project 2014: Australian Weather Detective, 7th ACRE Workshop, 25th – 27th August 2014, Toronto, Canada. (Oral Presentation).

Pudmenzky, C, 2015, 'The ABC Citizen Science Project 2014: Australian Weather Detective (update), 8th ACRE Workshop, 12th – 14th October 2015, Santiago, Chile. (Oral Presentation).

Table of Contents

List of Figures

List of Tables

Chapter 1: Introduction and Literature Review

Wind erosion is a common cause of land degradation in arid and semi-arid Australia, a process that can also lead to desertification. An estimated 110 Mt of dust is eroded by wind from the Australian continent each year, most originating from the arid and semi-arid rangelands (Chappell et al. 2013; Aubault et al. 2015). Climate factors, including rainfall, temperature, and wind play an important role in the wind erosion process (Figure 1.1). In particular, the quantity and distribution of rainfall influences vegetation cover. Reduced vegetation cover together with decreased soil moisture is a direct result of drought conditions. These drought conditions increase the risk of wind erosion under the right atmospheric conditions. Farming practices such as the clearing of native vegetation for farming and grazing, can also accelerate wind erosion rates above natural levels by reducing vegetation cover and soil surface stability.

At the same time, the increased dust load in the atmosphere from wind erosion events has the potential to alter the climate system and hydrological cycle through their radiative and cloud condensation nuclei effects (Choobari, Zawar-Reza & Sturman 2014). Considering this, understanding wind erosion is particularly important as it provides a foundation for developing appropriate and effective land management and erosion control processes and also in the forecasting of future climate. The landscape factors outlined above will be discussed further in Sections 1.2.1, 1.2.2 and 1.2.3.

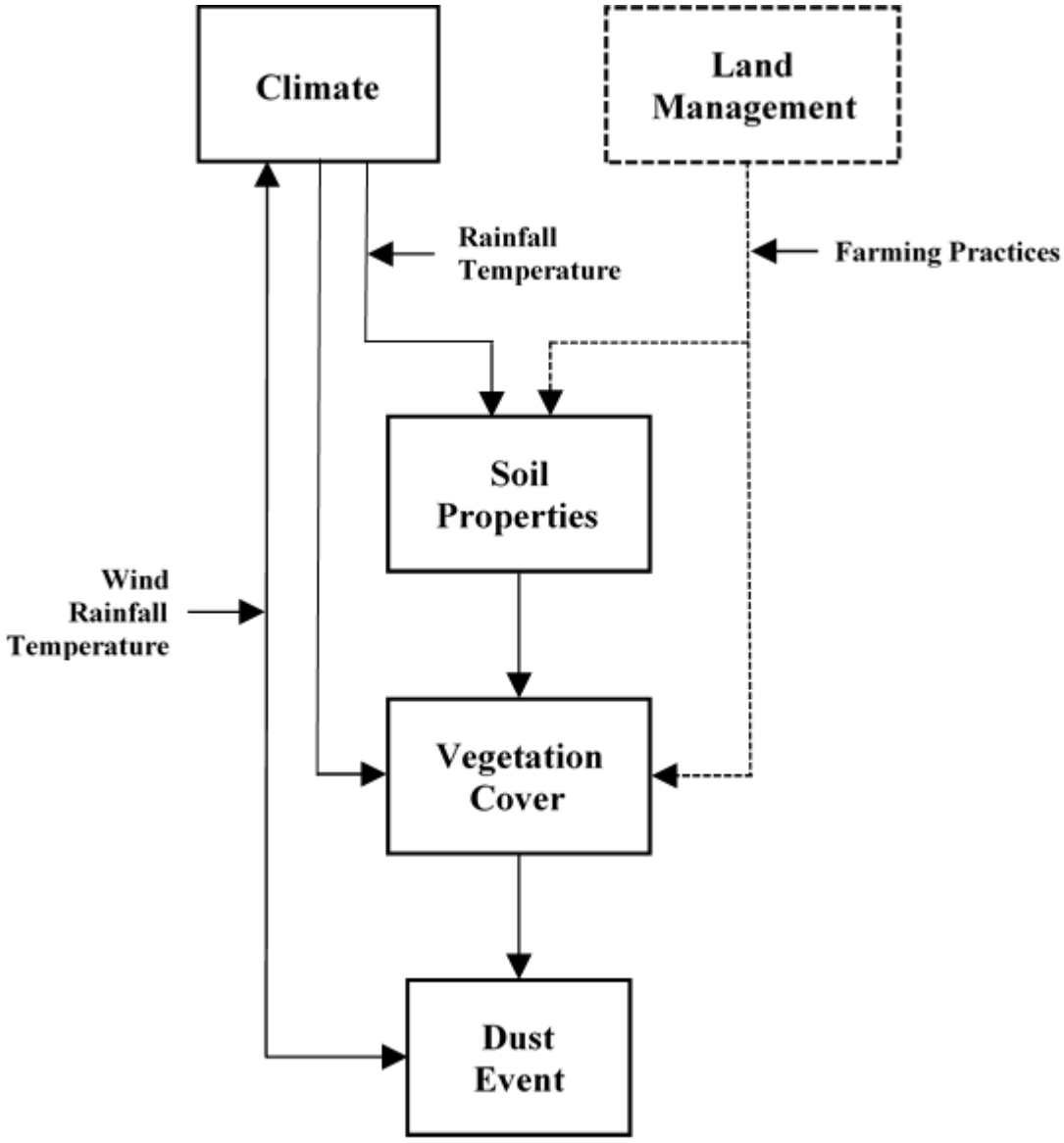

Figure 1.1: Both climate and landscape factors affect the susceptibility of soil to wind erosion and dust events.

1.1 Climate factors influencing dust in Australia

Climate is defined as the measurement of the long term average and variability of: precipitation, temperature, wind velocity and other weather variables in a particular region over a specific time scale (ranging from months to thousands or millions of years). The World Meteorological Organization (2015) has defined the "long term average climate" as reference points used by climatologists to compare current climatological trends to that of the past or what is considered "normal". A Normal is defined as the arithmetic average of a climate variable over a 30-year period. A 30 year

period is deemed long enough to filter out any interannual variation or anomalies, but also short enough to be able to show longer climatic trends. The Australian climate is characterised by extreme year-to-year rainfall variability compared to other major countries as illustrated in Figure 1.2 (Nicholls & Wong 1990; Love 2005; Bureau of Meteorology & CSIRO 2014).

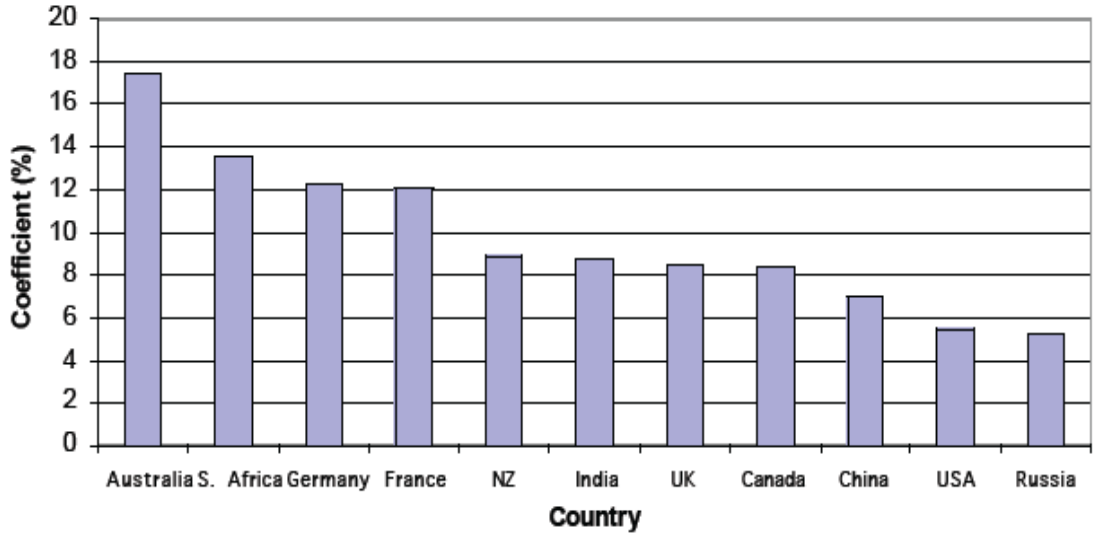

Figure 1.2: The coefficient of variation of national annual rainfall for Australia and 10 other countries for the period 1950 – 2000 (Love 2005).

Important key climate drivers in Australia include the El Niño-Southern Oscillation (ENSO), the Australian monsoon, the Madden-Julian Oscillation, the Southern Annular Mode (Risbey et al. 2009), and to a certain degree the Indian Ocean Dipole (IOD) (Allan et al. 2001; Compo & Sardeshmukh 2010; Frauen & Dommenget 2012; Zhao & Nigam 2015). Up to 50% of rainfall variability in northern and eastern parts of Australia is explained by ENSO variations (Allan, Lindesay & Parker 1996; Power et al. 2006; Risbey et al. 2009; Williams & Stone 2009). The ENSO phenomenon has a profound influence on climate variability and is predictable on interannual time scales (Frauen & Dommenget 2012). The origin of the ENSO lies in the interactions of the tropical atmosphere and the tropical Indo-Pacific Ocean, but the influence of ENSO reaches far beyond the tropical Pacific region. During different ENSO phases the areas of equatorial convection and subsidence are shifted, resulting in a change to the atmospheric circulation/rainfall patterns. ENSO fluctuates on a two to seven year time scale and alternates between its two phases: El Niño and La Niña (Allan, Lindesay & Parker 1996). El Niño events are associated with the warming of the surface layer

in the ocean in the eastern and central equatorial Pacific, a large scale weakening of the trade winds, and a reduction in rainfall in eastern and northern Australia that often results in drought conditions (Power & Smith 2007). La Niña events are associated with a cooling of the ocean in the eastern and central equatorial Pacific with above average rainfall over much of Australia often leading to flooding, similar to that observed in January 2011. The influence on amplitude and frequency of ENSO reach far beyond the tropical Pacific Ocean (Frauen & Dommenget 2012). Studies by Reason et al. (2000), Allan et al. (2001), Dommenget, Semenov and Latif (2006), Compo and Sardeshmukh (2010), Frauen and Dommenget (2012) and Zhao and Nigam (2015) suggest that the IOD is a manifestation of the ENSO in the Indian Ocean with a one season lag (Reason et al. 2000).

The Southern Oscillation Index (SOI) is a standardised index based on the observed sea level pressure difference between Tahiti and Darwin. The SOI is one measure of the large-scale fluctuations in air pressure occurring between the western and eastern tropical Pacific during El Niño and La Niña. A positive SOI generally indicates La Niña conditions, while a negative SOI generally indicates El Niño conditions.

Depending on the ENSO state, Australia experiences a higher frequency of drought, bushfires, and dust storms during an El Niño event, or a higher frequency of floods and an increased number of tropical cyclones during a La Niña event (Nicholls 1985; Evans & Allan 1992; Stone, Hammer & Marcussen 1996; Gallant, Hennessy & Risbey 2007; Risbey et al. 2011). The 2000s experienced extreme drought conditions with an increase in large dust storms and other wind erosion activity. Two extreme dust storms occurred in eastern Australia in October 2002 and September 2009 during the 'Millennium Drought' which lasted from 2001 – 2010. Through 2002 – 2003 Australia was under the influence of a weak to moderate El Niño which had a very strong impact on the continent. In the six months leading up to the October 2002 dust storm event, severe drought conditions in eastern Australia, plus above average maximum temperatures resulted in reduced vegetation cover (McTainsh et al. 2005). The 2009 – 2010 El Niño produced exceptionally dry conditions over much of the continent. They were the precursor conditions which, together with a passage of pre frontal northerlies with sufficiently strong winds, culminated in the very severe "Red Dawn" dust storm occurring in September 2009. South-eastern Australia had been experiencing drought conditions for several years and large parts of the country received below average

rainfall for the previous three and 36 months (Leys et al. 2011b). The influence of the El Niños explained approximately two thirds of the rainfall deficit that occurred in eastern Australia (van Dijk et al. 2013). The decline in rainfall and runoff contributed to widespread crop failures, livestock losses, dust storms, and bushfires. For example, the contribution of agricultural production to the Australian economy fell from 2.9% (financial years ending 1997 – 2002) to 2.4% of GDP (2003 – 2009) (Australian Bureau of Statistics 2011). The impact of bushfires to the Australian economy is estimated to average around $337 million per year and is predicted to increase by 2.2% annually (Deloitte Access Economics 2014).

Current studies (IPCC 2014) predict the Earth will continue to warm under the 'business-as-usual' scenarios for future greenhouse gas emissions. This global warming will likely cause widespread changes in the climate system and may affect climatic drivers, like ENSO, which will in-turn influence future climate variability. The degree to which these changes will impact on the future climate in Australia, and in particular the extreme dust storm events is uncertain (Timmermann et al. 1999; IPCC 2001; Trenberth et al. 2002; McTainsh et al. 2005; Gergis & Fowler 2009; Power 2014).

1.2 Landscape factors influencing dust

Wind erosion is a land degradation process which occurs in arid and semi-arid areas of the world. Australia is the driest inhabited continent (Peel, Finlayson & McMahon 2007) with 78% of its land area (Figure 1.3) classified as arid and semi-arid (Wilson & Graetz 1979). It is estimated that these arid to semi-arid areas receive, at the most, 400 mm rainfall annually (McTainsh & Pitbaldo 1987). Wind erosion is a natural process in the Australian landscape but has been accelerated due to human activities in rangelands and marginal cultivated lands. The loss of valuable fertile topsoil through erosion is a major threat to the Australian soil assets (Leys et al. 2009).

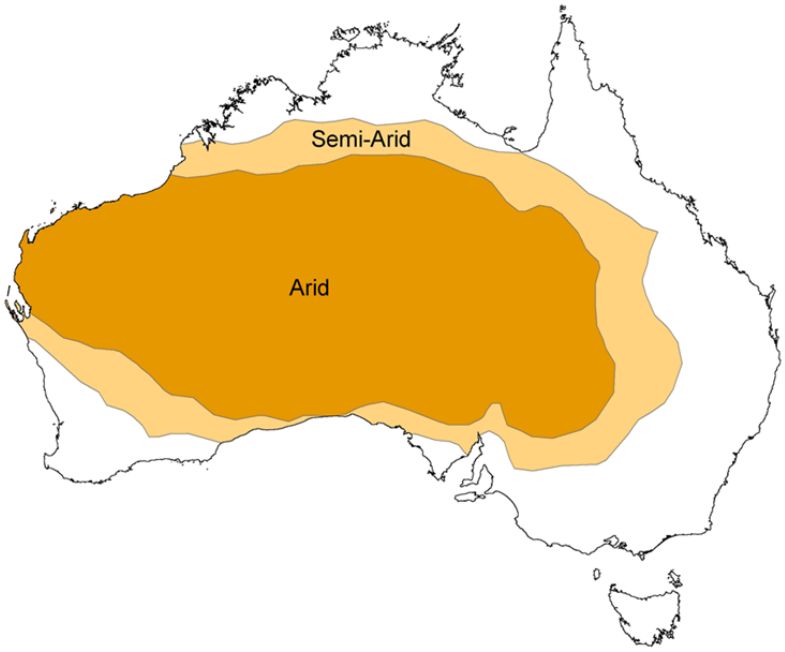

Figure 1.3: Arid and semi-arid zones in Australia (Desert Knowledge CRC 2006).

1.2.1 Soil properties

Australian soils are among the most ancient and fragile in the world and are a finite, non-renewable resource. The removal of valuable top soil adversely impacts on rural communities, biodiversity, carbon stores, and our ability to produce food & fibre. Increasing pressure on agricultural land to produce more food for a growing population, will lead to continued and increasing pressure to grow crops on drier more marginal lands, that are more vulnerable to wind erosion (Leys et al. 2009). At the same time, areas affected by moderate or severe wind erosion are likely to expand due to increased climate variability and associated droughts (Australian Government Land and Coasts 2010). Under the 'business-as-usual' climate scenarios, the frequency of major dust storms, such as those experienced in eastern Australia in September 2009, are likely to increase (NSW Government Office of Environment and Heritage 2014).

Wind erosion occurs when three environmental conditions coincide: i) the wind is strong enough to mobilise soil particles from the land surface; ii) the characteristics of the soil make it susceptible to wind erosion (soil texture, organic matter and moisture content); and iii) the surface is mostly devoid of vegetation cover, stones or snow cover (Bagnold 1941; Shao 2008; Borrelli et al. 2014). Recently burned areas would have minimal or no vegetation cover and therefore are more susceptible to wind erosion.

Sandy and loamy textured soils in low rainfall areas are most susceptible to wind erosion. Both biological and physical surface crusts (Strong 2007) are important in stabilising the soils surface in arid and semi-arid zones. The disturbance of these crusts drastically decreases soil surface resistance to wind erosion (Belnap & Gillette 1998). To maintain sediment control a crust cover of at least 20% is required (Eldridge 2003). Entrainment, transportation and deposition are three components of the wind erosion processes. The entrainment process represents an input into the aeolian (wind erosion) system, transport represents a throughput within the system and deposition an output from the system (McTainsh 1985). Kok et al. (2012) and Pye (1987) separated the transport of soil particles by wind into four physical regimes (Figure 1.4): long-term suspension (particles less than 20 μm diameter), short-term suspension (particles between 20 – 70 μm); saltation (particles between 70 – 500 μm), and surface creep (greater than 500 μm). Surface creep occurs when heavier larger particles (greater than 500 μm) are rolled across the soil surface (Shao 2008). This causes them to collide with, and dislodge, other particles. These large particles move only a few metres. Saltation is the bouncing motion of sand size particles (70 – 500 μm) across the surface. Such particles are light enough to lift off the surface but are too heavy to become suspended, and can travel a few kilometres (Raupach & Lu 2004). Suspended particles (less than 70 μm) can be moved into the air by saltation and may travel thousands of kilometres depending on size and are eventually delivered back to the surface through dry and wet deposition (precipitation) processes. Through these processes, Australian soil has been transported as far as the Tasman Sea, Great Southern Ocean, New Zealand, New Caledonia and Antarctica (McGowan & Clark 2008).

Wind erosion is the consequence of: 1) the aerodynamic forces and impacts that tend to remove particles from the surface; and 2) forces, such as gravity and inter-particle cohesion that resist the removal of particles (Shao 2008). Aerodynamic forces can be quantified by the friction velocity, which is a measure of wind shear at the surface and depends on vegetation cover which modifies surface roughness. Gravity and inter-particle cohesion forces can be quantified by the threshold friction velocity, which defines the minimum friction velocity required for wind erosion to occur. It is dependent on the particle size of the soil surface, atmospheric conditions and surface

conditions such as soil moisture, surface chemistry of the soil particle (Shao 2008), vegetation cover and soil type.

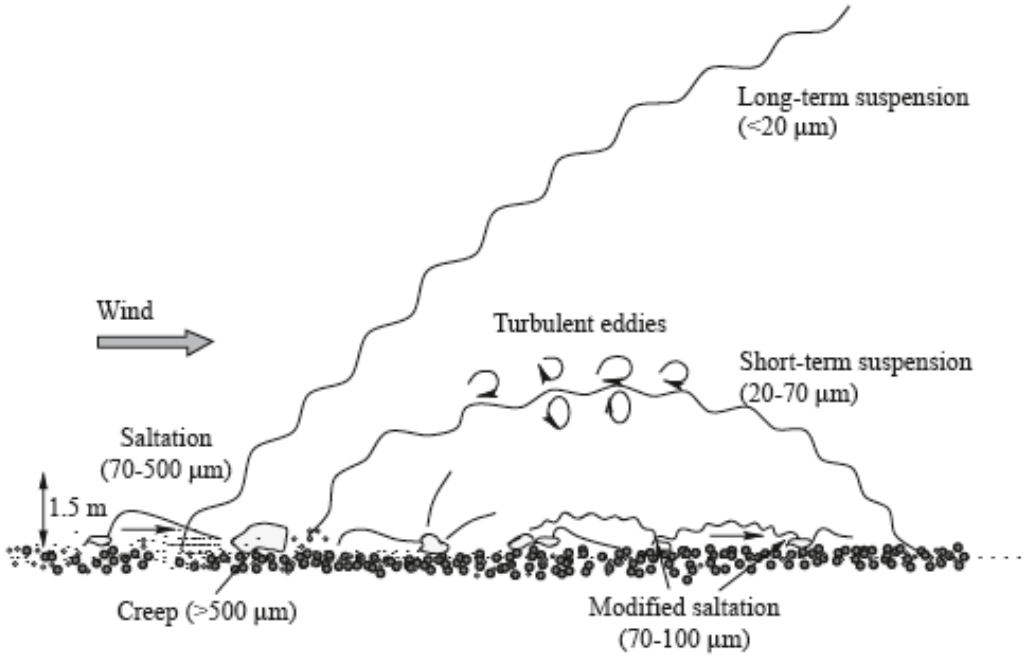

Figure 1.4: The three main modes of aeolian transport: surface creep, saltation and suspension of fine material. Modified from Pye (1987) and Kok et al. (2012).

Wind erosion rates vary spatially and temporally in relation to climatic and landscape factors. The impact of wind erosion can be measured, monitored and modelled but these approaches can be complicated by the physically complex nature of wind erosion processes, and the large spatial and temporal variability in erosion processes. Wind erosion can be measured over a set period of time but that approach is only suitable on a plot scale since it is not time or cost effective due to the large number of replications required to cope with field variability (Leys, McTainsh & Shao 1999). Monitoring wind erosion is a method used to quantify changes in erosion through time and can occur continuously on a plot, field or regional scale over days to years. With advances in modelling and computing power it is possible to calculate wind erosion at various scales and time intervals. Measuring, monitoring and modelling methods are discussed in more detail in Section 1.4.

The economic costs of wind erosion are substantial. The impact of a single severe dust storm event on the 23rd September 2009 is estimated to have cost $299 million to the NSW economy alone (Tozer & Leys 2013). Research by Williams and Young (1999)

estimated that the annual off-site cost of wind erosion was approximately $23 million for South Australia. Six prime cost centres were identified by the Williams and Young (1999) study: individual households, power supply, road safety, road maintenance, cost of air travel, and human health. The impact of wind erosion is very costly to the economy, human health and environment. Research into the impact of climate variability on wind erosion is needed to better understand future potential costs associated with the different climate change scenarios.

The interaction of dust aerosols with other components of the Earth System produces a wide range of both on-site and off-site impacts on the ecosystems, weather and climate, the hydrological cycle, agriculture, and human health (Kok et al. 2012).

On-site impacts include (Rutherford et al. 2003; McTainsh & Strong 2007; Leys et al. 2008; Shao 2008):

- loss of nutrient rich topsoil which reduces soil fertility;
- reduced soil water storage capacity;
- decreased ability of soils to sustain vegetation and livestock;
- decreased agricultural and pastoral productivity;
- spread of herbicides and pesticides off–farm;
- burying of farm infrastructure; and
- undermining infrastructure.

Off-site impacts are related to the transport & deposition of mineral dust and include (Webb 2008; Marx, McGowan & Kamber 2009; Zhao et al. 2011; Downs, Butler & Parisi 2016):

- reduced air quality which can lead to increased respiratory health risk;
- alters the radiation balance of the atmosphere through scattering and absorption of radiation with a potential to increase and decrease global air temperatures through radiative forcing;
- acts as a source of iron (Fe) that may be a limiting nutrient for phytoplankton and influencing nitrogen chemistry of the ocean; and
- acts as an effective vector for the transport of pathogens and pollutants.

1.2.2 Vegetation cover

The arid and semi-arid areas of inland Australia are defined by the presence of desert vegetation and landforms, and receive less than 400 mm of rainfall annually. The climate is characterised by highly erratic rainfall, extremes of long dry periods and occasional flooding. The Köppen-Geiger Climate Classification System is the most widely used system for classifying the world's climates (Peel, Finlayson & McMahon 2007). Its categories are based on the annual and monthly averages of temperature and precipitation.

The Köppen-Geiger system recognises five major climatic zones; each type is designated by a capital letter. The Australian continent is distinguished by three major climate zones (A – Tropical, B – Arid/Semi-Arid, C – Temperate) as shown in Figure 1.5 (Peel, Finlayson & McMahon 2007). The A climate zone (8.3% of Australia's land area) is located in the northern part of the continent and subdivided into three tropical climate zones. The arid and semi-arid B zone (77.8% of the continent) is the dominant climate type by land area and is described as a zone where precipitation is less than potential evapotranspiration. The temperate C type climate (13.9% in Australia) is the second largest climate type by land area and is described as having warm and humid summers with mild winters. The majority of Australia is categorised as arid and semi-arid B zone and this has direct implications for the type of vegetation cover (species) possible, the density and extent in 'good' and 'bad' years. A more detailed list explaining the individual criterion for each group can be found in Peel, Finlayson and McMahon (2007) and Figure 1.5.

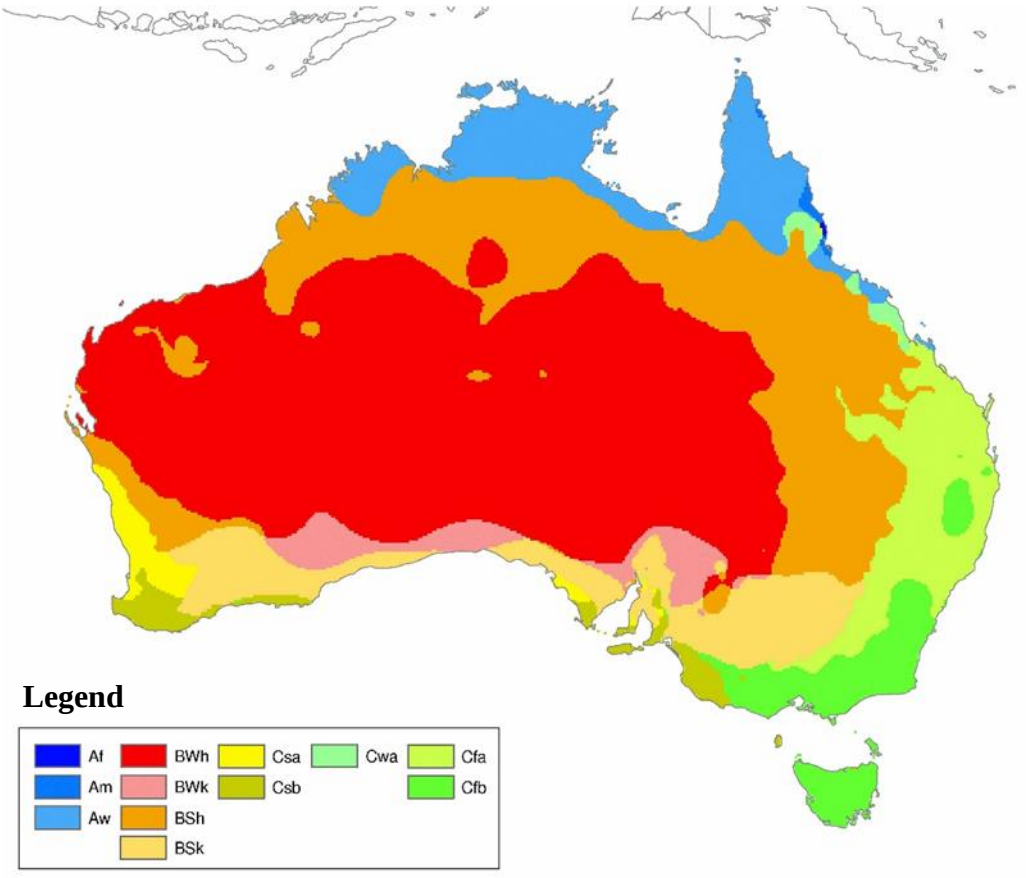

Figure 1.5: Köppen-Geiger climate type map of Australia. Modified from Peel, Finlayson and McMahon (2007).

The Australian arid and semi-arid ecosystems can be divided into herbaceous and woody vegetation comprising grasses and trees (or shrubs) respectively (Macinnis-Ng & Eamus 2007). The mix of these vegetation growth forms depends on interactions between climatic variables (amount of rainfall, temperature), soil factors (texture, depth, fertility and run-off) and disturbance regimes (fire regime, grazing by livestock and browsing by native animals).

The arid and semi-arid regions are dominated by species of acacia, casuarinaceae, chenopods and grasses. Acacia shrublands are widespread in southern areas where annual rainfall is less than 250 mm and occurs predominantly in winter. In northern regions, acacia communities predominate in areas receiving less than 350 mm annually. Within the central and western arid zone, particularly in the northwest and in the drier desert areas, acacia distribution is sparse and hummock grassland is the dominant vegetation cover (Johnson & Burrows 1994; Mott & Groves 1994). Chenopod shrubs, samphire shrubs and forblands occur extensively throughout southern Australia in both the semi-arid and arid zones where winter rainfall is reliable (Martin 2006).

Australian perennial grasses have adapted to the harsh conditions and can be classified as either C3 or C4 plants. The terms relate to the number of carbons and the different pathways that plants use to capture carbon dioxide during photosynthesis. Figure 1.6 illustrates the distribution of C4 grass relative to C3 grass and seasonality of rainfall (Lopes dos Aantos et al. 2013). C3 plants prefer cool seasonal regions in either wet or dry environments, are more tolerant to frost and are more dominant in the southern part of the continent, whereas C4 plants are more adapted to warm or hot seasonal conditions under moist or dry environments with a predominant distribution in the northern part of Australia. It is not uncommon to find both C3 and C4 species in one paddock. For example, C3 species are often more abundant in the shade of trees and on southerly aspects, while C4 species prefer full-sun conditions and northerly aspects (NSW Department of Primary Industries 2013). The ratio of C4 to C3 changes towards the higher latitudes as illustrated in Figure 1.6. This coexistence of both C3 and C4 species in one area has advantages in providing greater groundcover across a range of conditions and therefore a food source for both grazing and native animals.

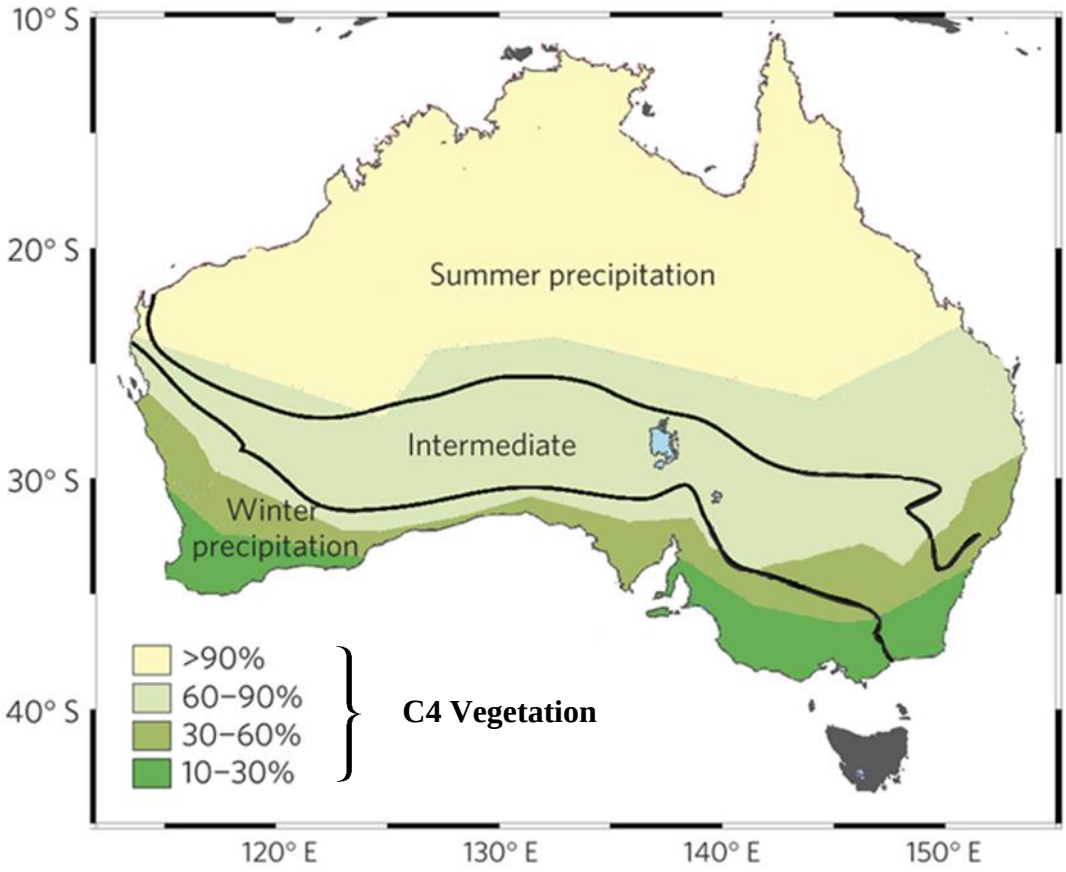

Figure 1.6: Map of Australia illustrating the distribution of C4 grass relative to C3 grass and seasonality of precipitation. Modified from Hattersley (1983).

1.2.3 Land management and usage

Soil and land degradation has been a major environmental, social and economic concern in Australia for over a century. Soil erosion by wind and the rate at which it occurs is dependent upon a number of factors, including geology, climate, soil type, and density of vegetation cover (Thompson 2014) as discussed in Section 1.2.1 and Section 1.2.2. Human activities, such as the clearing and burning of vegetation, cultivation practices, stocking (both domestic and feral) and overgrazing can disrupt the soil surface, remove vegetation cover and increase its susceptibility to erosion. The overall influence of climate can be exacerbated or mitigated by primary production methods and practices. Land management practices can have a major impact on ground cover in areas where inappropriate pastoral and cropping practices are used. Farming practices and land management are keys for sustainable agriculture. Effective land management practices maintain adequate ground cover to protect the soil from the erosive forces of wind and water (Leys 2003).

Increasing pressures on dryland environments from land use change and climate variability may increase the vulnerability of these areas to wind erosion. Climate change projections suggest that wind erosion will increase in Australia over the next 30 years due to increased droughts and increased climate variability (NSW Government Office of Environment and Heritage 2014). The hotter and drier conditions projected under these climate scenarios will impact on plant productivity and increase the risk of severe wind erosion events. Maintaining adequate vegetation cover is the most critical factor, not only in the protection of soils from wind erosion but also in maintaining pasture productivity and soil health. The relationship between percentage of ground cover and wind erosion is demonstrated in Figure 1.7. Threshold levels are indicated as green for low risk, orange for medium risk and red for high risk of soil erosion. The impact of wind erosion can be minimised by retaining a vegetation cover of more than 50% (Leys 2003). To further reduce the risk of erosion a minimum ground cover of 30% is required (Bowman & Scott 2009).

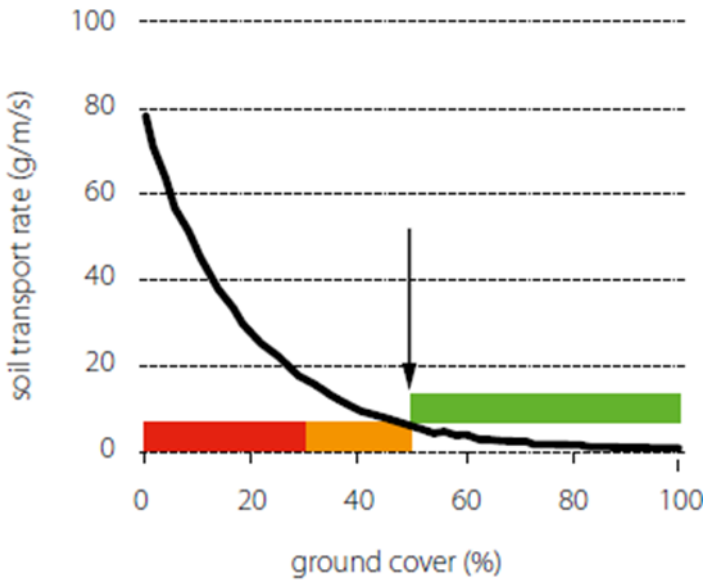

Figure 1.7: Relationship between wind erosion and percentage ground cover. Threshold levels are indicated as green for low risk (> 50%), orange for medium risk (> 30%) and red for high risk of soil erosion (Barson & Leys 2009).

1.3 Wind erosion in Australia

Australia is the driest continent on Earth (excluding Antarctica) and the largest source of atmospheric dust in the Southern Hemisphere (Pye 1987; Prospero, Ginoux & Torres 2002; Tanaka & Chiba 2006). Dust storms, which are defined as visibility less

than 1000 m according to the World Meteorological Organization (1995), are a common feature of the arid and semi-arid areas of Australia. This research focuses on the 20th and 21st century. The 1940s, 1960s and 2000s were very 'dusty' periods in Australia (O'Loingsigh et al. 2015). During 1941, 1942 and 1944 visibility of less than 1 km was recorded at Sydney Airport and less than 0.4 km on the 23rd September 2009 (Leys et al. 2011b).

In Australia large dust storms are often related to the passage of cold fronts across the continent. The strong pressure gradients creating wind strong enough to exceed the threshold friction velocity required to mobilise the sediments. The track of these fronts are seasonal with varying intensity.

Australian dust is transported offshore via two main dust pathways to the southeast and northwest (Bowler 1976) as illustrated in Figure 1.8. Three main dust transporting wind systems feed into these dust pathways and are associated with the passage of weather systems from west to east across the continent – prefrontal northerlies, frontal westerlies and postfrontal south easterlies (Sprigg 1982; Strong et al. 2011). The first type of wind system involves hot northerlies which blow out of Central Australia before the passage of a cold front, the second type involves the westerlies associated with the passing of the cold front. Finally, postfrontal south easterlies result in dust transport along the northwest corridor. The occurrence and effects of frontal systems are most prominent in the southern part of Australia, with the prefrontal northerlies being responsible for significant dust entrainment within the Lower Lake Eyre and Murray-Darling Basins (McTainsh 1989). Research by McGowan and Clark (2008) which was based on air parcel trajectory, identified a number of possible dust pathways from Australia over to the Tasman Sea and Southern Ocean. The core of the southeast dust transport pathway (Figure 1.8) extends 10º further south than previously assumed by Hesse and McTainsh (2003). Dust and associated aerosols from Lake Eyre and eastern Australia have the potential to impact most of the Southern Pacific, affecting marine productivity over a vast region. Dust from Lake Eyre Basin can also be transported to Antarctic from March to November, and has been identified in ice cores (Revelrolland et al. 2006; De Deckker et al. 2010). The dust from Lake Eyre Basin is iron rich and when deposited into ocean environments off the Australian coast, has the potential to stimulate cyanobacterial blooms, which are strongly iron or phosphorus

limited nutrients in oceans off the Australian coast (Mills, Ridame & Davey 2004; Pulido-Villena, Rerolle & Guieu 2010; Cropp et al. 2013).

The northwest dust path (Figure 1.8) may be subdivided into a northwest trajectories frequently passing over southern Philippines, Indonesia including the tropical rainforests of Borneo, New Guinea and the Indonesian archipelago, and the coral reefs of northern Australia including the Great Barrier Reef, and Broome, Western Australia, and north trajectories passing over the Gulf of Carpentaria (McGowan & Clark 2008).

Wind erosion activity is linked to a seasonal pattern in Australia (McTainsh & Boughton 1993; McTainsh, Lynch & Tews 1998). The eastern part of Australia (east of longitude 138º E) can be divided into two wind erosion regions, with north-eastern Australia (north of latitude 33º S) recording a high frequency of dust storms from September – December and in south-eastern Australia (south of latitude 33º S) from December – April. The seasonality has been linked to rainfall and the penetration of cold fronts deeply over the Australian continent (McTainsh, Lynch & Tews 1998; Reeder & Smith 1998) which influences the source area in terms of erodibility (vegetation cover, soil surface moisture, soil surface roughness and soil–inherent wind erodibility) and wind erosivity (rain, wind speed and surface runoff).

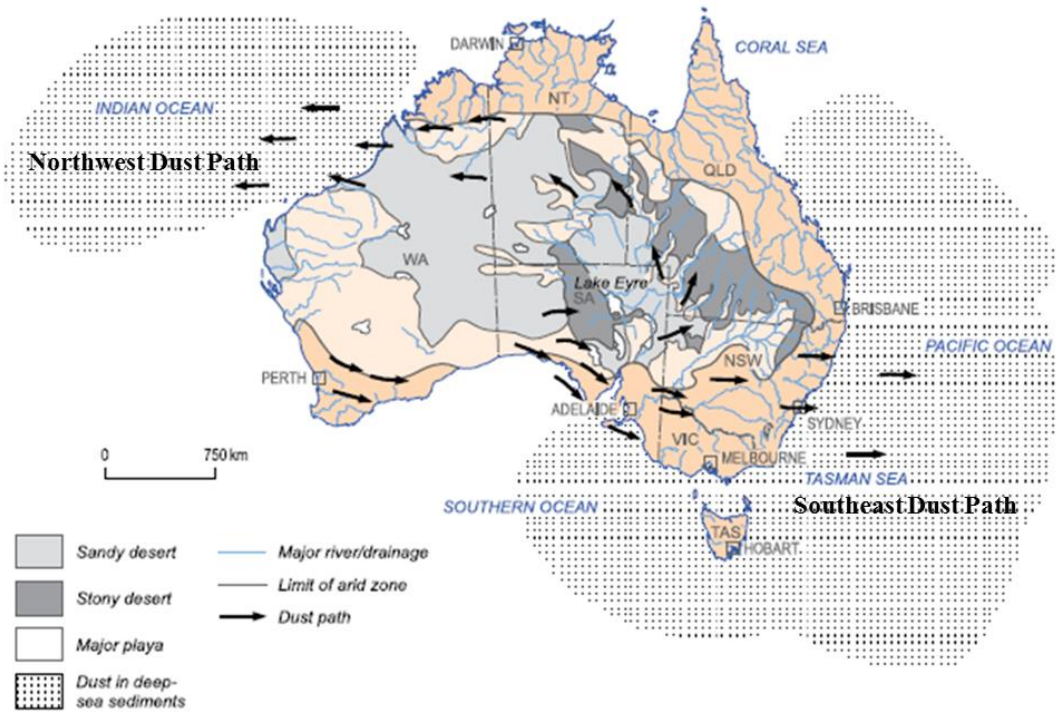

Figure 1.8: Location map showing Lake Eyre Basin, Channel Country and Mallee region and the general location of the Northwest and Southeast Dust Pathways (Bowler 1976; Fujioka & Chappell 2010).

Large dust storms are a common phenomenon in Australia with diary records dating back to the 1900's (Liversidge 1902; Chapman & Grayson 1903). Historical accounts of land degradation in Australia show that wind erosion was very active during the drought periods of the 1890s, 1901 – 1903, 1920s, 1930s, 1940s (McTainsh et al. 2011), 1960s (Ekström, McTainsh & Chappell 2004), 1980s (McTainsh et al. 2007) and 2000s (McTainsh et al. 2011). The first spatial study of dust storm occurrence over Australia by Middleton (1984) indicated that the highest frequency of dust events have occurred in the centre of Australia (Alice Springs), where there was a mean of 10.8 and a maximum of 65 events per year. Research by McTainsh and Pitbaldo (1987) supported these findings by demonstrating that the regions of maximum dust storm occurrence are in central Australia and in coastal Western Australia. Anecdotal reports describe dramatic images of huge dust storms engulfing rural towns but it has never been unequivocally established whether the 1940s "dusty years" were due to extreme drought and/or poor land management (McTainsh et al. 2011). In the 2000s, Australia was in a grip of the Millennium drought with extreme drought conditions and an increase in large dust storms and other wind erosion activity. Two extreme dust storms

impacted eastern Australian cities on 23rd October 2002 and 22nd – 23rd September 2009. These events have raised questions as to whether this recent period of wind erosion is more or less active than the 1940s and 1960s.

A study by Lamb et al. (2009) based on surface dust observations between the months of September – February during 1959 – 2006 has shown that a multidecadal oscillation of dust frequency occurred in central eastern Australia since the late 1950s. From 1959 to 1973, there was a distinct and consistent dust maximum, followed by a sharp decline with a less active period from 1977 – 2006. The 1940s and 1960s were part of the dust maximum period whereas 2002 fell within the less active period. The 2009 events were outside the Lamb et al. (2009) study period. The transition between dust maximum and a much more dust-free period coincided with a La Niña period between 1973 – 1976 with well above average rainfall for most of the Australian continent (Allan 1983). A time series of surface and 925 hPa winds showed that the dust oscillation was linked to strengthening and then weakening of the southerly component of the low level surface and tropospheric wind over the dust-prone central eastern Australian region (Lamb et al. 2009). The results of this research indicate that the 1940s and 1960s were affected by severe droughts and therefore experienced more dust storm events than in the 2000s.

Australian dust emissions via the two dust pathways (Figure 1.8) impacts in the Southern Hemisphere due to the potential for dust plumes to travel thousands of kilometres (Zhou et al. 2007). Dust from the centre of Australia may travel far beyond the continent, to the southeast over New Zealand (Raupach, McTainsh & Leys 1994; Knight, McTainsh & Simpson 1995) into the Southern Ocean (McGowan et al. 2000; Boyd et al. 2004), to the northwest over the Indian Ocean (McTainsh 1989) and accumulate in east Antarctica (Revelrolland et al. 2006; De Deckker et al. 2010). The possible future increase of extreme dust storm events in Australia as a result of anthropogenic activities and climate change, will impact upon the environment, including radiative forcing, and biogeochemical cycling and will have global implications (Goudie 2009).

An example of an extreme dust event experienced in Australia during a dry El Niño phase occurred on 22nd and 23rd September 2009 and is colloquially known as the "Red Dawn" dust storm. The "Red Dawn" event was the largest to pass over the east coast

of Australia since the 1940s (Leys et al. 2011b; Cork et al. 2012; Reynolds et al. 2014). This extreme event was the result of extended drought conditions in north-western New South Wales, north-eastern South Australia and western Queensland. The dust storm was associated with a deep low pressure system of 980 – 990 hPa and a cold front that produced average 24 h wind speed of 11 m s^{-1} in the Sydney region on 23rd September 2009 (Aryal et al. 2012). The visibility was reduced to 0.4 km in Sydney during this event. O'Loingsigh et al. (2015) estimated that 2.54 Mt of topsoil was transported and lost off the eastern coast of Australia during the event.

Although most dust storms are not as extreme as the 'Red Dawn' event, they are common in the arid and semi-arid inland of Australia and a natural part of the Australian landscape. They can have far reaching ecological, economical, and social consequences. With a projected mean temperature increase of 1.0 – 5.0 °C by 2070 (CSIRO 2011), understanding historical wind erosion periods provides a foundation for developing appropriate and effective land management and erosion control strategies.

1.4 Dust modelling, satellite remote sensing analyses and wind erosion research

Understanding spatial and temporal patterns in land susceptibility to wind erosion is a vital component to developing methods for managing land degradation. As mentioned in Section 1.2.1, a mixture of measuring, monitoring and modelling tools have been developed and employed to assess the spatial and temporal patterns of wind erosion and climate in Australia. To gain an understanding of wind erosion processes, portable wind tunnels have been used to measure and assess soil erodibility on a plot scale (Leys & Raupach 1991; Leys, McTainsh & Shao 1999; Van Pelt et al. 2010). In contrast, wind erosion monitoring methods are used to quantify changes in erosion through time and have been undertaken at a field scale to regional scales. Field scale monitoring relies on instrumentation such as deposition traps, high volume air samplers (HVS) and DustTrak® instruments (Shao et al. 1993; Leys, McTainsh & Shao 1999; Leys et al. 2008) which make it possible to monitor the transport and deposition of eroded sediments. DustWatch was established to supplement the Australian Bureau of Meteorology (ABoM) network by strategically adding a community network of

observers and instruments. The instrument sites, called DustWatch Nodes (DWN), utilise HVS to collect total suspended sediment (TSS) and/or DustTrak® sensors to collect PM10 data (Leys et al. 2008). These methods provide a picture of the extent and severity of individual dust storm/wind erosion events through surrogate measures. Maps describing the location and extent of areas prone to wind erosion have been developed based on field scale surveys of particular regional study areas (Mezösi & Szatmári 1998). However, these maps provide only snapshots of the landscape condition relevant to the climatic conditions at the time when the survey was undertaken. Regional scale long term monitoring tends to focus on the transport phase of wind erosion. This method provides information of the dust concentration in the air and based on the use of meteorological records of dust events from a large number of stations over a wider area and can be used to monitor the intensity of wind erosion, over a particular time period. The low spatial resolution of meteorological stations particularly in the arid and semi-arid region of Australia (Figure 1.9 & Figure 1.10), where wind erosion is the most active, is a weakness of this approach (Leys, McTainsh & Shao 1999).

The earliest meteorological recordings in Australia date back to 1789 (Gergis, Karoly & Allan 2009; Gergis, Brohan & Allan 2010; O'Loingsigh et al. 2015) but the temporal record has been interrupted by changes to the meteorological recording protocol in 1959 and 1974. The recording methods, weather code ranking and number of observations per day changed through time. The reclassification of dust-related weather codes after 1960 introduced an inconsistency in the classification of these codes before this year (Ekström, McTainsh & Chappell 2004; O'Loingsigh et al. 2010). Since 1996, the number of Automated Weather Stations (AWS) has increased substantially, and in some areas manned weather stations where staff and volunteers collected weather data have been replaced by AWS's. The increased use of AWS's has both advantages and disadvantages for research into wind erosion at a regional scale. The advantages include: 1) increased number of daily measurements, 2) more consistent measurements which provide data at a significantly greater frequency in all weather conditions and 3) the AWS's can be installed in sparsely populated areas. Some of the disadvantages of using AWS's include: 1) a reduced number of data variables the system can record and 2) a change in methodology from manual observations to instrument measurements will introduce different types of errors.

AWS's do not record dust and can only record visibility if fitted with instruments designed for that purpose (O'Loingsigh et al. 2010). Hence, dust haze and smoke are not recorded. This has added to the subsequent discontinuity in the dust record. In summary, measurement and monitoring approaches provide site data for specific points across the landscape under observation but it is not possible to get the full picture of the magnitude of wind erosion on a spatial and temporal scale (Leys, McTainsh & Shao 1999) from these methods alone.

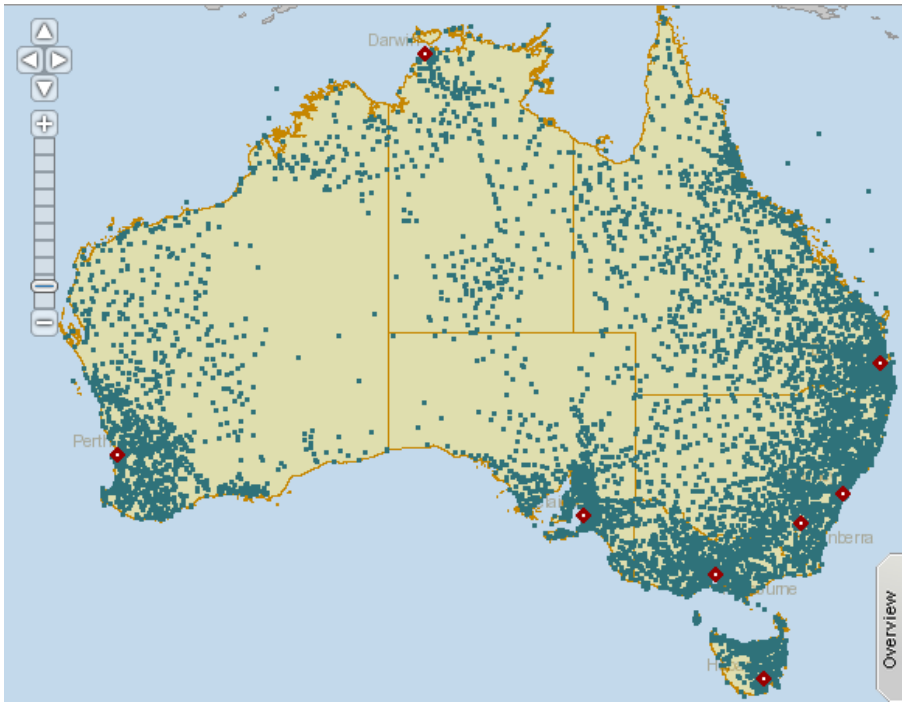

Figure 1.9: Meteorological stations locations recording rainfall in Australia. Note the increase of density in the south east corner of the continent (Bureau of Meteorology 2015).

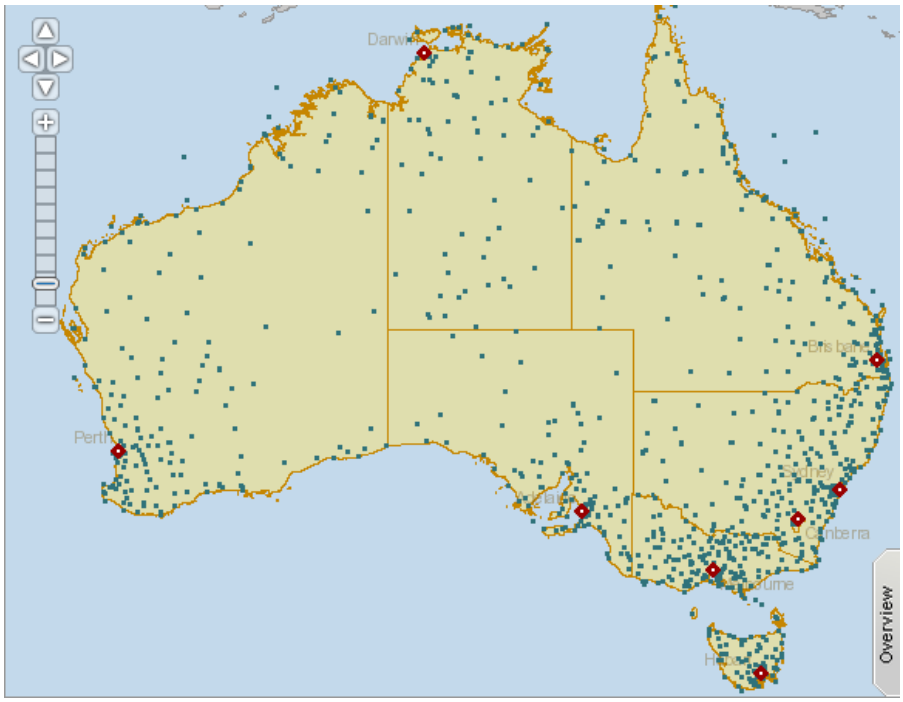

Figure 1.10: Meteorological stations locations recording temperature in Australia. Note the low spatial distribution of stations particularly in the arid and semi-arid region (Bureau of Meteorology 2015).

Empirical models relate management and environmental factors directly to soil loss and/or sediment yields through statistical relationships. The Wind Erosion Prediction System (WEPS) is an integrated semi-empirical model describing the influences between environmental and climatic factors on wind erosion (Hagen 1991). WEPS is an empirical process-based, daily time-step model that predicts soil erosion by simulating weather, field conditions and wind erosion on crop land (Wagner 1996). WEPS consists of a number of sub-models and databases which require detailed information on soils, hydrology, management, crop type, decomposition rates, erosion rates and weather. Obtaining this extensive amount of data and validating the empirical relevance for the Australian continent is relatively costly and not always available.

Burgess, McTainsh and Pitblado (1989) based the development of the climate index of effective soil moisture (E_m Index) of potential wind erosion in Australia on the empirical relationship between soil moisture and wind erosion (Chepil 1965). This empirical model describes the spatial extent and severity of wind erosion in Australia. The E_m Index is calibrated against meteorological data on dust storm frequencies and it is used to identify regions where wind erosion rates are increased by local environmental factors and/or human activities. In a modified version of the model,

wind run was also included in order to describe how wind speed and soil moisture interact during different seasons (McTainsh, Lynch & Tews 1998). This technique concentrates on the transport phase of the wind erosion process but lacks the ability to identify source areas.

The Dust Storm Index (DSI) utilises meteorological observations of dust phenomena to calculate the frequency and intensity of dust events at a range of spatial scales from regional to national and at temporal scales from three-hourly to annually covering 48 years (Yang & Leys 2014). This empirical climatic modelling approach has the advantage that access to nationwide long term meteorological data is readily available and a distinction between natural and accelerated wind erosion is possible (Leys, McTainsh & Shao 1999). On the other hand, disadvantages include low spatial resolution of rainfall and temperature meteorological stations in different areas (Figure 1.9 & Figure 1.10) and the change in measurement criteria used to record visibility has meant that results are not directly comparable across years.

Satellite remote sensing of soils has been demonstrated to have considerable potential for the assessment of soil erodibility and soil erosion (Ben-Dor, Irons & Epema 1999). Remote sensing can be used to estimate the percentage of ground cover and to measure the percentage of eroded ground surface based on changes in the reflectance of the mapped surface before and after a wind erosion event. The ground cover information can be used to estimate the impact of past events and approximate the potential wind erosion risk in the future. Remote sensing can be valuable in approximating dust plumes based on the temperature difference between the dust and the ground and to estimate an aerosol index of the column of dust in the atmosphere (Yang & Leys 2014). Sensors on board satellites detect the radiances of various surfaces of the Earth through different spectral channels. Channels are set in correspondence to the atmospheric radiation windows and water vapour absorption bands (Shao 2008). Various satellite-sensed signals are combined to identify and monitor dust storms in real time, to derive land-surface and atmospheric parameters for dust modelling, to retrieve dust quantities, (such as dust load, optical thickness and particle size), and to derive long-term dust climatology. The global annual dust emission rate is estimated to be ~1877 Tg yr^{-1}, of which Australia contributes ~5.6% (Tanaka & Chiba 2006). Australian desert dust is rich in iron oxide, hence the reddish colour (Figure 1.11) which is characteristic for hematite (Bullard, McTainsh & Pudmenzky 2004, 2007;

Radhi et al. 2010), in contrast to the Sahara which is more yellow. Hematite is an iron oxide dominant in the clay fraction (Journet, Balkanski & Harrison 2014) and has the potential to travel thousands of kilometres in a dust storm. Dust particles rich in iron oxide show a prominent depression in single scattering albedo in the blue spectral range due to absorption of hematite (Qin & Mitchell 2009). The hematite absorption capability is the reason the volume of dust in an Australian dust plume is very often underestimated in remote measurements.

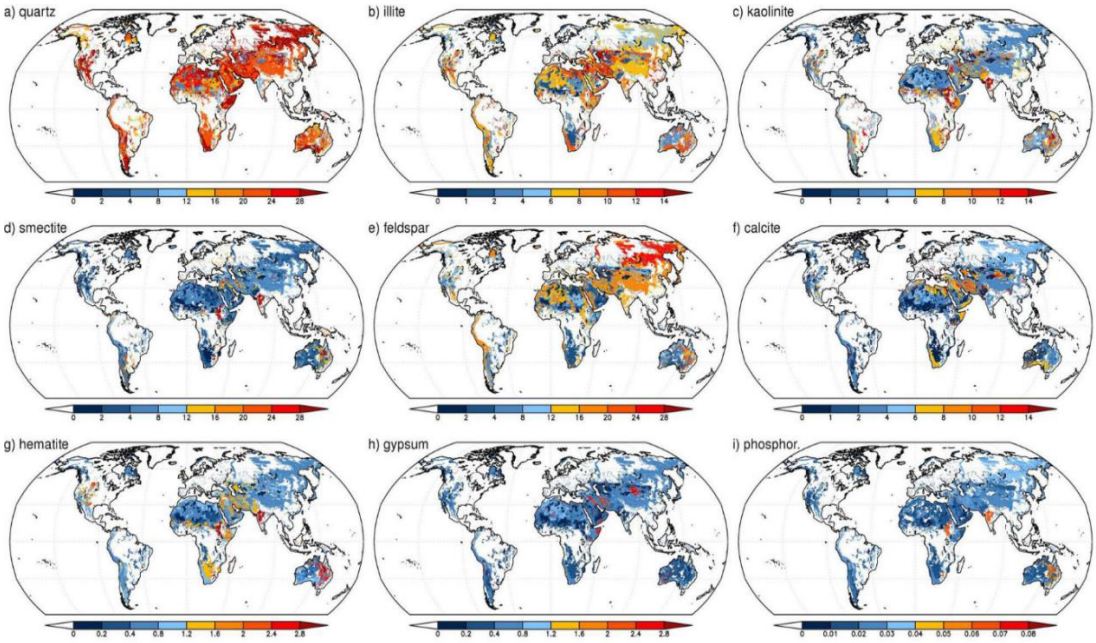

Figure 1.11: Global distribution of the effective mineral content in soil in percentages for (a) quartz, (b) illite, (c) kaolinite, (d) smectite, (e) feldspar, (f) calcite, (g) **hematite**, (h) gypsum and (i) phosphorus. (Nickovic et al. 2012).

The CEMSYS (Computational Environmental Management System) prediction system is a physical based model incorporating integrated climate, wind erosion and geographical information systems (based on remote sensing data) to predict the location and intensity of wind erosion at large spatial and temporal scales. This model is applied to analyse the spatial extent and severity of wind erosion from 2000 – 2012 across Australia (Leys et al. 2011a). This model is applied to Australian conditions regularly. To gain a quantitative estimate of wind erosion, input variables like atmospheric conditions (rainfall, temperature and wind speed), soil conditions (soil moisture and texture) and vegetation cover are incorporated into the model. The integrated modelling system (Figure 1.12) couples an atmospheric prediction model, a

wind erosion model, a dust transport model, a dust deposition model together with a Geographical Information System (GIS) (Shao, Raupach & Leys 1996; Shao & Leslie 1997). The system has the capability to model wind erosion on a continental and regional scale at a very high spatial and temporal resolution. It can also estimate dust emission, dust transport and dust deposition rates. One of the limitations of this approach is that vegetation cover information is one of the variables required in the model which is estimated from the satellite remote sensing data. However, for periods where no satellite data are available there is currently no simple, broadly applicable method or index to realistically estimate vegetation cover levels. This includes any time prior to the early-1990s (prior to satellite remote sensing) and any future forecasting. Without remote sensed vegetation cover estimates (Malthus et al. 2013), integrated wind erosion modelling systems (Shao et al. 2007) currently cannot confidently be used to estimate wind erosion rates.

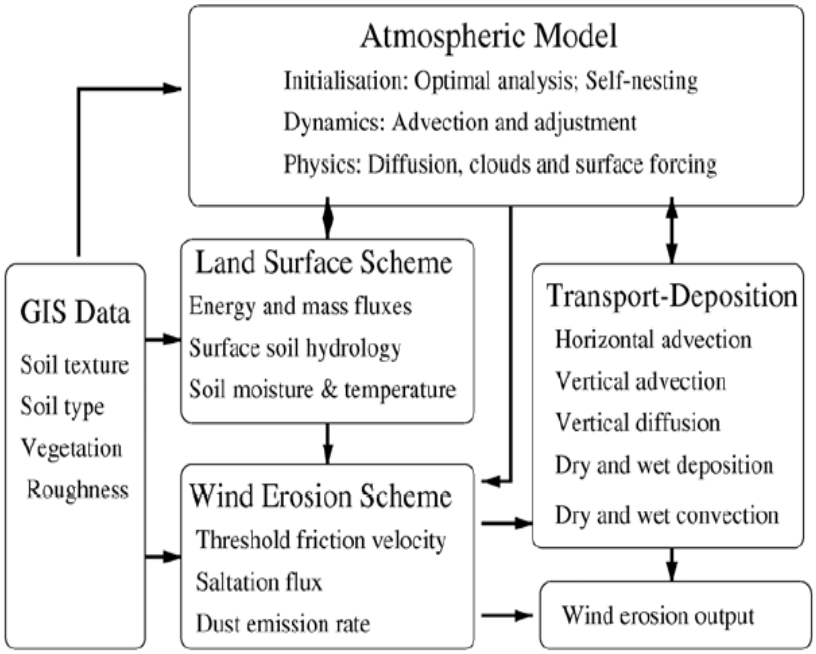

Figure 1.12: The structure of the integrated wind erosion modelling system CEMSYS (Butler et al. 2007). Soil texture, soil type, vegetation cover and roughness are part of the GIS Data.

The Australian Grassland and Rangeland Assessment by Spatial Simulation (AussieGRASS) is a vegetation modelling tool used to monitor key biophysical processes associated with pasture degradation and recovery, and in the assessment of drought conditions and is reliant on remotely sensed satellite data. It was developed in

1996 and provides a three month grass production forecast across Australia down to a 5 km grid scale (Carter et al. 2000). The AussieGRASS spatial framework includes inputs of key climate variables from the Bureau of Meteorology's SILO database (rainfall, evaporation, temperature, vapour pressure and solar radiation), soil and pasture types, remote sensed tree and shrub cover density, domestic livestock and other herbivore numbers. Since historical land usage and vegetation cover information is difficult to obtain on a broader scale prior to remotely sensed satellite data, the use of AussieGRASS is restricted to the period post 1996 and excludes the possibility to provide any future projection outside a three month window.

A range of Aridity Indices have been used as a classification tool to determine the climatic conditions of a region (Baltas 2007; Paltineanu et al. 2007). The De Martonne Aridity Index is based on mean monthly rainfall and mean temperature data from meteorological stations and classifies regions from arid to very humid. The De Martonne Aridity Index expresses the ratio of rainfall to temperature and uses temperature as a proxy for potential evaporation rate (Maliva & Missimer 2012). This classification approach works well in Mediterranean climates where rainfall data is consistently available for every month. Australia, on the other hand, with 78% land area classified as arid and semi-arid rangelands (Peel, Finlayson & McMahon 2007), often experiences extreme dry conditions with no rainfall for a few months for a large number of stations. The Aridity Index would be zero for months with no rainfall. Hence, it does not convey any history of the length in has been dry. Therefore the use of this aridity index without modification is not informative. However, the simplicity and reliance on only rainfall and temperature data of the De Martonne Aridity Index provided a template for the development of an index appropriate to Australian conditions.

In Australia there has been an increased interest in understanding if periods of wind erosion have been more or less active over the past few decades and if changes in land management have played a role (Leys et al. 2009). Of particular interest is comparing the 1940s drought period with that of 2000 – 2009 (McTainsh et al. 2011). Using one or more of the methods described above, historical dust events could be modelled with readily available meteorological data. However, most methods are constrained by the limited availability of vegetation cover data which restricts modelling to periods where remotely sensed satellite information is available.

1.5 Potential impacts of climate change

Climate change and associated climate variability is one of the greatest ecological, economic, and social challenges facing civilisation today. Evidence suggests that most of the observed global warming since the mid-20th century is due to increases in human activities such as the burning of fossil fuels, agriculture and land clearing (Bureau of Meteorology & CSIRO 2012). Human activities have influenced ocean warming, sea-level rise, rainfall variability and temperature extremes. The extra heat in the climate system affects atmospheric and ocean circulation, which influence global rainfall and wind patterns. In Australia, daily mean temperature has increased by around 0.9 ºC since 1910, and each decade has been warmer than the previous one since the 1950s (CSIRO 2011). Australian mean temperatures are projected to rise by 1.0 – 5.0 °C by 2070 when compared with the climate of recent decades (Bureau of Meteorology & CSIRO 2012).

The Australian continent faces significant environmental and economic impacts from climate change and associated variability across a number of sectors, including water security, agriculture, coastal communities, infrastructure, increased urban pollution, threat to public health (Chan et al. 2005) and an increase in the spread of poverty and hunger (Edwards, Gray & Hunter 2008; Smith & Leys 2009). In 2015 Australia was under the influence of a very strong El Niño and by December 2015, 86% of Queensland was drought declared (Queensland Government Department of Agriculture and Fisheries 2015). Projections into the future for Australia indicate that heatwaves, fires, floods, and southern Australian droughts are all expected to become more frequent and more intense in the coming decades (Bureau of Meteorology & CSIRO 2012).

Recent studies by Nicholls (2006, 2009), and Cai et al. (2010) have shown a decline in rainfall over austral autumn (March – May) and winter rainfall (June – August) over portions of southern Australia for the past several decades, particularly in southwestern Australia. The decline is, in part, attributed to anthropogenic changes in levels of greenhouse gases and ozone in the atmosphere (Delworth & Zeng 2014). The Millennium Drought, which affected southern Australia in 2001 – 2010, has been described as the most severe drought since instrumental records began in the 1900s (van Dijk et al. 2013; Cai et al. 2014). The long lasting drought conditions, which

included two severe El Niño events, explained about two thirds of the rainfall deficit in eastern Australia. The Coupled Model Intercomparison Project Phase 5 (CMIP5) model results by Cai et al. (2014) confirm that the drought over southern Australia is at least in part attributable to a recent anthropogenic-induced change in the climate.

As previously discussed in Section 1.2.1, the impact of climate on wind erosion can have numerous effects at regional to global scales (Miller & Tegen 1998; Raupach & Lu 2004). Increased temperatures and a decrease in rainfall will influence the soil moisture and therefore reduce the amount of vegetation cover to protect the soil surface (Figure 1.1). Under these climatic conditions the probability of wind erosion events and subsequent dust storm are increased. Dust emission caused by wind erosion can have far reaching effects by interacting with physical, chemical and bio-geochemical processes between the atmosphere, land and ocean (Harrison et al. 2001; Shao et al. 2011). On a global scale, each year approximately 2 000 Mt of dust is emitted into the atmosphere, of which 1 500 Mt is deposited on land and the remaining 500 Mt in the ocean (Shao et al. 2011). Mineral dust particles significantly impact on the climate system by changing the global energy balance in areas where dust is entrained in the atmosphere (Sokolik & Toon 1999; Wurzler, Reisin & Levin 2000; Rotstayn et al. 2009). They influence the climate system directly by scattering and absorbing shortwave and longwave radiation, semi-directly by changing the atmospheric cloud cover through evaporation of cloud droplets, and indirectly by acting as cloud and ice condensation nuclei, which changes the optical properties of clouds. The increased dust particles in the atmosphere can suppress rainfall by increasing the number of cloud condensation nuclei in warm clouds (Hui et al. 2008) and may decrease or increase precipitation formation (Choobari, Zawar-Reza & Sturman 2014).

A reduction of surface wind speed due to radiative cooling may also reduce soil erosion (Zhao et al. 2011). Radiative forcing by mineral dust is associated with changes in the atmospheric dynamics that may alter the vertical profile of temperature and wind speed, through which a feedback loop on dust emission can be established. Changes in the radiative energy budget of the Earth induced by dust aerosols could also affect the glacial–interglacial climate evolution (Bauer & Ganopolski 2014). The radiative forcing impact of mineral dust in the atmosphere is an area of high uncertainty as illustrated in Figure 1.13 due to the incomplete understanding concerning the diverse nature, the transport and removal processes, and the chemical and physical properties

of the particles. Mineral aerosols can have a warming and/or cooling effect on the atmosphere.

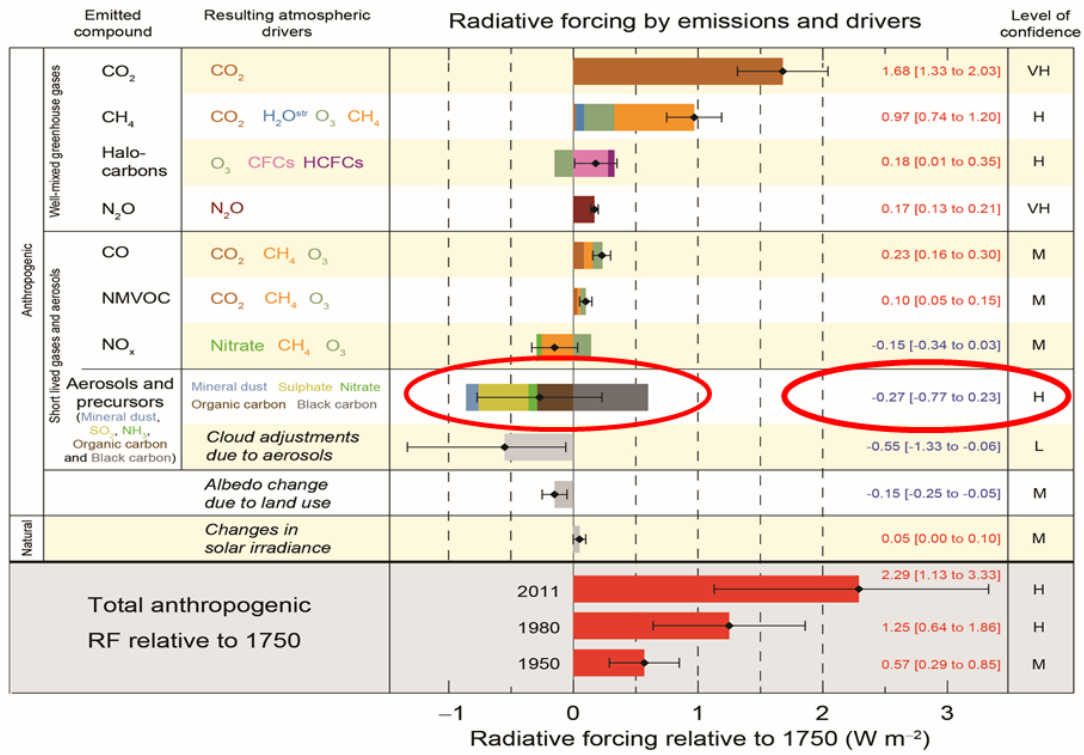

Figure 1.13: Radiative forcing estimates in 2011 relative to 1750 and aggregated uncertainties for the main drivers of climate change. Positive (or negative) radiative forcing indicates a warming (or cooling) effect on climate. The impact of mineral dust in the atmosphere is an area of high uncertainty. Mineral dust can have a cooling and/or warming effect as highlighted here (red circles). Modified from IPCC (2013).

1.6 Research objectives

Given the susceptibility of the Australian landscape to wind erosion and dust storm events and the potential for increased frequency and intensity of such events due to climate change, the relationships between climate factors and vegetation cover are of major interest. Broad-scale estimation of spatial changes in vegetation cover is of value in many areas of research and land-use management. For periods before the early 1990s (prior to satellite remote sensing) and for any future forecasting, there is currently no simple, broadly applicable modelling method or index to realistically estimate vegetation cover levels.

The research presented here, based on historical archived information, firstly aims to investigate the historic relationship between climatic conditions and recorded dust

events from diaries and other historic information across Australia. Next, the relationship between climate variables and vegetation cover is thoroughly explored, in particular the potential for using long-term climate information to predict broad scale vegetation cover. Without estimates of vegetation cover, integrated wind erosion modelling systems, such as Shao et al. (2007), cannot confidently be used to estimate historical or future wind erosion rates and dust source areas. This information would significantly aid in the decision making processes in regards to land management practices under future climate conditions.

The key objectives of this research are:

1. To establish a Historical Dust Event Database (HDED) from a wide number of sources including personal experiences, diaries, book excerpts, newspaper articles, journal articles, and other reports. (Chapter 2)
2. To compare the HDED to the climatic history of ENSO, rainfall and temperature to the historical dust event data, to establish if HDED dust records match climate records. (Chapter 3)
3. To develop a simple, broad scale, Climate Aridity Vegetation Index (*CAVI*) for the arid to semi-arid regions in Australia based solely on rainfall and temperature data. Then, investigate if reliable spatial and temporal vegetation cover maps can be produced based on the *CAVI* without modelling individual vegetation type responses, seasonality and land-use. (Chapter 4).
4. To investigate and validate if the *CAVI* can be used as a surrogate for vegetation cover for integrated wind erosion modelling where no satellite remote sensing data are available. (Chapter 5).
5. The results of the research are drawn together in Chapter 6, which discusses the usefulness of the *CAVI* and suggests possible improvements to the effectiveness of the index to allow for the modelling and mapping of vegetation cover for periods where rainfall and temperature data are available but satellite data and fine scale remote sensing data are not.

Chapter 2: Sources of climate and dust storms data and their history

This chapter describes the individual quantitative and qualitative data sources used to address four research objectives as outlined in Section 1.6. To address the second research objective, quantitative gridded rainfall and temperature data was accessed through the Australian Bureau of Meteorology (ABoM), and is discussed in Section 2.1. Satellite remote sensing vegetation cover data, obtained from the Department of Agriculture, Fisheries and Forestry (DAFF) and the Commonwealth Scientific and Industrial Research Organisation (CSIRO), has been accessed to address the third research objective and will be discussed in Section 2.2. To address the fourth research objective, quantitative gridded atmospheric data for the wind erosion modelling were accessed through the National Centre for Environmental Prediction and the National Center for Atmospheric Research (NCEP/NCAR) and the 20th Century Reanalysis website, and are discussed in Section 2.3. In order to address the first research objective, a comprehensive, qualitative, anecdotal dust event database was assembled from diaries, newspapers and other sources and will be discussed further in Section 2.4. Section 2.5 provides a qualitative overview of the history of dust events in Australia from 1852 – 2010 based on the collection of records from various sources to supplement the information to address the first research question.

The timeline in Figure 2.1 illustrates the temporal availability of the individual data sets. The earliest observation uncovered in the literature for this study was found in the diaries by Mrs Charles Clacey (1853) and dates back to December 1852. 20th Century Reanalysis (20CR) atmospheric data goes back to 1851 at the present time but as earlier weather observations are added to the 20CR database, it is hoped that reliable atmospheric reanalysis data will go back even further in time. Rainfall and temperature grid data became available in 1900 and 1910 respectively but some individual stations started recording data earlier but information is not continuous. Reliable satellite remotely sensed vegetation cover information for Australia has only became available from April 1992 onwards (AusCover 2012). The number of documented dust events varies considerable through time whereas atmospheric, rainfall, temperature and vegetation cover information has been fairly consistent throughout their respective availability time periods.

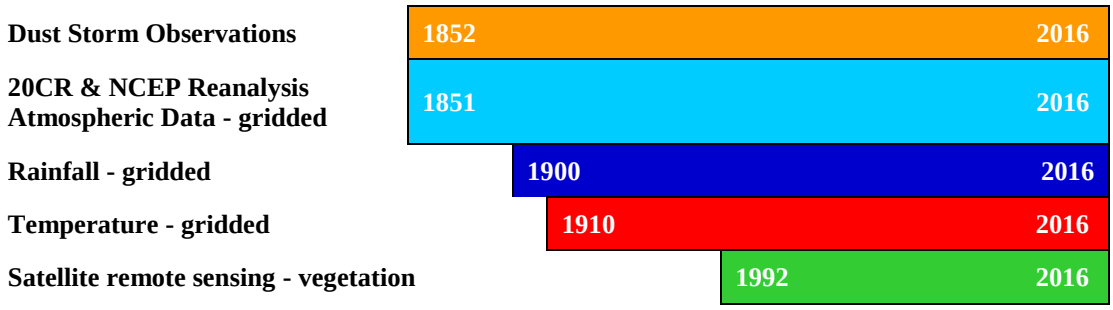

Figure 2.1: Timeline showing the data record availability of dust event observations, atmospheric data, rainfall, temperature and satellite remotely sensed vegetation cover data.

2.1 Measured climatic data from the Australian Bureau of Meteorology

Climate has been the longest documented and measured natural phenomenon in Australia, recorded at different places and observed by many people. The earliest written historical weather records date back to 1788 during the European settlement in Australia (Gergis, Karoly & Allan 2009).

For this research gridded 'daily rainfall' (1900 – 2014) and 'maximum daily temperature' data (1910 – 2014) were sourced from the Australian Bureau of Meteorology (ABoM - Figure 2.1). Daily rainfall is measured in millimetres (mm) and recorded at individual stations throughout Australia at 9.00am local time and is the record of total rainfall for the preceding 24 hours. Daily temperature is measured in degree Celsius (ºC) in a shaded enclosure at a height of approximately 1.2 m above the ground. Maximum daily temperature for the previous 24 hours are recorded at 9.00am local time. Both rainfall and maximum temperature are measured at individual weather stations and regridded by the ABoM at a 0.025°/2.5 km grid resolution to cover the Australian continent. Once sourced from the ABoM the gridded rainfall and temperature data were further regridded for this research to a spatial resolution of 5 km to match the spatial resolution of other data used for this study. All data had a spatial coverage of 110.00 to 155.00º E and -10.00 to -45.00º N. The regridding of the rainfall and temperature data were carried out by Dr Harry Butler from the University of Southern Queensland based on Shao (2008). The quantitative rainfall and temperature data are further discussed in Chapter 3.

2.2 Satellite remote sensing data

Remotely sensed satellite vegetation cover data for Australia became available from 1992 onwards as illustrated in Figure 2.1. For this study, monthly remote sensed fractional ground cover data (Guerschman et al. 2009) for both the photosynthetically active (green) fraction (f_{PV}) and the bare soil fraction (f_{BS}) at a 500 m resolution from February 2000 (110.00 to 155.00^{o} E and -10.00 to -45.00^{o} N) were sourced from the Department of Agriculture, Fisheries and Forestry (DAFF) and the Commonwealth Scientific and Industrial Research Organisation (CSIRO). The data were then post processed (re-sampled) and re-gridded to a monthly 5 km grid using the nearest-neighbour method to match the rainfall and temperature grid structure of the ABoM data set. The post processing algorithm was written by Dr Harry Butler, University of Southern Queensland before the data was re-gridded to a 5 km grid. This procedure was similar to that used by Shao (2008) to combine different spatial resolution GIS data sets for use in the Computational Environmental Management System (CEMSYS) model.

2.3 Atmospheric data used for wind erosion modelling

Quantitative gridded atmospheric data is required for historical wind erosion modelling and presented in Chapter 5. This data was accessed from the National Centre for Environmental Prediction and the National Center for Atmospheric Research (NCEP/NCAR) and the 20th Century Reanalysis. Air temperature, surface pressure, geopotential height, relative humidity, surface height, *u*-wind, *v*-wind and sea surface temperature are required to calculate atmospheric properties such as wind fields, rainfall, radiation and clouds for wind erosion modelling. The NCEP/NCAR Reanalysis data has a global grid size of 2.5 x 2.5 degree and is currently available from January 1948 and is constantly updated. For wind erosion modelling periods prior to 1948, atmospheric data can be accessed from the 20th Century Reanalysis (20CR) project website (http://www.esrl.noaa.gov/psd/data/20thC_Rean/). The data has a resolution of 2.0 degree global grid size.

The 20CR project has produced a reanalysis dataset spanning from 1851 – 2012 (and is periodically being updated), assimilating only surface observations of synoptic

pressure, monthly sea surface temperature and sea ice distribution. The observations have been assembled through international cooperation and collaboration with the Atmospheric Circulation Reconstructions over the Earth (ACRE) initiative from the UK Met Office, in which 20CR is a key component. Newly recovered worldwide historical weather observations are continuously added to the ACRE database, fed into the International Surface Pressure Databank (ISPD) and the International Comprehensive Ocean-Atmosphere Data Set (ICOADS), and then assimilated into 20CR data set.

Part of this project was also to collect any historical weather data which can be added to the ACRE database. Through the ABC Science Citizen Science Award the 'Weather Detective' project (Allan et al. 2016) was launched and over 8,000 photographed images of extracts from historical weather observations recorded in ship logbooks are being transcribed by 'citizen scientists'. These logbooks were collected by Clement Wragge, the former Government Meteorologist of Queensland and cover the period from 1882 – 1903. Thus, thousands of new weather measurements are being added to the ACRE database and processed by the 20CR initiative. The inclusion of additional historical weather data increases the capability of climate models to make better projections and extending the research applications of 20CR data, to areas like wind erosion modelling, possible.

2.4 Observation and records of dust events database

There are many references in historical records and research literature of dramatic dust storm events in Australia. Diary and journal entries from pioneering times, paintings, slides, poetry, book excerpts, newspaper clippings, journal articles, reports from the Australian Bureau of Meteorology and weather stations, DustWatch and the NSW Government of Environment and Heritage, satellite images, online news reports and information on multimedia websites are some of the resources available (Table 2.1). Records from the 1800's and the start of 1900's, when settlers had to brave devastating floods, droughts, dust storms, diseases and hardship with limited support, present a dramatic picture of early life in Australia. Anecdotal diary entries are often very descriptive and paint a vivid image of the conditions. For example, a diary entry by O'Shaughnessy (1903) mentioned the loss of the roof of his house during a big dust

storm on the 7th October 1898. Three months later he lost the roof again after another dust storm.

A large number of occurrences of dust storms in the 19th and 20th century have been reported in newspapers which have been digitised and can be accessed on websites such as Trove Digitised Newspapers (http://trove.nla.gov.au/newspaper). Information on more recent dust events (2000s onwards) are often not archived in the form of newspaper articles, diaries or other material, but have instead been recorded on websites. However, websites are often only active for a certain period of time and therefore records of these more recent events can be more difficult to obtain. For example the ABoM provides live weather observations which are constantly updated, but only available free of charge for a short period of time. Getting access to long term data can be time consuming and very expensive.

For this project, an extensive dust storm event list has been collated from 347 different sources covering the years from 1852 – 2010 (Table 2.1). The quality of the data is further discussed in Chapter 3.

Table 2.1: Historical dust event data sources and number of records used in this study based on the time from 1852 – 2010.

Source of dust event data	Number of records
Books	9
Diaries	106
Newspaper articles	122
Journals, Articles	18
Picture	1
Bureau of Meteorology	19
NASA Satellites	11
NSW Government of Environment & Heritage - DustWatch	57
News online	2
Multimedia Websites	2
Total	**347**

2.5 Decadal description of dust event records

The Historical Dust Event Database (HDED) has been compiled from diaries, newspapers and other sources starting from 1852. The database does not include any observations based on the weather code ranking system used by the ABoM and is

purely based on recorded observations by the 'general public'. McTainsh et al. (2007) developed a Dust Storm Index (DSI) which draws upon meteorological observational wind erosion data from the ABoM with records dating back to the 1960s. The use of the DSI has revealed weaknesses in the data as a result of changes to the ABoM definitions of dust event codes and inconsistent observer adherence to the codes (O'Loingsigh et al. 2015). The results of this study will be compared to the results based on McTainsh's DSI to verify if similar trends in dust storm activity to that found by McTainsh and Tews (2007) can be extracted purely from qualitative historical data sources.

Colonial reports, personal diaries and newspaper articles provide rich accounts about past drought, floods and other significant weather events since the first European settlement at Sydney Cove, New South Wales in 1788 (Nicholls 1988). One of the earliest dust storm reports by Europeans in Australia is by Charles Darwin in the '*The Voyage of the Beagle*' where he describes travelling from Sydney to Bathurst through the Blue Mountains, and being enveloped in a dust storm on his way to Bathurst on the 20th January 1836 (Darwin 1839):

> "We experienced this day the sirocco-like wind of Australia, which comes from the parched deserts of the interior. Clouds of dust were travelling in every direction; and the wind felt as if it had passed over a fire."

The earliest observation uncovered in the literature for this research was found in the diaries of Mrs Charles Clacey (1853) dating back to December 1852 and describing life in the gullies around Bendigo. Since then, 585 dust storm events have been found in unofficial records over 331 days to the end of 2010. The definition of a 'dust storm event' as recorded in the diaries and other documents is dependent on what the observer deems to be an event, and hence are likely to under estimate the actual number (i.e. haze, dust devil etc.).

Figure 2.2 illustrates the number of observations which have been retrieved from various sources from 1852 – 2010 with the number of days when observations have been recorded in brackets for the individual decade. It is acknowledged that the list is incomplete since the arid and semi-arid area of Australia is and has always been sparsely populated, with the highest density of people living along the east coast and

in the Perth region of Western Australia. Therefore, it is highly likely that a large number of events may have past unnoticed and/or unrecorded.

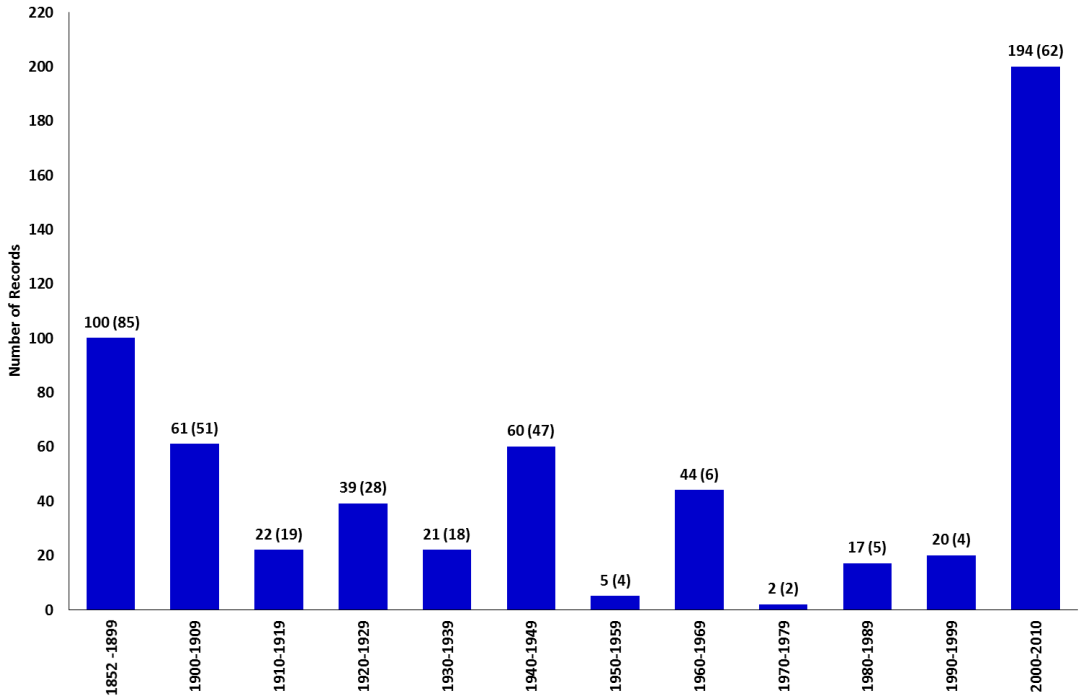

Figure 2.2: 585 dust storm events were documented by the public on 331 days (shown in brackets) over 16 decades.

During 1852 – 1899, 100 dust storm events were documented in diaries, newspapers, books and journals (Figure 2.2). On occasions more than one event was recorded by the public on the same day in a number of locations. This either relates to a large event travelling over a vast distance or there were a number of localised events reported on the same day. In the following paragraphs a small selection of anecdotal recorded events are discussed in more detail.

The diary by Mrs Charles Clacey (1853) describes the harsh working conditions in the goldfields near Bendigo in the summer of 1852/53. Not only had the gold diggers survived the night with "murder here—murder there—revolvers cracking—blunderbusses bombing—rifles going off" but also mother nature "working hard under a burning sun, tortured by the mosquito and the little stinging March flies, or feel his eyes smart and his throat grow dry and parched, as the hot winds, laden with dust, pass over".

Between 1864 – 1866, Victoria (VIC), South Australia (SA), New South Wales (NSW), Queensland (QLD) and Western Australia (WA) experienced a severe drought (Australian Bureau of Statistics 1988). During the 1866/67 spring/summer season, the Adelaide region was affected by numerous dust events which have been mentioned in Mary Jacob's diaries on the 25th May 1866, 6th September 1866, 5th, 16th, 25th & 26th December 1866 and 2nd & 26th January 1867 (Durdin 2010). The severity of these early dust storm events is unknown. Currently it has not been possible to model these periods and compare to modern events before land management changes were adopted.

From 1880 – 1886, parts of VIC (northern areas and Gippsland), NSW (mainly northern wheat belt, northern Tablelands and south coast), QLD (1881 – 1886, the south-east, Central Highlands and central interior in 1883 – 1886), and the agricultural areas of SA (1884 – 1886) were severely affected by a major drought (Australian Bureau of Statistics 1988). The severity of this drought is reflected in the 24 dust storm events recorded for the HDED. A newspaper article in 'The Australasian Sketcher' describes the violent nature of a dust storm sweeping over large areas of VIC on the 10th January 1882 (Australasian Sketcher 1882).

> "The temperature was very high in Melbourne, and the atmosphere was obscured by great clouds of dust all day."

The storm was so severe that seven children escaped serious injuries when the wind lifted the heavy shingle roof off and tossed it over, burying the children underneath. A large number of houses lost their roofs and chimneys were blown over.

In 1888, VIC (northern areas and Gippsland), southern Tasmania (TAS) (1887 – 1889), NSW and QLD (1888 – 1889), SA and WA (central agricultural areas) were influenced by a short but major drought. A newspaper article in The Sydney Morning Herald (1888) described the dust storm on the 5th October 1888 so destructive that a large number of houses were damaged. Due to the increased wind speed, ships anchored in the harbour had lost their moorings.

The Federation drought (1895 – 1903) impacted the whole of Australia but most persistently the coast of QLD, inland areas of NSW, SA, and central Australia (Australian Bureau of Statistics 1988). The agricultural and grazing sectors were severely affected. The Barrier Miner (1895) reported on the 6th February 1895 that a

frightful dust storm blew into Melbourne. Two clergymen were blown from Queen's Bridge. On the 10th April 1896, The Argus (1896) reported that Broken Hill experienced a "record breaking" dust storm. At 4pm the impact of this dust storm was described as being a "total eclipse of the sun".

Until 1903, the Australian continent was under the influence of the Federation Drought which saw a large number of dust events in the earlier years of the decade. Of the 61 dust storms events found in records, 48 occurred from 1900 – 1903 (Figure 2.2). The Advertiser (1904) reported on the 19th October 1904 that dust storms lasting a few days had caused severe damage in parts of SA. Hot blasts of wind whipped up dust and had "penetrated the houses" which was "disagreeable" with housewives in Adelaide. The damage was more widespread in the regional areas. Large areas of crops were flattened and ships anchored in Port Adelaide lost their mooring. Several people died from flying debris and others sustained severe injuries. Trees were uprooted, fences blown over, houses, sheds and churches lost their roofs which were often carried away for some distance. Areas in NSW were also affected. Figure 2.3 illustrates the severity of a dust storm approaching Broken Hill in NSW on the 15th December 1907.

Figure 2.3: Dust storm approaching Broken Hill, News Souths Wales, 15th December 1907. Photo from the Jim Davidson Australian postcard collection, 1880 – 1980.

During 1910 – 1919 only 22 minor events were documented (Figure 2.2) in Adelaide (Apr 1910), Cobar (Nov 1910), Williamstown (Dec 1910), Melbourne (Nov 1911, Jan 1916, Dec 1918), Broken Hill (Nov 1912, Dec 1913, Dec 1918, Jan 1919), Brewarrina (Dec 1912), Hobart (Nov 1913), Bordertown (Jan 1914), Booleroo and Wilmington (Mar 1914), Melrose, Crystal Brook, Quron and Wirrabara (Mar 1914), Wangaratta (Dec 1914), Riverina area (Jan 1915), Queanbeyan (Mar 1915), and Narrandera (1915). According to the Australian Bureau of Statistics (1988), areas in VIC and TAS (1913 – 1915 & 1918 - 1920) and NSW, QLD, Northern Territory (NT), SA and WA (1910 – 1914 & 1918 – 1920) were in drought. Figure 2.4 illustrates the approach of a dust storm in Narrandera, NSW in 1915.

Figure 2.4: Dust storm approaching Narrandera, New South Wales, 1915. Photo courtesy of National Library of Australia.

Throughout the 1920 – 1929 decadal period, 39 dust events have been documented (Figure 2.2). On the 4th April 1922 a report in The Argus (1922) describes a "fierce dust storm visited Melbourne and the conditions in the city caused great discomfort".

The gusts had reached 54 miles an hour (~ 87 km/h). Railways were interrupted and overhead electricity wires were damaged. Galvanised iron sheets came off the wheat sheds and fences were blown over. The Barrier Miner (1924) reported that the people of Broken Hill were of the opinion that the 27th October 1924 "was a terrible day". It was very hot and from the early morning until late at night the city was enveloped in dust. Housewives had to worry about the inside conditions which was most unpleasant. Dust had to be tipped out of the bottom of the cups. During mealtime, the teeth frequently grated on fine particles of sand but people consoled themselves with the thought that the sand might assist digestion. During October 1928, large number dust storms occurring for more than a week covering the Desert Channels and southwest QLD, and parts of NSW (The Queenslander 1928). The shipping men on the Sydney harbour had an anxious time. When the storm reached its maximum severity with wind speeds of 142 km/h, the coastal steamer Pulganbar broke away from its moorings and dragged her anchors but was safely re-moored.

Towards the end of the 1930 – 1939 decade, Australia was in the grip of the World War II (WWII) drought but only 21 dust storm events were collated in HDED (Figure 2.2). During the WWII period, newspapers were most likely to have focused on reporting about the war and the reporting of dust events might have been of a lesser importance and have not been documented to that extent. On the 10th February 1937, the ABoM mention for the first time a dust storm which surrounded the wheat belt of WA. The drought was most severe in NSW, SA, QLD, WA, VIC, NT and parts of TAS due to extremely low rainfall during 1935 – 1936 (Australian Bureau of Statistics 1988). The Advocate (1937) reported on the 16th October 1937 that aviator Jean Batten's record attempt to fly solo from England to Australia was delayed by a day due to a dust storm in Bedourie, QLD.

Until halfway through 1940 – 1949, Australia was still under the influence of the WWII drought which was reflected in the increased number of documented records (60) as shown in Figure 2.2. In late spring and summer of 1944/45, a large number of dust storms occurred over the southeast of Australia. The number of diary entries by Margaret Harris (1956) from Darby's Falls near Cowra, NSW indicate that the period between October 1944 and February 1945 was a very active dust storm period. The Canberra Times (1944) reported on the 15th December 1944 that dust storms "enveloped three states". Meteorologist Mr Mares commented that "one felt as though

one was eating dust all day". Visibility on Sydney Harbour was reduced to a few hundred yards and Sydney bound planes had to be diverted. Dust events were also reported in QLD, SA and TAS. The dust storm in Broken Hill on the 30th January 1945 was described as the worst ever experienced (The Advertiser 1945) and the sky turned black in the middle of the day. Dust events continued through to the end of the decade.

In the 1950 – 1959 period records of only five dust events were found (Figure 2.2). The Canberra Times (1950) reported the first dust storm for the summer on the 14th December 1950. Gusty westerly winds "whipped up soil from bare surface patches in local rural areas, and spread a low pall of brown over the city". Similar conditions were reported from Goulburn and Wagga Wagga and aeroplane pilots reported dust up to a height of 1,000 feet (~305 m). A news article in the Cairns Post (1951) reported that on the 10th November 1951, two new P2V-5 Neptune long-range bombers narrowly escaped disaster while landing during a dust storm at Richmond. The two planes arrived at Richmond, NSW from California, US after an uneventful flight across the Pacific. One of the planes was swept off the airport's main runway, but it landed smoothly among piles of heavy equipment used for building a new airstrip. Workmen and two press photographers had to jump for their lives as the huge aircraft "bore down on them". Flight Lieutenant Boyle said that this was the worst landing he had ever experienced. The dust-filled air tore every bit of paint off the propellers. On 20th October 1953 (Barrier Miner 1953), a dust storm which swept across Broken Hill was described by some residents as a real "old-timer" – the worst since 1944. Visibility was reduced to about 50 yards (~ 46 m) and motor vehicles had to move along the streets at a snail's pace with headlights on. Lights in shops and offices had to be switched on and the insides of buildings were covered with a thick blanket of dust. Strong winds during the night gave an indication that the day would be unpleasant. Gale force winds which reached a velocity of 48 miles an hour (~ 72 km/h), swept the city and by 10am a red hue had descended. The radio communications on the Flying Doctor network were disrupted by the storm. The City Council's electricity mains and services were also interrupted. Street trees and household gardens took a severe battering and branches were torn from trees. Minor damage was caused in most parts of the city, fences being flattened and iron blown from roofs. An interesting observation was made by Mr. R. Hinchcliffe, of Belmont Station. He commented: "At 10 o'clock this morning instrument readings at Belmont Station showed that 99.9 per

cent of the light which usually reaches the vegetation was being cut off by a dust haze. At the rate which dust was falling, Broken Hill should expect about 1500 tons of dust to pass over the city." Another dust storm followed on the 19th November 1954 which arrived from the west and provided a spectacular sight as it billowed over Broken Hill and was followed by 15 points of light rain, according to the Barrier Miner (1954). It spread to the north and south, and within minutes the city was shrouded with blinding dust in a wind which reached 59 miles an hour (~ 95 km/h) at 6pm. The radio reported that the velocity of 59 mph was the highest recorded at the aerodrome for some time. Some minor damage was caused in the city and loose sheets of iron were torn from fences. In late 1958, a 10 year drought period started to take hold in central Australia, with vast areas of QLD, SA, WA, NSW, and northern Australia affected to varying intensities (Australian Bureau of Statistics 1988).

During 1960 – 1969, this 10-year drought period continued until 1967. Severe dust storms were so widespread that several events affected a large number of states. Overall 44 observations were found (Figure 2.2). In the book 'Swanton in Australia - with MCC 1946–1975', Ernest Swanton (1975) reported on the 11th November 1965 that the "Adelaide Oval was the flattest in Australia, but the Sheffield Shield match beforehand had been affected by a dust-storm followed by a sudden 22 degree drop in frontal system temperature". Another severe dust storm event starting on the 23rd – 27th November 1965 affecting the Lake Eyre region and Strzelecki Lakes in SA, western and north west NSW and south west QLD (Jaeger 1988). A newspaper article in the The Canberra Times (1965) published on the 26th November 1965 reported that a six-mile pall of red dust, which choked 500,000 square miles of QLD, was starting to engulf northern cities and towns. The dust "blanket" was creating a nightmare for pilots and a curse for housewives. ABoM estimated that 1,000 million tonnes of western QLD earth was being blown out to sea during this event.

In 1970 – 1979, the Australian continent was under the influence of alternating La Niña and El Niño events starting in 1970 and resulted in major flooding in 1970, 1971, 1974 and 1975. A more detailed description of the extreme events is provided in Section 3.2. Due to the seesaw pattern between La Niña and El Niño and the increased occurrence of rainfall during the decade, only two dust storm were found and documented in HDED (Figure 2.2). The Bureau of Meteorology (2015) reported a dust storm event on the 4th April 1978. Strong winds and the dry conditions produced

extensive dust storms that reduced visibility over a large area of the southwest of WA. The deposition of dust on power lines also caused a failure of the electricity distribution system.

From 1980 – 1989, the dust storm activity increased to 17 events due to continued dry conditions and a severe drought in south-east Australia (Figure 2.2). On the 8th February 1983, Melbourne (Figure 2.5) was enveloped in a thick cloud of dust. At its height of the event visibility was reduced to 100 m and the three airports were temporarily closed (Dineley 2013). The power to 150,000 homes was cut as winds brought down powerlines and dust clogged junction boxes shorting circuits. The cold front that carried the dust in brought gusts of 85 km/h, uprooted trees and tore the roofs off at least 50 houses. Another intensive dust storm occurred on the 2nd December 1987 which originated in inland Australia and was recorded in the NT, QLD, NSW, VIC and SA.

Figure 2.5: Dust storm engulfed Melbourne on the 8th February 1983. Photo courtesy of Crystalink.

The 1990 – 1999 period was under the influence of a very long El Niño lasting from 1991 – 1995 (Allan & D'Arrigo 1999). This extended El Niño was accompanied by a

persistent drought over parts of QLD, NSW and other regions of the Australian continent. Overall 20 dust storm events were recorded in 1994 (Figure 2.2) in the Lake Eyre region, Strzelecki Lakes, Southern Simpson Desert, western QLD, northwest NSW and Murrumbidgee District NSW (Bureau of Meteorology 2006).

During the 2000 – 2010 decade, Australia was influenced by a very persistent and strong El Niño associated with above maximum temperatures. This is reflected in the 194 documented dust storm events for the decade (Figure 2.2). It appears that this decade experienced a large increase in dust storm activity but the surge in the number of documented events in the HDED is also attributed to the advances in technology, easy access to the World Wide Web, the establishment of DustWatch and the availability of satellite data. Earlier decades might also have experienced a large number of dust storm events but were not documented due to low population density in Australia and access to modern technology.

Between 2001 and 2010 the "Millennium Drought" set in, southeast Australia experienced the most persistent rainfall deficit since the start of the 20th century and was described as the worst drought on record. Two particular events have received news coverage worldwide and research attention. The 23rd October 2002 (Figure 2.6) and 22nd – 25th September 2009 (Figures 2.7 and 2.8) events were amongst the largest recorded in Australian history. The 23rd October 2002 severe dust storm was a result of drought conditions in eastern Australia caused by the 2002 El Nino event. The Australian Weather News (2002) reported that the dust storm was at its worst in western NSW and QLD, with visibility reduced to 50 m in places as fresh dust was whipped up from bone dry soil with reduced vegetation cover. A few years later another severe dust storm event took place between the 22nd – 25th September 2009, nicknamed 'Red Dawn' by the media and was described as "bigger than Ben Hur!" by Dr John Leys in *The Australian* newspaper (Leys, Heidenreich & Case 2009). Nigel Lawrence from Broken Hill commented that "I have never seen or experienced anything like it. You have to be 60 years plus to have seen a dust storm as bad as this!"

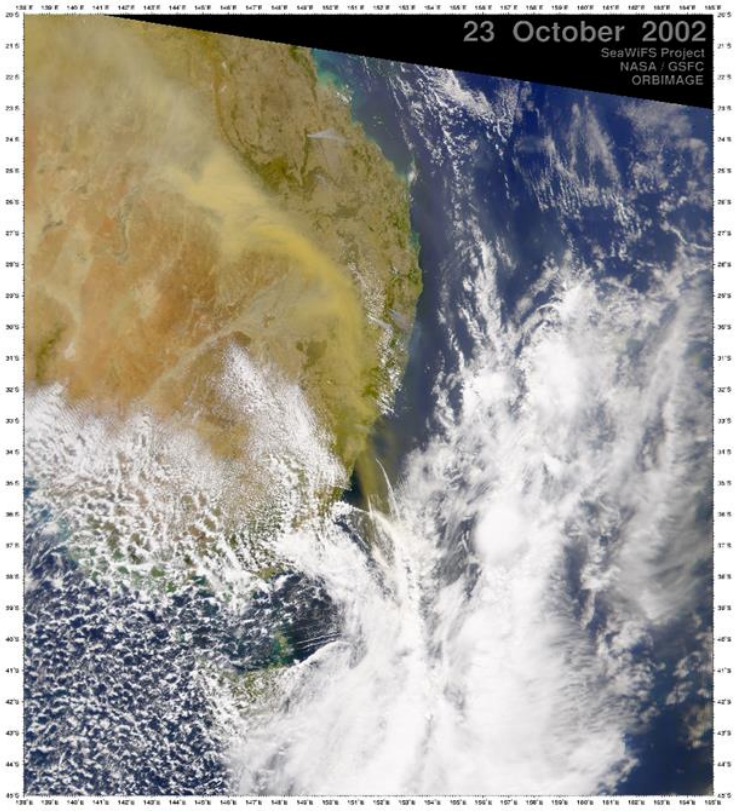

Figure 2.6: Large dust storm blowing across eastern Australia on 23rd October 2002. Photo courtesy of the SeaWiFS Project, NASA/Goddard Space Flight Center.

Figure 2.7: Dust storm approaching the Fregon Community in the Anangu Pitjantjatjara lands, South Australia, 22nd September 2009. Photo courtesy of a Remote Area Nurse.

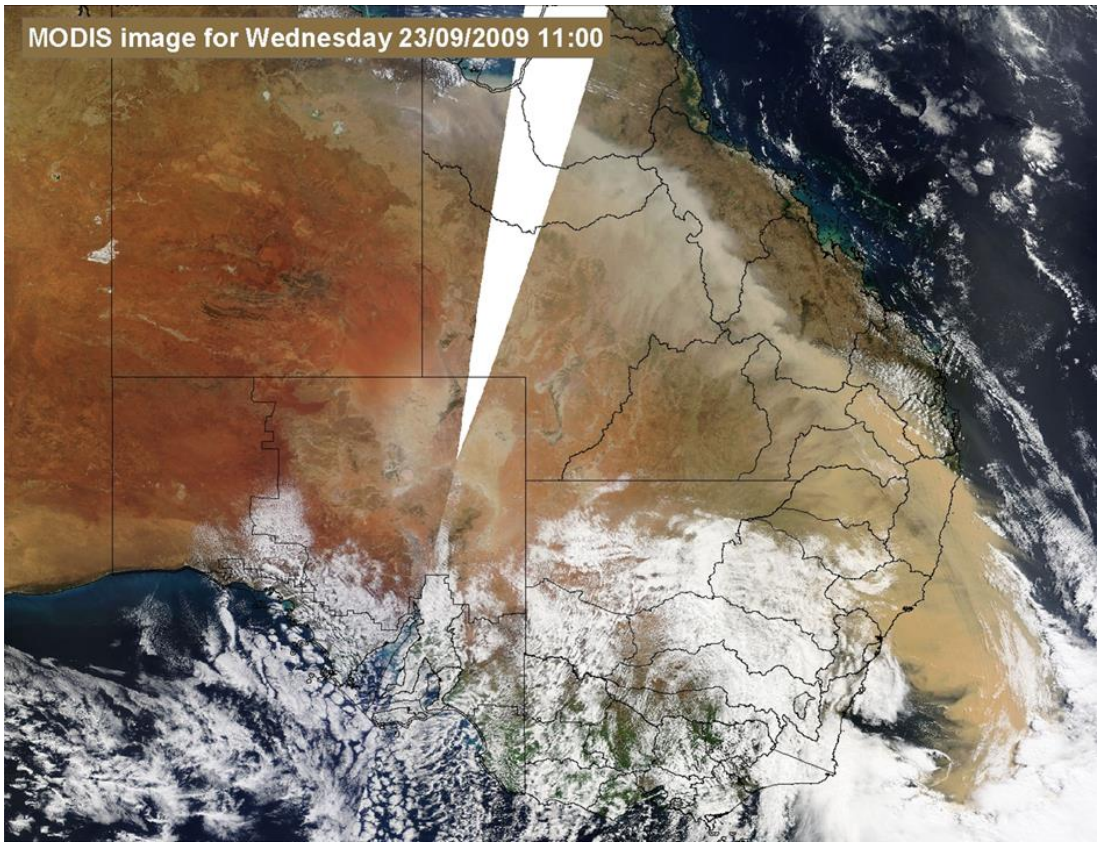

Figure 2.8: Dust storm swept across parts of inland South Australia, Victoria, New South Wales and Queensland. By 24th September, the dust plume measured more than 3,450 km from the northern edge at Cape York to the southern edge of the plume. NASA image by Jeff Schmaltz, MODIS Rapid Response Team, Goddard Space Flight Center.

In summary, the earliest dust storm events collated for the HDED was in 1852. To the end of December 2010, 585 dust storms were documented on 331 days. This list is by no means complete, but is continuing to be updated as new documented events are being uncovered. Figure 2.2 provides a good overview of the trend of the number of dust storms which have occurred over the last 16 decades. An increased number of dust storm events can be observed in the 1900s, 1940s, 1960s and 2000s. From historical documents it is known that these periods were affected by severe droughts which is reflected in the high numbers. But it is very likely that the actually number is much higher. Possibly a large number of events were not noticed or were not reported due to the sparse population in arid and semi-arid areas. Others might have been written down in diaries but have not been archived in museums or libraries.

Chapter 3: Decadal summary of quantitative and qualitative data of dust events

This chapter aims to address the second key objective as outlined in Section 1.6 by linking the climatic history of ENSO, rainfall and temperature to the HDED to establish if HDED dust records reflect climate records. Section 3.1 describes the Natural Resource Management regions of Australia and highlights the key wind erosion regions which will be used in this study. Section 3.2 links the climatic history of ENSO, rainfall and temperature to the HDED to establish and confirm if dust records match climate records between 1852 – 2010. The 159 years have been divided into decades except for the years from 1852 – 1899 which have been grouped together since there were a sparse number of historical dust storm events in the HDED for this period.

3.1 Wind erosion regions of Australia

The Australian continent has been divided into 65 Natural Resource Management (NRM) regions by the Department of Agriculture, Fisheries and Forestry as shown in Figure 3.1 and Table 3.1. The analysis in Section 3.2 utilises the NRM regions to further explore the HDED records collected for this study (Figure 2.2). Nine NRM regions out of the total 65 have been identified as being susceptible to wind erosion from long-term data. These nine regions are shown in Figure 3.1 and are listed in bold in Table 3.1. These nine regions are located within the arid and semi-arid part of Australia and are suspected to be the major source areas of dust storms activity during drought periods (Leys et al. 2010). Other NRM regions may have recorded events during 1852 – 2010, however these are most likely to be transported dust or deposition areas due to their environmental conditions and locations. The analysis of the HDED dust storm history of the individual NRM regions through time will show if there have been any spatial changes.

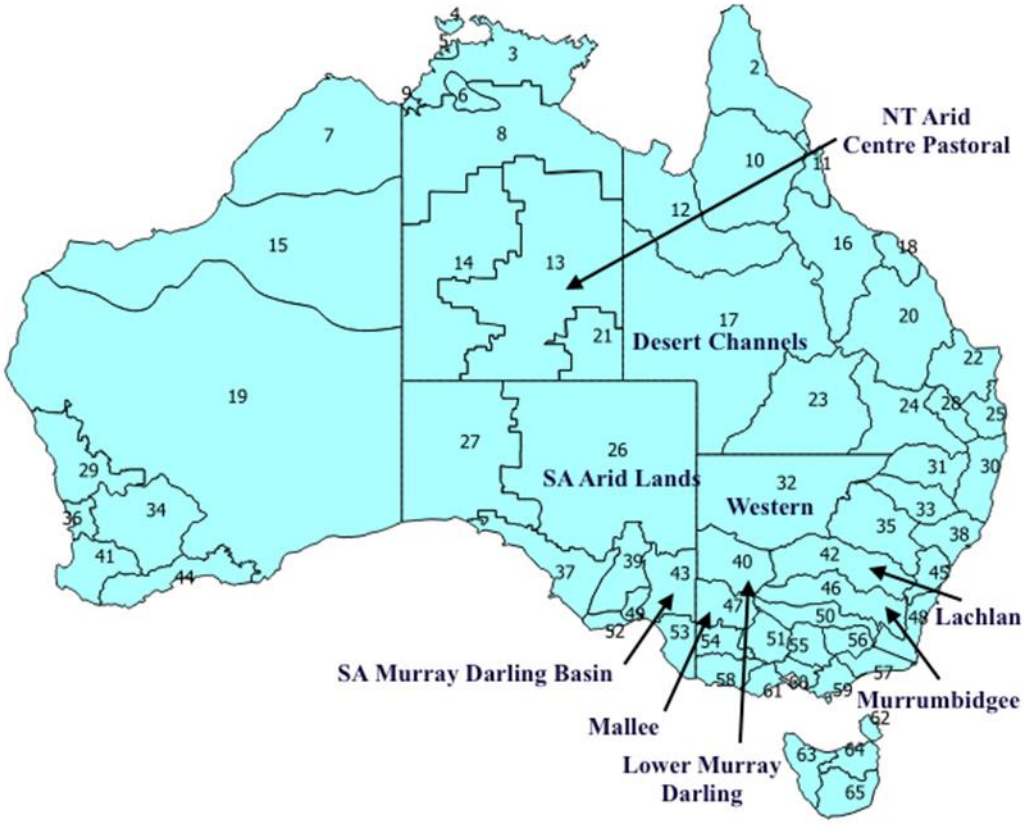

Figure 3.1: Australia's 65 NRM regions including the nine regions susceptible to wind erosion.

Table 3.1: 65 NRM regions including the nine regions susceptible to wind erosion highlighted in bold.

ID	NRM Regions	ID	NRM Regions
1	Torres Strait	34	Avon
2	Cape York	35	Central West
3	NT - Top End	36	Swan
4	NT - Melville Island	37	Eyre Peninsula
5	NT - Darwin	38	Hunter-Central Rivers
6	NT - Katherine-Douglas	39	Northern & Yorke
7	Rangelands - Kimberley	**40**	**Lower Murray Darling**
8	NT - Savanna	41	South West
9	NT - Victoria River	**42**	**Lachlan**
10	Northern Gulf	**43**	**SA Murray Darling Basin**
11	Wet Tropics	44	South Coast
12	Southern Gulf	45	Hawkesbury-Nepean
13	**NT - Arid Centre - Pastoral**	**46**	**Murrumbidgee**
14	NT - Arid Centre - Non Pastoral	**47**	**Mallee**
15	Rangelands - Gascoyne Murchison	48	Southern Rivers
16	Burdekin	49	Adelaide & Mount Lofty Ranges
17	**Desert Channels**	50	Murray
18	Mackay Whitsunday	51	North Central
19	Rangelands - Goldfields Nullarbor	52	Kangaroo Island
20	Fitzroy	53	South East
21	NT - Arid Centre Simpson	54	Wimmera
22	Burnett Mary	55	Goulburn Broken
23	South West Queensland	56	North East
24	Border Rivers Maranoa - Balonne	57	East Gippsland
25	South East Queensland	58	Glenelg Hopkins
26	**SA Arid Lands**	59	West Gippsland
27	Alinytjara Wilurara	60	Port Phillip & Westernport
28	Condamine	61	Corangamite
29	Northern Agricultural	62	TAS - Flinders
30	Northern Rivers	63	TAS - North West
31	Border Rivers-Gwydir	64	TAS - North
32	**Western**	65	TAS - South East
33	Namoi		

3.2 Decadal rainfall and temperature history

This section examines the dust storm history in the context of the climatic conditions (ENSO, rainfall and temperature). The aim is to investigate if the historical documented events in the database reflect meteorological records. The NRM wind erosion region maps in Figures 3.2 and Figures 3.4 – 3.14 show the spatial distribution

of the dust storm events in each decade. Each Figure shows three parts (with the exception of Figure 3.2). The decadal map in part (a) displays the NRM regions with the number of reported dust storm sightings. This Figure also includes the number of dust events in the NRM dust source areas. Part (b) displays the number of documented dust storm events in NRM dust source areas only. Part (c) shows the difference from the long-term average rainfall and temperature graphs for the NRM dust source areas.

The collated HDED results for the 1852 – 1899 years are shown in Figure 3.2 and Table 3.2. No rainfall and temperature data is shown here since recording of this gridded data Australia wide only started in the 1900s. The Lachlan NRM region (42) recorded the highest number of events particularly from 1890 – 1899. Other NRM regions in the eastern states and WA had dust storm recordings as well but the major dust source areas in the centre of Australia (SA and NT) seemed to have been much less active. The reduced number of documented events may also be due to the low population density in these areas during 1852 – 1899, whereas Lachlan was in the grip of a gold rush with a large number of prospectors in the area (Clacey 1853).

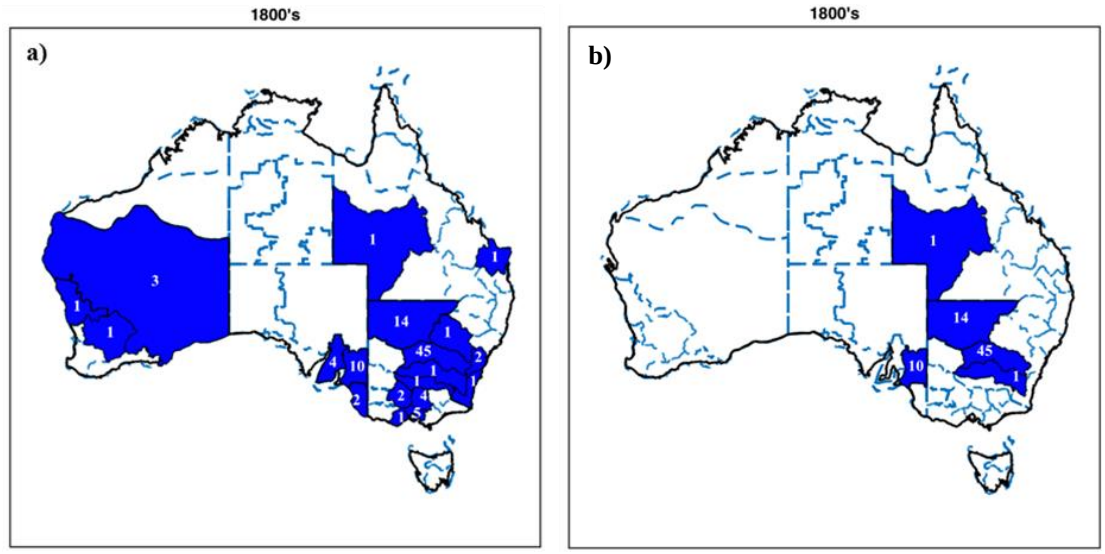

Figure 3.2: Decadal maps (1852 – 1899) showing NRM regions with a) the number of sighted dust storm events, b) the number of documented dust storm events in dust source areas.

Table 3.2: NRM wind erosion regions with the number of recorded dust events from 1852 - 1899.

No	NRM Regions	1852-59	1860-69	1870-79	1880-89	1890-99	Total
17	Desert Channels					1	**1**
32	Western				3	11	**14**
42	Lachlan				8	37	**45**
43	SA Murray Darling Basin		8		1	1	**10**
46	Murrumbidgee				1		**1**

The El Niño and La Niña climate drivers have possibly the strongest influence on year-to-year climate variability in Australia and are part of a natural ENSO cycle (Section 1.1). Rainfall and temperature are closely linked to the ENSO. El Niño affects the eastern and north-eastern region of Australia most strongly, particularly in winter and spring with below average rainfall across northern and eastern Australia, and above average temperatures across southern Australia. La Niña is associated with above average rainfall in northern and eastern Australia and below average daytime temperatures across southern Australia. Consequently, there is strong interannual variability in floods and droughts, and associated dust storm events.

The following HDED analysis is based on all dust storm events recorded from 1900 – 2010 with a particular focus on the nine NRM dust source regions (Figure 3.1) which are most susceptible to wind erosion. Figure 3.3 summaries the ENSO history starting in 1900 to 2010. In general, an El Niño, La Niña and Neutral year starts around May and goes to April the next year (Personal conversation with Prof. Roger Stone 2015, ICACS, University of Southern Queensland).

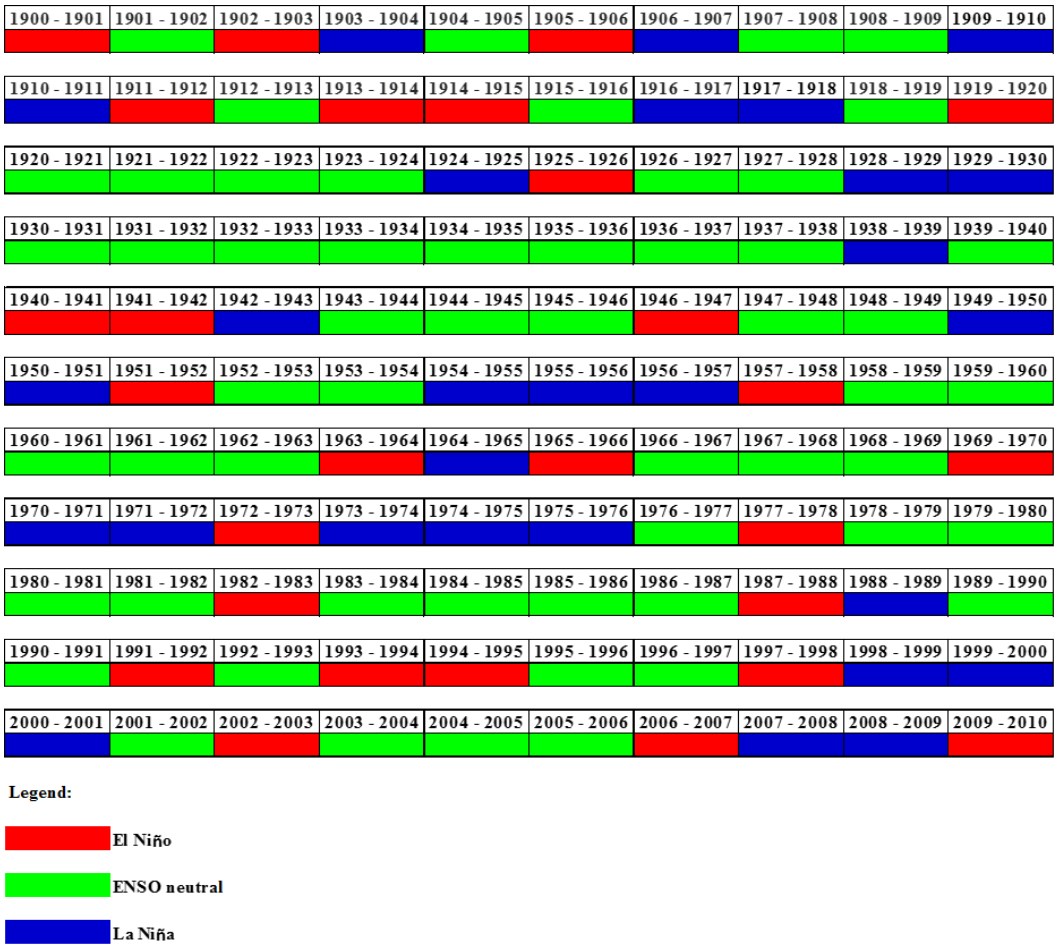

Figure 3.3: Australian ENSO history from 1900 – 2010.

The recording of gridded daily rainfall data dating back to 1900 and gridded daily temperature data at a large number of weather stations Australia wide starting in 1910 and were downloaded from the ABoM website. To determine if particular months had above or below average rainfall or temperatures, the difference from the average has been calculated. The difference in rainfall for each month is based on the long-term average of monthly rainfall calculated over 113 years (1900 – 2012), subtracted from the month of interest. Positive values represent above long-term average rainfall and negative values below long-term average rainfall on the following graphs. The same method was also applied to the temperature data using the average calculated over 103 years (1910 – 2012). These long periods (113 years – rainfall, 103 years – temperature) have been chosen to identify if long-term changes in rainfall and temperature have occurred since they have the potential to directly or indirectly impact on the environmental, social and economic sector.

The collection of documented dust storm events in the HDED between 1900 – 1909 show 45 events in six NRM regions which are susceptible to wind erosion and are of interest. The highest number of events (19) occurred in 1901 (Table 3.3) and of these, 13 are from the NT - Arid Centre. Lachlan (4), Western (1) and the Mallee (1) regions also noted one or more dust storms (Figure 3.4). Other years in this decade were less affected by wind erosion activity according to the collated records as shown in Table 3.3. According to the records in the HDED no dust storm events were documented in the Channel Country in QLD which has been identified as a major dust source area. This may be due to the sparse population in western QLD during the early 1900s.

The decadal difference rainfall graphs (Figure 3.4) for NT – Arid Centre, Lachlan, SA Arid Lands, SA Murray Darling Basin, Western and Mallee reflect the dry conditions expected to result in the number of dust event records collated. The negative values on the graphs (left hand side) represent the rainfall below the long-term average, whereas positive values (right hand side) represent the rainfall above the long-term average. The decade started with an El Niño affecting the Australian continent. In particular the NT – Arid Centre which recorded the largest number of events (13) in 1901, had well below long-term average rainfall until February 1903. Some periods had up to 60 mm less than the long-term average. The SA Arid Lands, Western, Lachlan, SA Murray Darling Basin and Mallee region also recorded below long-term average rainfall (Figure 3.4). The La Niña during August 1906 – January 1907 (Figure 3.3) which produced above long-term average rainfall over most of the continent resulting in extensive vegetation cover and therefore reducing the potential for wind erosion to occur. Overall, the percentage of months receiving below average rainfall from the long-term average (113 years) ranged from 58 – 70% for this decade as illustrated in Table 3.4 and Figure 3.4. No temperature data is available for this period. These results show that the collated records of historical dust storms reflect the quantitative climate data for this decade.

Table 3.3: NRM wind erosion regions showing recorded dust events 1900 – 1909.

No	NRM Region	1900	1901	1902	1903	1904	1905	1906	1907	1908	1909	Total
13	NT - Arid Centre		13									**13**
26	SA Arid Lands			1							1	**2**
32	Western		1	1		2			3	1	1	**9**
42	Lachlan	3	4	5	6							**18**
43	SA Murray Darling Basin					1						**1**
47	Mallee		1	1								**2**

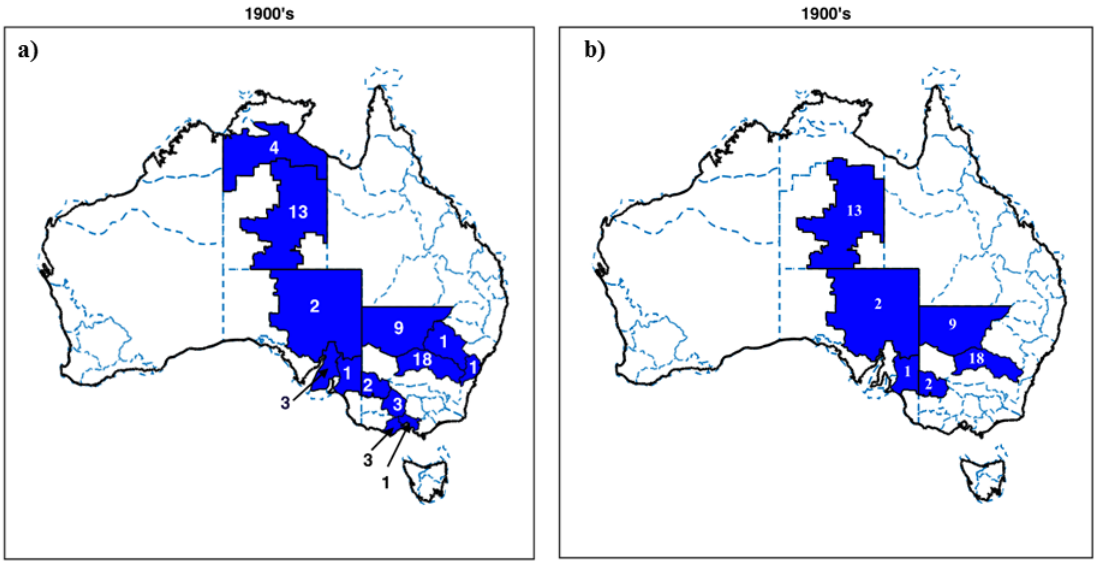

Figure 3.4: Decadal maps (1900 – 1909) showing NRM regions with a) the number of noted dust events, b) the number of documented dust events in dust source areas, and c) the difference from the long-term average rainfall (mm) data for the dust source areas. Figure continues over next page.

c) **Rainfall difference**

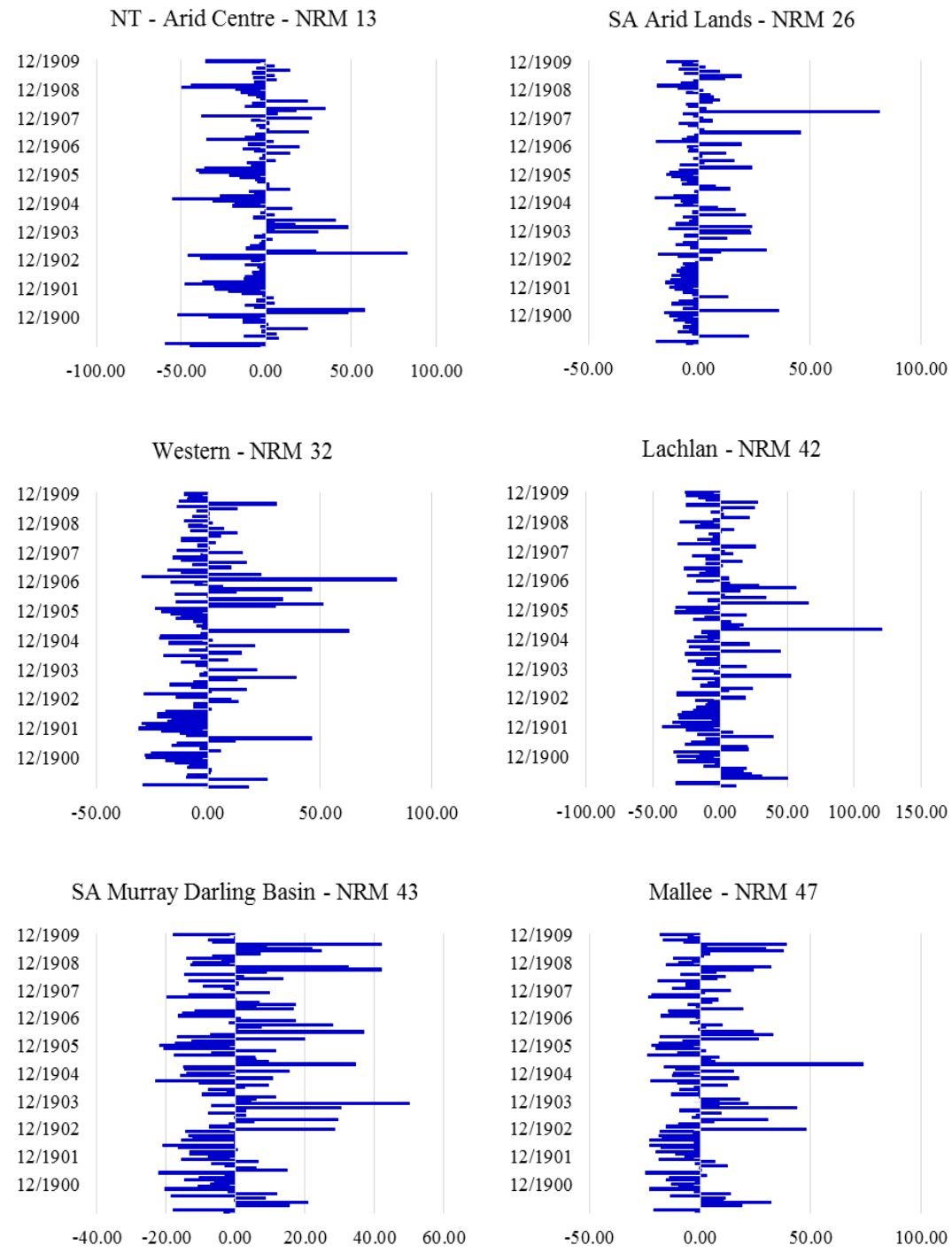

Figure 3.4: Decadal maps (1900 – 1909) showing NRM regions with a) the number of noted dust events, b) the number of documented dust events in dust source areas, and c) the difference from the long-term average rainfall (mm) data for the dust source areas.

Table 3.4: The percentage of months when rainfall was below the long-term average in the NRM dust source regions during 1900 – 1909.

1900 - 1909	13	26	32	42	43	47
% of months below average Rainfall	68	70	66	65	58	61

From 1910, long-term gridded temperature data is available from the ABoM. As mentioned in the previous section the difference in rainfall for each month is based on the long-term average of monthly rainfall calculated over 113 years (1900 – 2012), subtracted from the month of interest. The same approach was used to calculate the difference in temperature for each month based on the long-term average of monthly temperature calculated over 103 years. Negative values on the graphs (left hand side) represent below long-term average rainfall (blue) or below long-term average temperatures (red) data.

The collated historical records from 1910 – 1919 show 11 dust storm events occurred in the Western (7), Mallee (2) and SA Murray Darling Basin (2) NRM regions (Table 3.5). The low number of dust events during this decade may be attributed to the influence of the La Niña starting in 1909 – 1911 (Figure 3.3). An El Niño followed in 1911 – 1912 and another from 1913 – 1915. A second La Niña occurred between 1916 – 1918, and the decade concluded with an El Niño from 1919 – 1920. This see-saw pattern of ENSO extremes is reflected in the difference from long-term average rainfall and temperature graphs for the Western, SA Murray Darling Basin and Mallee graphs in Figure 3.5. In particular the influence of the 1916 – 1918 La Niña is clearly displayed in the rainfall and temperature Figure 3.5. Table 3.6 shows the percentage of months receiving below average rainfall from the long-term average (113 years) for the three NRM regions ranging from 51 – 63% for this decade. The temperatures were between 49 – 56% of the time above the long-term average as shown in Table 3.7. The Western NRM region experienced below long-term average rainfall for 63% of the decade and above long-term average temperatures for 56% of the time (Table 3.6 & Table 3.7). This may explain why the largest number of dust storm events occurred in this region. During periods of below average rainfall, temperatures are often higher than normal and vice versa. Since these regions received intermittent above average rainfall during the decade, green and dead vegetation would have covered a substantial

part of the soil surface. The potential for dust storm events to occur was therefore reduced.

Table 3.5: NRM wind erosion regions showing recorded dust events 1910 – 1919.

No	NRM Region	1910	1911	1912	1913	1914	1915	1916	1917	1918	1919	Total
32	Western	1		2	2					1	1	7
43	SA Murray Darling Basin					1						2
47	Mallee	1				1		1				2

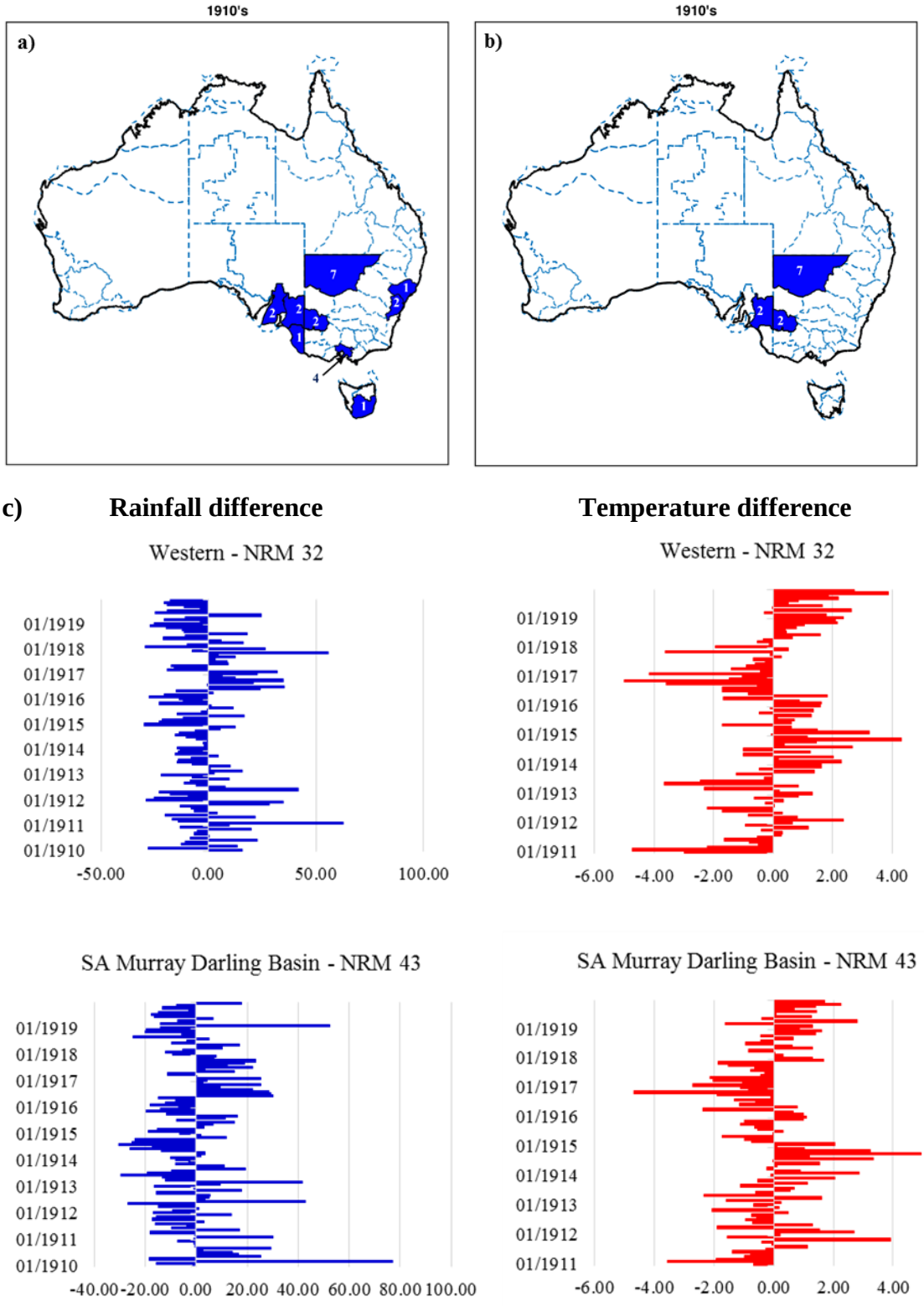

Figure 3.5: Decadal maps (1910 – 1919) showing NRM regions with a) the number of noted dust events, b) the number of documented dust events in dust source areas, and c) the difference from the long-term average rainfall (mm) and temperature (ºC) data for the dust source areas. Figure continues over next page.

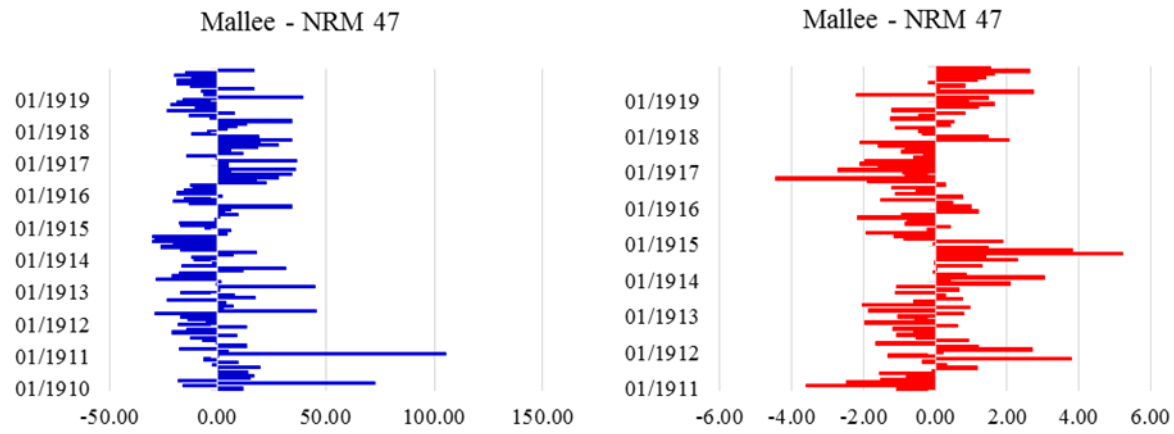

Figure 3.5: Decadal maps (1910 – 1919) showing NRM regions with a) the number of noted dust events, b) the number of documented dust events in dust source areas, and c) the difference from the long-term average rainfall (mm) and temperature (ºC) data for the dust source areas.

Table 3.6: The percentage of months when rainfall was below the long-term average in the NRM dust source regions during 1910 – 1919.

1910 - 1919	**32**	**43**	**47**
% of months below average Rainfall	63	56	51

Table 3.7: The percentage of months when temperatures were above the long-term average in the NRM dust source regions during 1910 – 1919.

1910 - 1919	**32**	**43**	**47**
% of months above average Temperature	56	50	49

Analysis of the HDED for the 1920 – 1929 decade show 18 dust storm events in the following NRM regions: Desert Channels (5), Western (9), SA Murray Darling Basin (3) and Mallee (1) as listed in Table 3.8. This decade was under the influence of two La Niña (1924 – 1925 & 1928 – 1930) and one El Niño (1925 – 1926) in between (Figure 3.3). The decadal difference from long-term average rainfall and temperature graphs (Figure 3.6) for Desert Channels, Western, SA Murray Darling Basin and Mallee reflect the mixed climatic conditions for the decade. From mid-1920 – mid-1921 these regions received above long-term average rainfall and therefore increased vegetation cover in the following months. From mid-1921, rainfall was below long-term average for the majority of the years until the end of the decade. Table 3.9 illustrates that all four NRM regions (Desert Channels, Western, SA Murray Darling

Basin, Mallee) experienced between 62 – 67% below the long-term average rainfall and between 44 – 55% above the long-term average temperatures in this decade (Table 3.10). The below average rainfall coupled with above average temperatures for Western may explain the higher number of recorded dust storm events. The meteorological conditions for the decade are consistent with the low numbers of documented anecdotal dust storm.

Table 3.8: NRM wind erosion regions showing recorded dust events 1920 – 1929.

No	NRM Regions	1920	1921	1922	1923	1924	1925	1926	1927	1928	1929	Total
17	Desert Channels									5		**5**
32	Western		1	3		2				1	2	**9**
43	SA Murray Darling Basin								2		1	**3**
47	Mallee									1		**1**

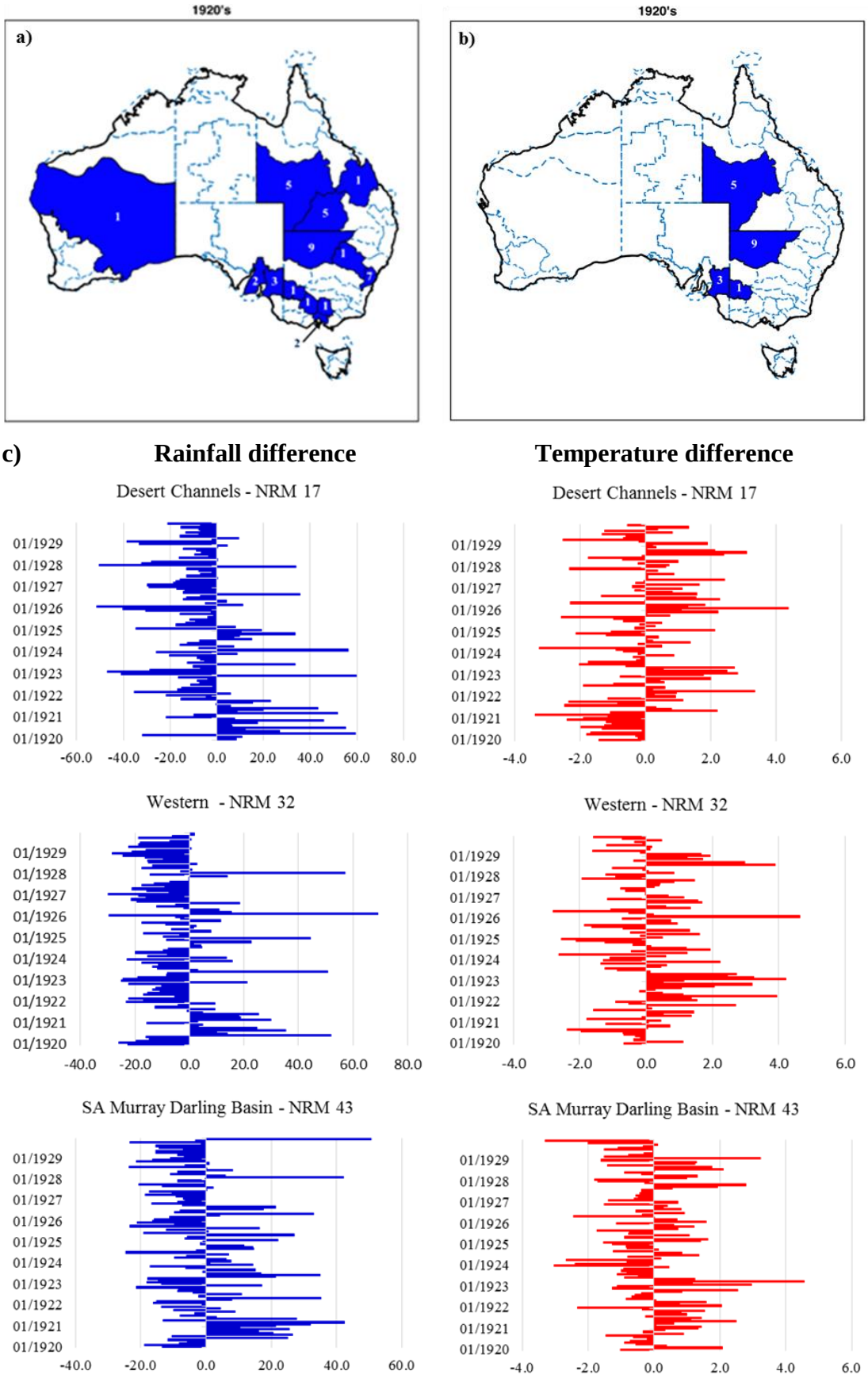

Figure 3.6: Decadal maps (1920 – 1929) showing NRM regions with a) the number of noted dust events, b) the number of documented dust events in dust source areas, and c) the difference from the long-term average rainfall (mm) and temperature (ºC) data for the dust source areas. Figure continues over next page.

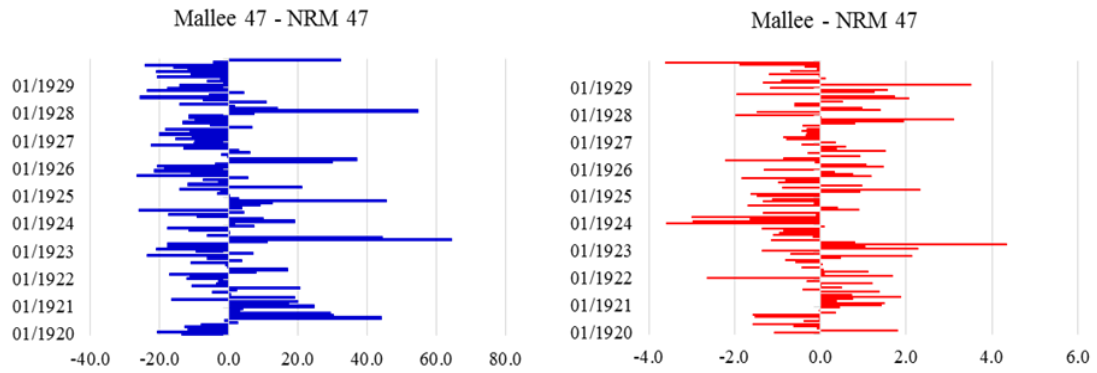

Figure 3.6: Decadal maps (1920 – 1929) showing NRM regions with a) the number of noted dust events, b) the number of documented dust events in dust source areas, and c) the difference from the long-term average rainfall (mm) and temperature (ºC) data for the dust source areas.

Table 3.9: The percentage of months when rainfall was below the long-term average in the NRM dust source regions during 1920 – 1929.

1920 – 1929	**17**	**32**	**43**	**47**
% of months below average Rainfall	67	67	63	62

Table 3.10: The percentage of months when temperatures were above the long-term average in the NRM dust source regions during 1920 – 1929.

1920 – 1929	**17**	**32**	**43**	**47**
% of months above average Temperature	49	55	46	44

During the 1930 – 1939 decade only a small number (15) of dust events were documented from 1934 onwards in the Desert Channels (1), Western (2), Lachlan (7), SA Murray Darling Basin (1), Murrumbidgee (1) and Mallee (3) NRM regions (Table 3.11, Figure 3.7). The small number of events may be explained when linking it to the climatic conditions for this period. During the last three years of the previous decade (1928 – 1930) Australia was under the influence of a long La Niña which was then followed with an eight year ENSO neutral from 1930 – 1938 (Figure 3.3). The oscillation of rainfall and temperatures between above and below long-term average resulted in the low count of dust events during this decade (Figure 3.7). The difference from the long-term average rainfall and temperature graphs in Figure 3.7, reflect this trend. All regions received well above 50 mm of rainfall in some of the months but overall between 54 – 63% received below the long-term average for the entire decade

(Table 3.12). The temperatures were for most of the decade below the long-term average. Only for 37 – 51% of the months it exceeded the long-term average (Table 3.13). The below average temperatures also influenced soil moisture favourably. The increased rainfall and below average temperatures during the first few years of the decade had a positive influence on vegetation growth. The extensive vegetation cover, which includes green and died off vegetation reduced the occurrence of wind erosion events.

Table 3.11: NRM wind erosion regions showing recorded dust events 1930 – 1939.

No	NRM Regions	1930	1931	1932	1933	1934	1935	1936	1937	1938	1939	Total
17	Desert Channels								1			**1**
32	Western								1	1		**2**
42	Lachlan						3			2	2	**7**
43	SA Murray Darling Basin					1						**1**
46	Murrumbidgee								1			**1**
47	Mallee					1				2		**3**

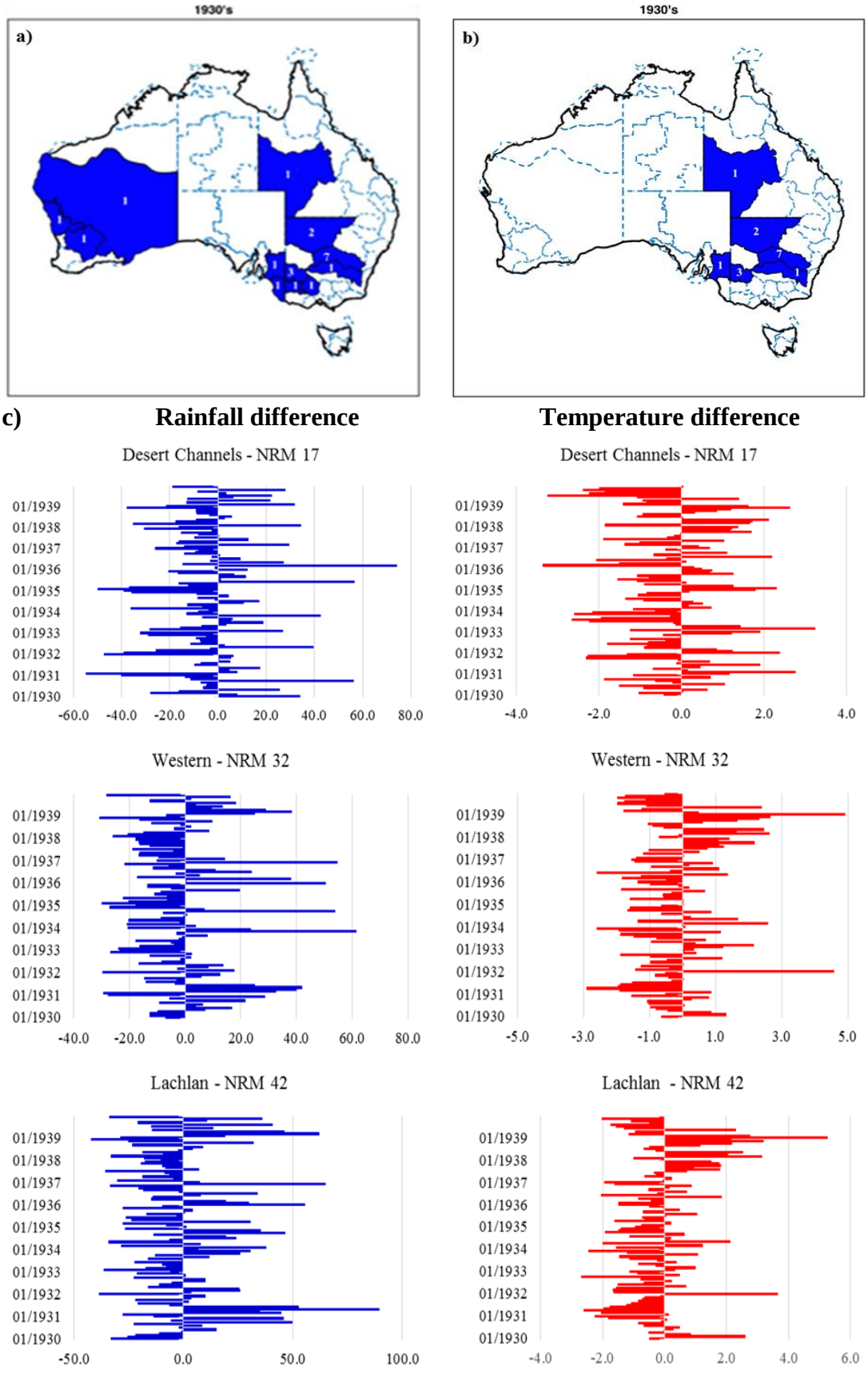

Figure 3.7: Decadal maps (1930 – 1939) showing NRM regions with a) the number of noted dust events, b) the number of documented dust events in dust source areas, and c) the difference from the long-term average rainfall (mm) and temperature (ºC) data for the dust source areas. Figure continues over next page.

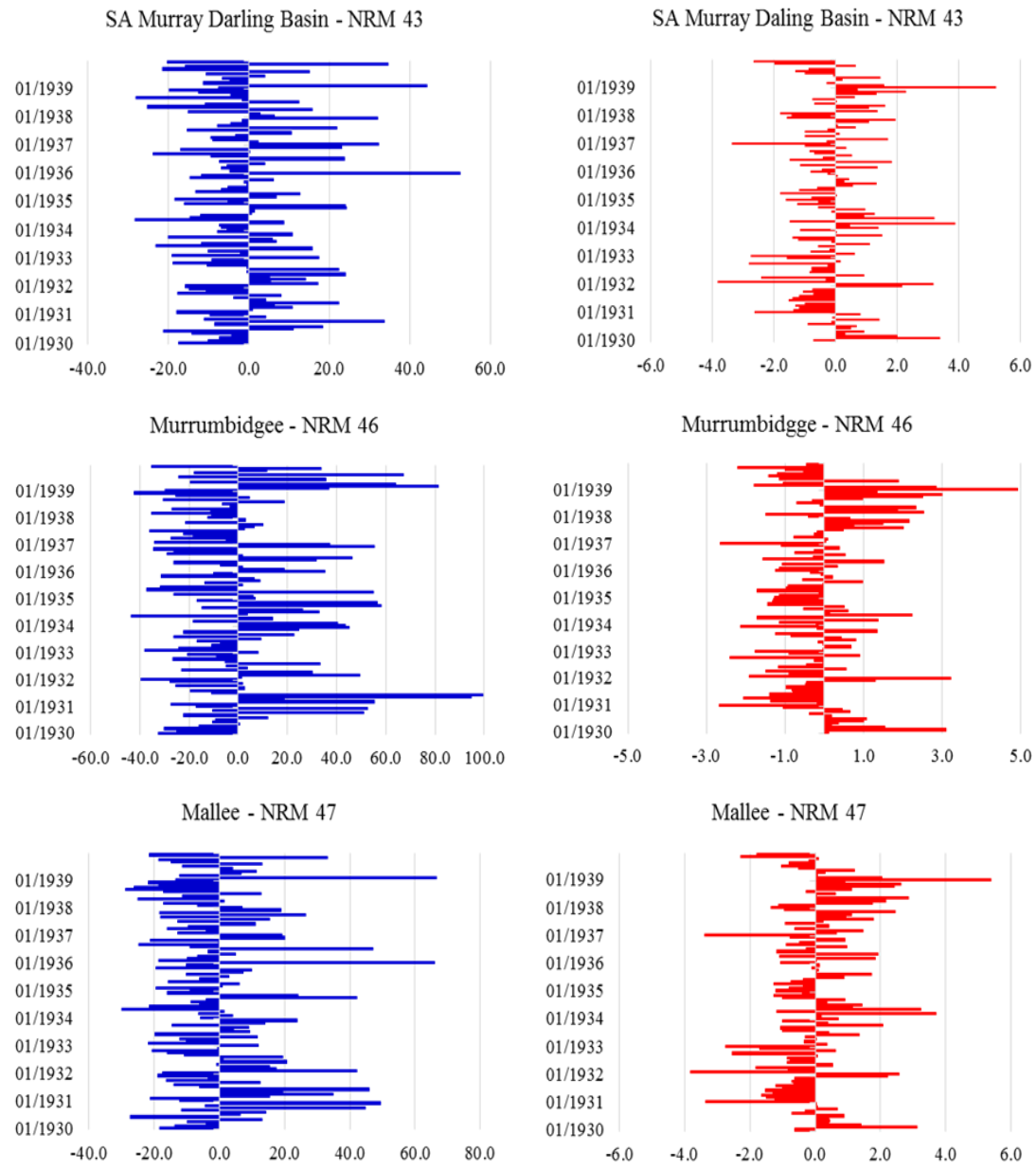

Figure 3.7: Decadal maps (1930 – 1939) showing NRM regions with a) the number of noted dust events, b) the number of documented dust events in dust source areas, and c) the difference from the long-term average rainfall (mm) and temperature (ºC) data for the dust source areas.

Table 3.12: The percentage of months when rainfall was below the long-term average in the NRM dust source regions during 1930 – 1939.

1930 - 1939	17	32	42	43	46	47
% of months below average Rainfall	63	63	59	61	54	58

Table 3.13: The percentage of months when temperatures were above the long-term average in the NRM dust source regions during 1930 – 1939.

1930 - 1939	17	32	42	43	46	47
% of months above average Temperature	43	42	37	43	39	51

The 1940 – 1949 decade was influenced by two strong El Niños (1940 – 1942, 1946 – 1947) and one La Niña (1942 – 1943). During 1943 – 1946 ENSO neutral conditions influenced the climate in Australia (Figure 3.3). By the beginning of the 1940 decade the WWII drought, which started in 1937 had a solid grip on Australia. Nine NRM regions reported 50 events collectively over the whole decade (Table 3.14). The HDED indicate an active wind erosion season particularly in 1944 and 1945 with 18 and 12 dust events respectively. Lachlan reported 12 events, Western 3, Mallee 2 and SA Arid Lands 1 for 1944 alone (Table 3.14).

The decadal graphs showing the difference from long-term average rainfall and temperature in Figure 3.8, provide a good overview of the climatic condition during 1940 – 1949. All seven NRM regions received between 63 – 72% of the time below the long-term average rainfall for the decade (Table 3.15) and temperatures were below the long-term average for 37 – 50% of the months (Table 3.16). From the beginning of 1942 to the end of 1945, the seven NRM received very much below the long-term average rainfall. The deficiency of rainfall reduced soil moisture, and therefore vegetation cover, and increased the risk and impact of wind erosion in these regions. In particular Lachlan with 18 dust storm event stands out. Twelve of these occurred in 1944. The decadal rainfall graph in Figure 3.8 shows that before 1944 the region received well below average rainfall for a number of years which will have influenced soil moisture and consequently vegetation cover and explains the increased dust storm activity during that period.

Table 3.14: NRM wind erosion regions showing recorded dust events 1940 – 1949.

No	NRM Regions	1940	1941	1942	1943	1944	1945	1946	1947	1948	1949	Total
13	NT - Arid Centre				3			1			1	**5**
17	Desert Channels						1		1	2		**4**
26	SA Arid Lands					1						**1**
32	Western		1			3	4			2		**10**
42	Lachlan		1			12	2	2	1			**18**
43	SA Murray Darling Basin	1		2					2			**5**
47	Mallee					2	5					**7**

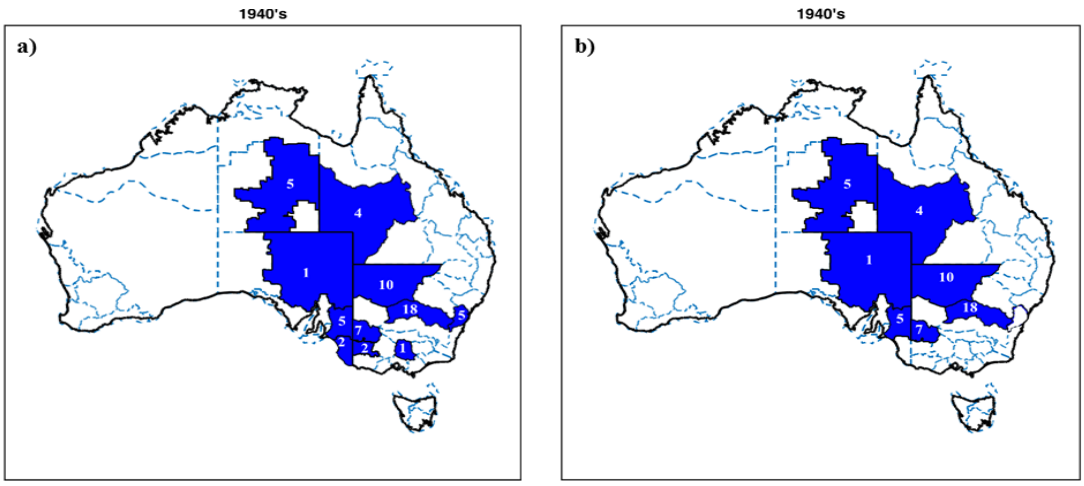

Figure 3.8: Decadal maps (1940 – 1949) showing NRM regions with a) the number of noted dust events, b) the number of documented dust events in dust source areas, and c) the difference from the long-term average rainfall (mm) and temperature (ºC) data for the dust source areas. Figure continues over next page.

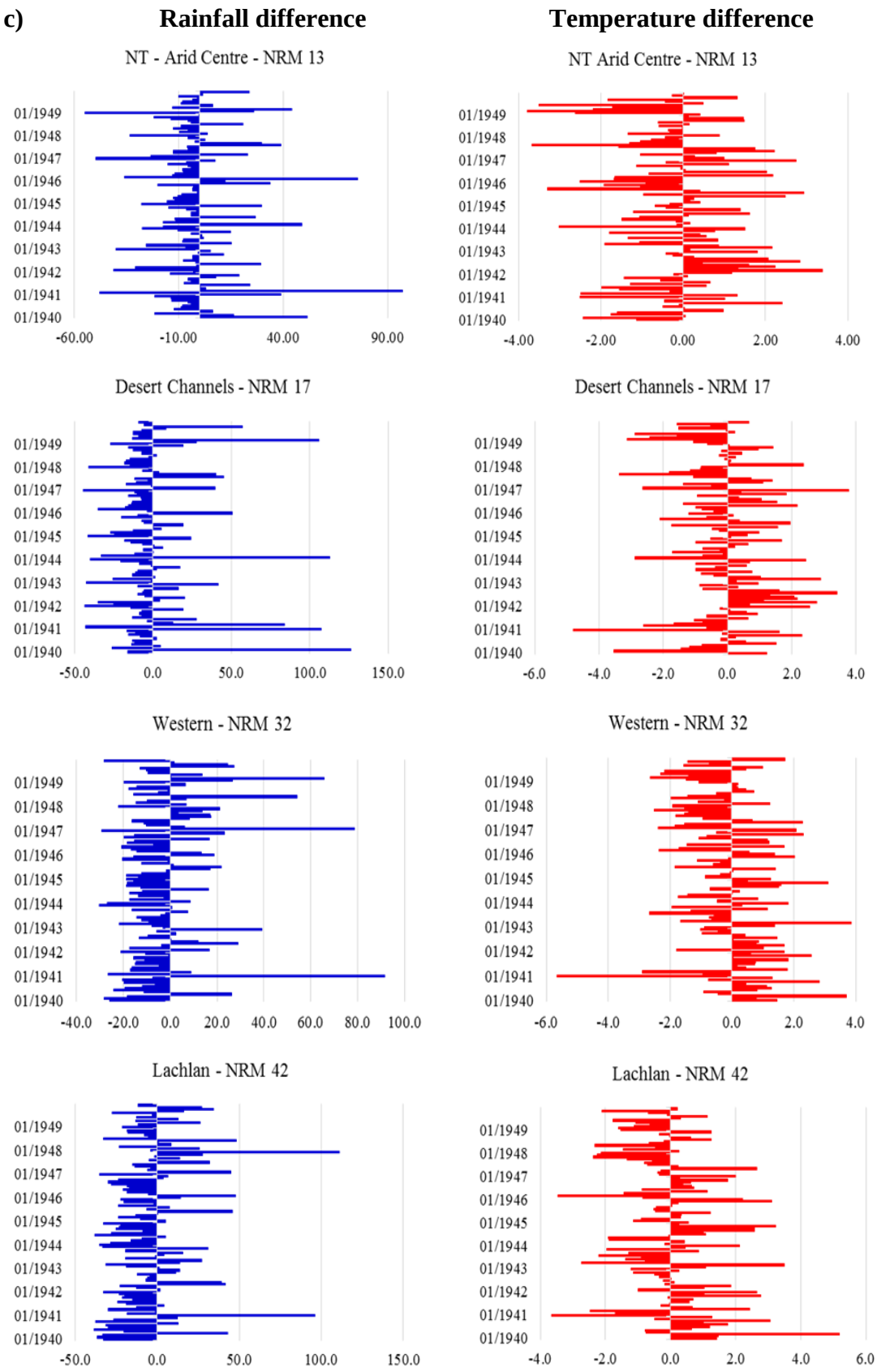

Figure 3.8: Decadal maps (1940 – 1949) showing NRM regions with a) the number of noted dust events, b) the number of documented dust events in dust source areas, and c) the difference from the long-term average rainfall (mm) and temperature (ºC) data for the dust source areas. Figure continues over next page.

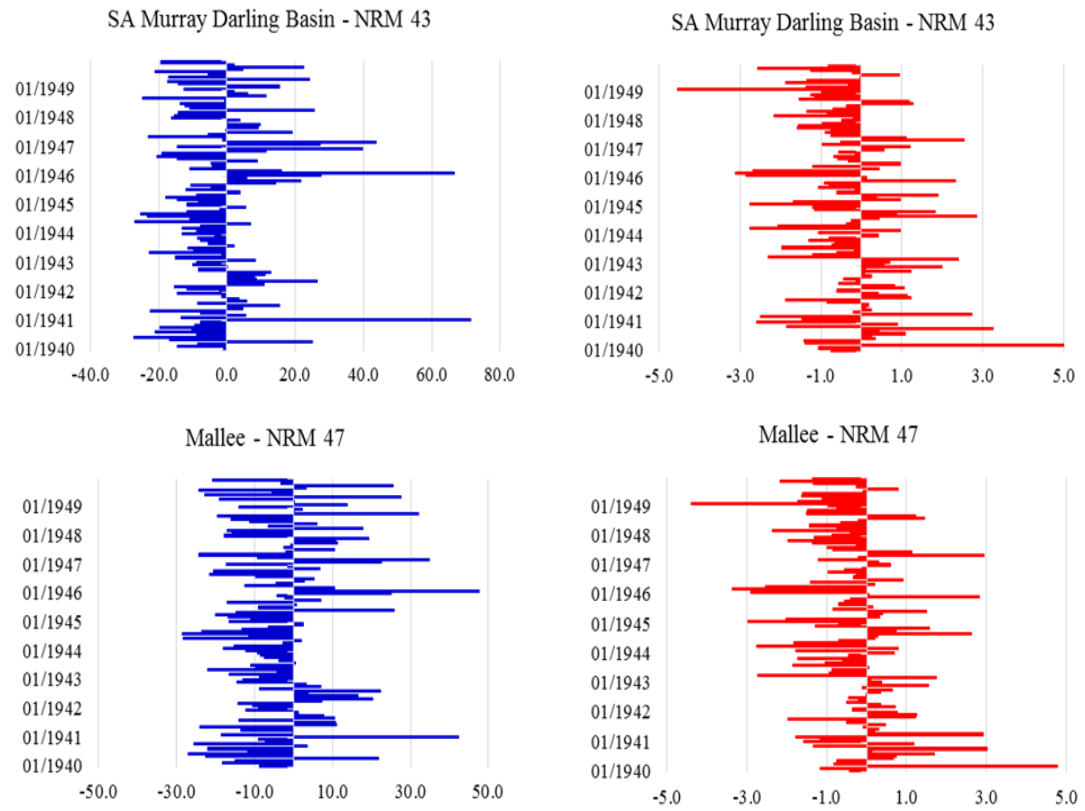

Figure 3.8: Decadal maps (1940 – 1949) showing NRM regions with a) the number of noted dust events, b) the number of documented dust events in dust source areas, and c) the difference from the long-term average rainfall (mm) and temperature (ºC) data for the dust source areas.

Table 3.15: The percentage of months when rainfall was below the long-term average in the NRM dust source regions during 1940 – 1949.

1940 - 1949	**13**	**17**	**26**	**32**	**42**	**43**	**47**
% of months below average Rainfall	71	72	68	68	68	63	64

Table 3.16: The percentage of months when temperatures were above the long-term average in the NRM dust source regions during 1940 – 1949.

1940 - 1949	**13**	**17**	**26**	**32**	**42**	**43**	**47**
% of months above average Temperature	47	38	40	50	48	37	37

Historical records in the HDED indicate that between 1950 – 1959 only two dust storm events were found. Both occurred in the Western NRM region in 1953 and 1954 (Table 3.17). The reduced number of events may be attributed to the influence ENSO neutral conditions from 1952 – 1954 follwed by a long lasting La Niña between 1954 – 1957 (Figure 3.3). The decadal rainfall and temperature graph of the Western NRM region (Figure 3.9) reflects the imapct of the La Niña. In March 1956, rainfall peaked at 131

mm above the long-term average but over the decade 55% of the time rainfall was below the long-term avarage (Table 3.18). Temperatures were above the long-term avarage for 38% of the months in the western NRM region (Table 3.19). The wetter conditions were favourable for vegetation growth and therefore reduced the risk of dust storm events.

Table 3.17: NRM wind erosion regions showing recorded dust events 1950 – 1959.

No	NRM Regions	1950	1951	1952	1953	1954	1955	1956	1957	1958	1959	Total
32	Western				1	1						2

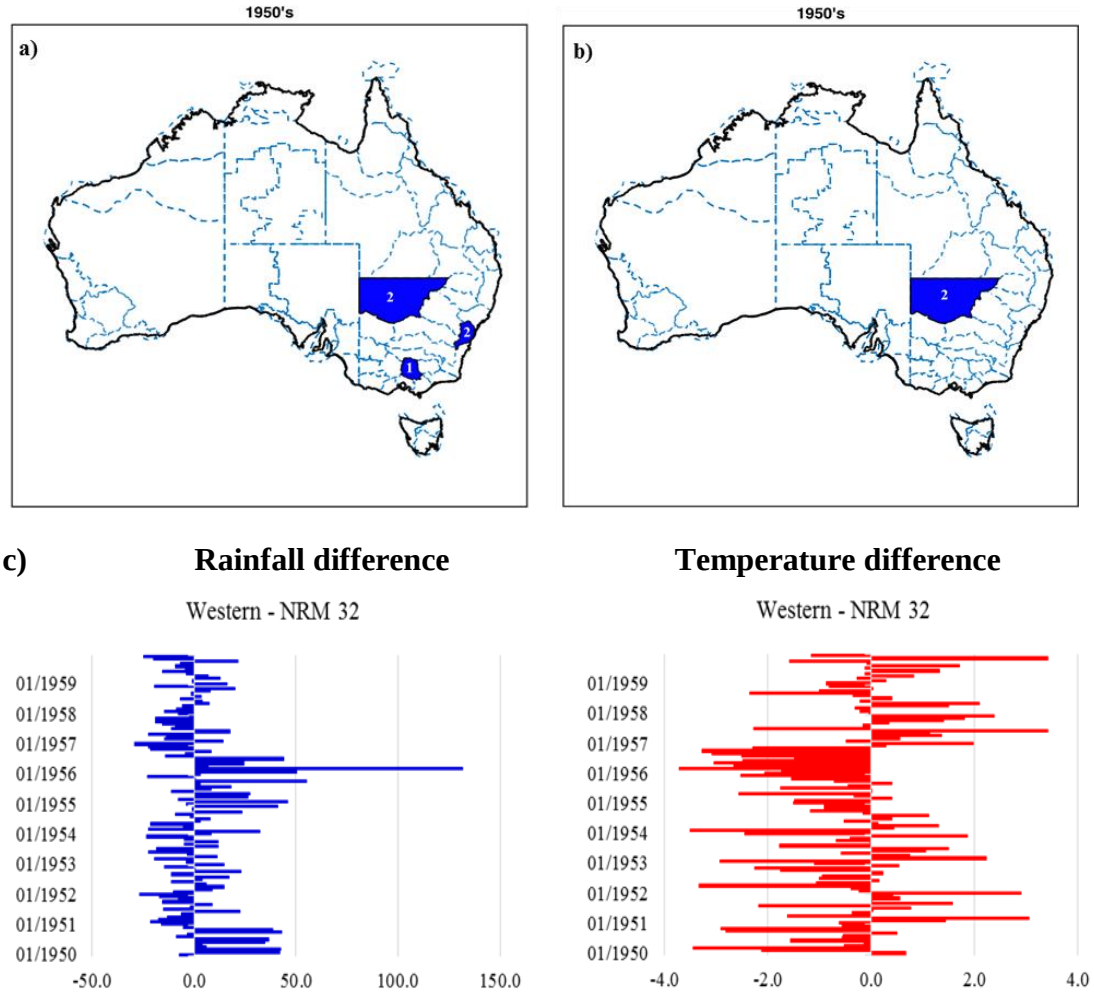

Figure 3.9: Decadal maps (1950 – 1959) showing NRM regions with a) the number of noted dust events, b) the number of documented dust events in dust source areas, and c) the difference from the long-term average rainfall (mm) and temperature (ºC) data for the dust source areas.

Table 3.18: The percentage of months when rainfall was below the long-term average in the NRM dust source regions during 1950 – 1959.

1950 - 1959	32
% of months below average Rainfall	55

Table 3.19: The percentage of months when temperatures were above the long-term average in the NRM dust source regions during 1950 – 1959.

1950 - 1959	32
% of months above average Temperature	38

The collected anecdotal dust storm records in the HDED for the 1960 – 1969 decade provided additional confirmation that Australia was experiencing a severe drought from 1965 – 1968. In particular the year 1965 stands out in the dust storm event list

with 21 recordings in five NRM wind erosion regions over five days (Table 3.20). All recorded dust events, apart from one (1963), occurred from the 23 – 27 November 1965. The Desert Channels, NT – Arid Centre, SA Arid Lands and Western recorded five events each and one for Murrumbidgee in November 1965. In 1963 one dust storm record was found in the NT – Arid Centre.

The decadal rainfall graphs (Figure 3.10) for the Desert Channels, NT – Arid Centre, SA Arid Lands, Western and Murrumbidgee highlight the dry conditions which lead to the increased number of recorded severe dust storm events in November 1965. The decade started with ENSO neutral conditions from 1958 – 1963 which was followed with an El Niño from 1963 – 1964 (Figure 3.3). A short lived La Niña had a modest impact on parts of southern and eastern Australia. Long periods of below average falls prevailed over NSW and the southern half of QLD as a prelude to the 1965 El Niño which took hold in March 1965 as can be seen in the Figure 3.10. The five NRM regions received 53 – 72% of the time below the long-term average rainfall (Table 3.21) and temperatures were between 37 – 50% of the months above the long-term average (Table 3.22). The years leading up to November 1965 where very dry and as a consequence vegetation cover was reduced leaving the soil surface exposed.

Table 3.20: NRM wind erosion regions showing recorded dust events 1960 – 1969.

No	NRM Regions	1960	1961	1962	1963	1964	1965	1966	1967	1968	1969	Total
13	NT - Arid Centre				1			5				**6**
17	Desert Channels						5					**5**
26	SA Arid Lands							5				**5**
32	Western						5					**5**
46	Murrumbidgee						1					**1**

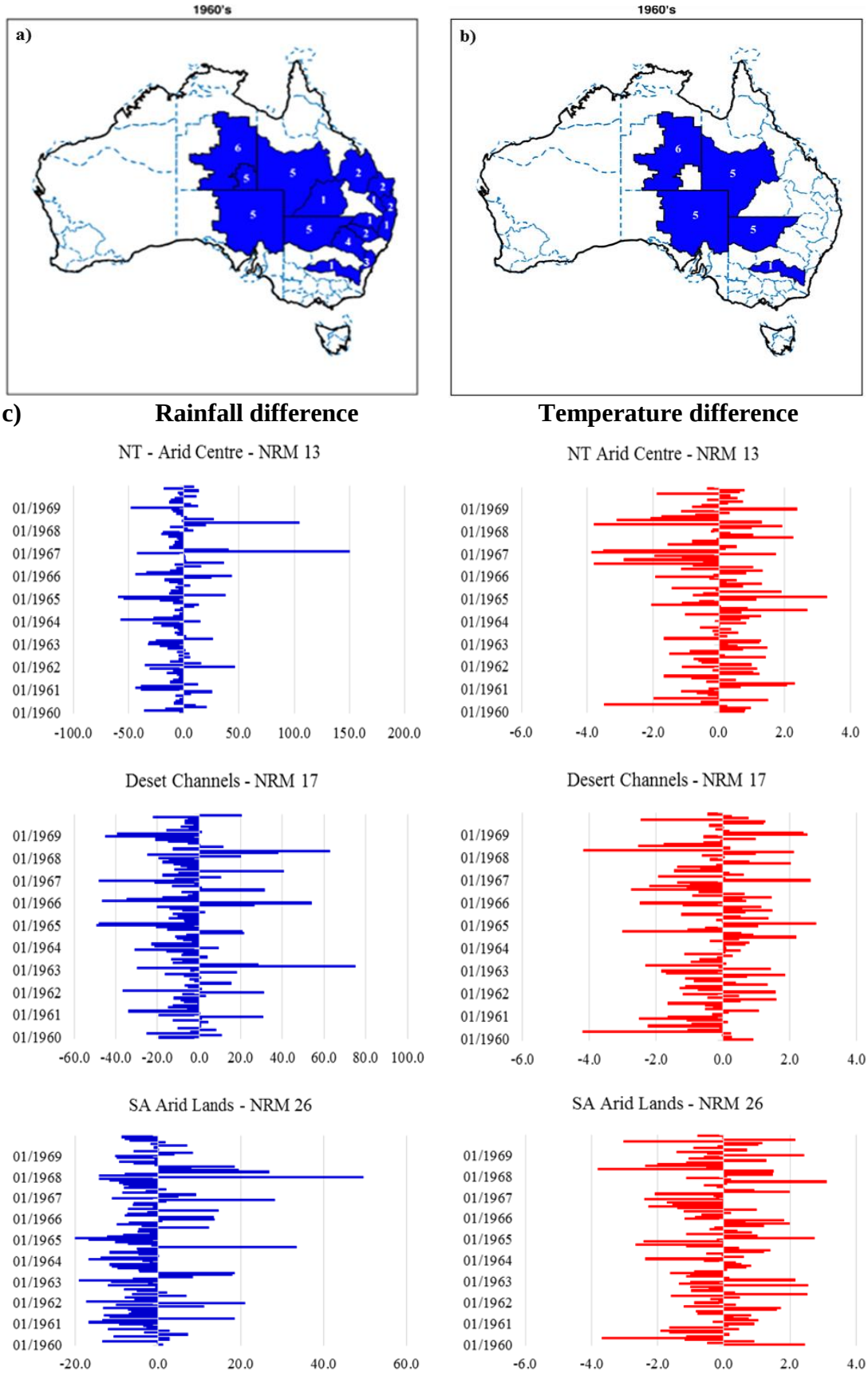

Figure 3.10: Decadal maps (1960 – 1969) showing NRM regions with a) the number of noted dust events, b) the number of documented dust events in dust source areas, and c) the difference from the long-term average rainfall (mm) and temperature (ºC) data for the dust source areas. Figure continues over next page.

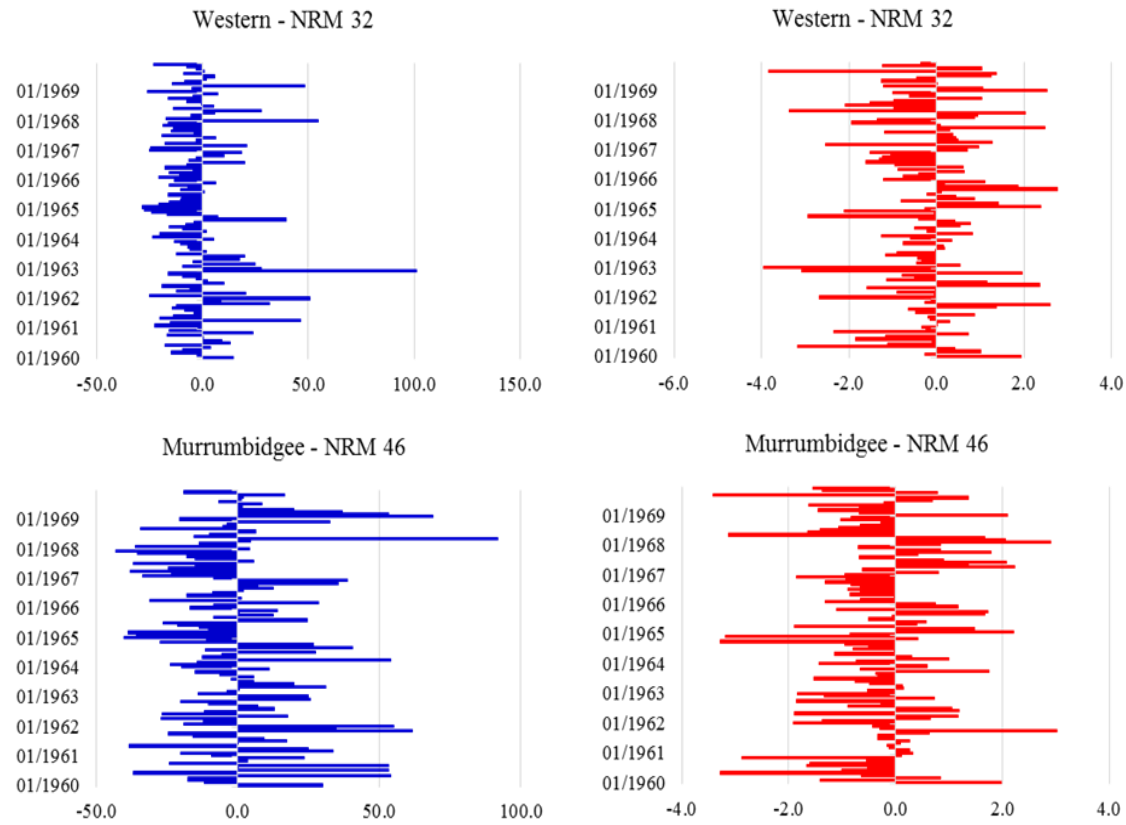

Figure 3.10: Decadal maps (1960 – 1969) showing NRM regions with a) the number of noted dust events, b) the number of documented dust events in dust source areas, and c) the difference from the long-term average rainfall (mm) and temperature (ºC) data for the dust source areas.

Table 3.21: The percentage of months when rainfall was below the long-term average in the NRM dust source regions during 1960 – 1969.

1960 - 1969	13	17	26	32	46
% of months below average Rainfall	68	72	71	68	53

Table 3.22: The percentage of months when temperatures were above the long-term average in the NRM dust source regions during 1960 – 1969.

1960 - 1969	13	17	26	32	46
% of months above average Temperature	50	48	45	42	37

In the 1970 – 1979 decade one dust event was documented in the HDED, occurring in the SA Arid Lands NRM region in 1971 (Table 3.23 & Figure 3.11). The months leading up to the event were very dry with rainfall below average in the SA Arid Lands region (Figure 3.11). For the decade, 58% of the months experienced below the long-term average rainfall (Table 3.24) and 47% of the time above the long-term average

temperatures (Table 3.25). The decadal long-term average difference rainfall and temperature graphs for SA Arid Lands illustrates the impact of the La Niña events, particularly from the 1973 – 1976 resulting in above average rainfall which explains the low number of dust storm events for this decade.

The reduced occurrence of dust storm events was due to a number of La Niñas (Figure 3.3) during this decade with the first one lasting from 1970 – 1972. Drier than average conditions followed as the climate began a shift into an El Niño mode in 1972 when rainfall totals were very much below the long-term average. Following is relatively short intense El Niño, one of the longest La Niña developed in 1973 which lasted to 1976 (Figure 3.3) with excessive rainfall resulting in widespread floods (Allan 1983). As an example, the exceptionally wet spring together with the additional rainfall from Cyclone Wanda produced widespread and severe flooding in Brisbane, QLD. In the early morning of 25th January 1974, heavy rain began to fall and during a 36-hour period the city received 642 mm of rain. Large areas were inundated with flood waters and at least 6,700 homes were flooded. Fourteen people lost their lives. The SA Arid Lands received 128 mm above the long-term average rainfall in January 1974 (Figure 3.11) and 92 mm in February 1976. The extensive rain produced abundant vegetation growth in central Australia. The 1970 – 1979 decade received well above average falls over large areas of the continent, increasing vegetation cover and therefore reducing the risk of wind erosion.

Table 3.23: NRM wind erosion regions showing recorded dust events 1970 – 1979.

No	NRM Regions	1970	1971	1972	1973	1974	1975	1976	1977	1978	1979	Total
26	SA Arid Lands		1									1

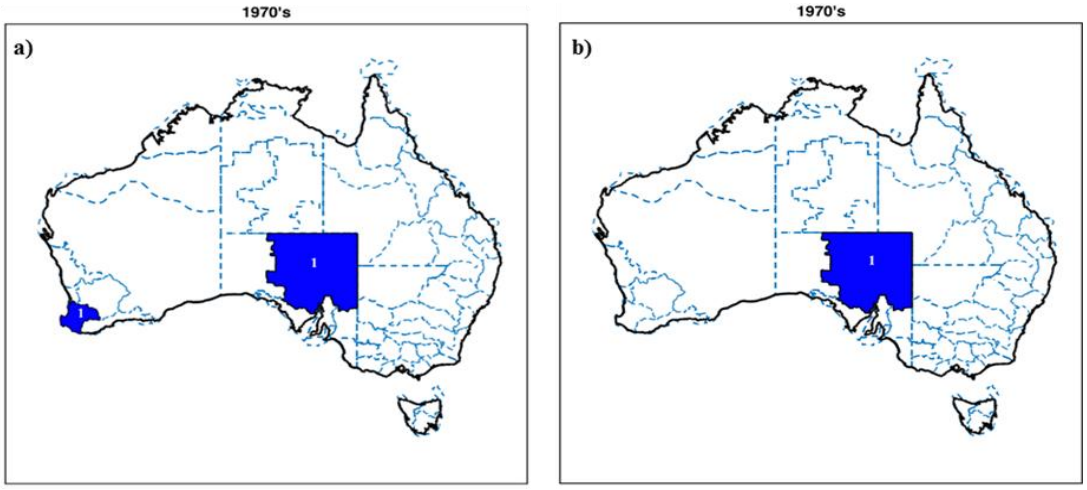

Figure 3.11: Decadal maps (1970 – 1979) showing NRM regions with a) the number of noted dust events, b) the number of documented dust events in dust source areas, and c) the difference from the long-term average rainfall (mm) and temperature (ºC) data for the dust source areas. Figure continues over next page.

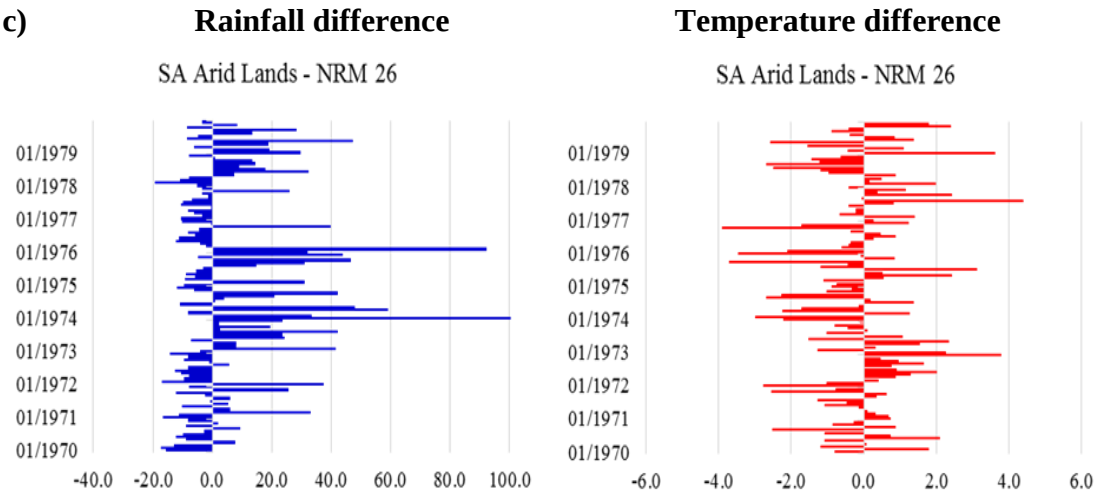

Figure 3.11: Decadal maps (1970 – 1979) showing NRM regions with a) the number of noted dust events, b) the number of documented dust events in dust source areas, and c) the difference from the long-term average rainfall (mm) and temperature (ºC) data for the dust source areas.

Table 3.24: The percentage of months when rainfall was below the long-term average in the NRM dust source regions during 1970 – 1979.

1970 - 1979	26
% of months below average Rainfall	58

Table 3.25: The percentage of months when temperatures were above the long-term average in the NRM dust source regions during 1970 – 1979.

1970 - 1979	26
% of months above average Temperature	47

The long period of above average rainfall in the previous decade had a 'protective' influence in terms of wind erosion potential for the 1980 – 1989 decade. Overall 11 dust storm events were documented in the HDED (Table 3.26) with Desert Channels (2), SA Arid Lands (2), Western (3) SA Murray Darling Basin (2) Murrumbidgee (1) and Mallee (1).

The decadal rainfall graphs in Figure 3.12 display the rainfall deficiency throughout the decade, in particular during the period from early 1980 to late 1982 and mid-1983 to mid-1986. The difference rainfall and temperature graphs (Figure 3.12) for the six NRM regions indicate that the occurrence of dust events were reduced due to increased vegetation cover in the previous years following above average rainfall and below

average temperatures. Overall, the six NRM regions received 57 – 64% of the months below long-term average rainfall (Table 3.27) and 47 – 58% above the long-term average temperatures (Table 3.28). The dust storm events in 1983 may be linked to the influence of the El Niño in 1982 – 1983 (Figure 3.3), when eastern Australia recorded very much below long-term average to lowest on record rainfall totals. The extreme dry conditions were replaced by flooding rain in March 1983 affecting central and southern Australia for several months. The second El Niño during 1987 – 1988 was the trigger for the dust storm events in 1987 and 1988.

Table 3.26: NRM wind erosion regions showing recorded dust events 1980 – 1989.

No	NRM Regions	1980	1981	1982	1983	1984	1985	1986	1987	1988	1989	Total
17	Desert Channel								2			**2**
26	SA Arid Lands								2			**2**
32	Western				1				2			**3**
43	SA Murray Darling Basin				1							**2**
46	Murrumbidgee								1			**1**
47	Mallee				1							**1**

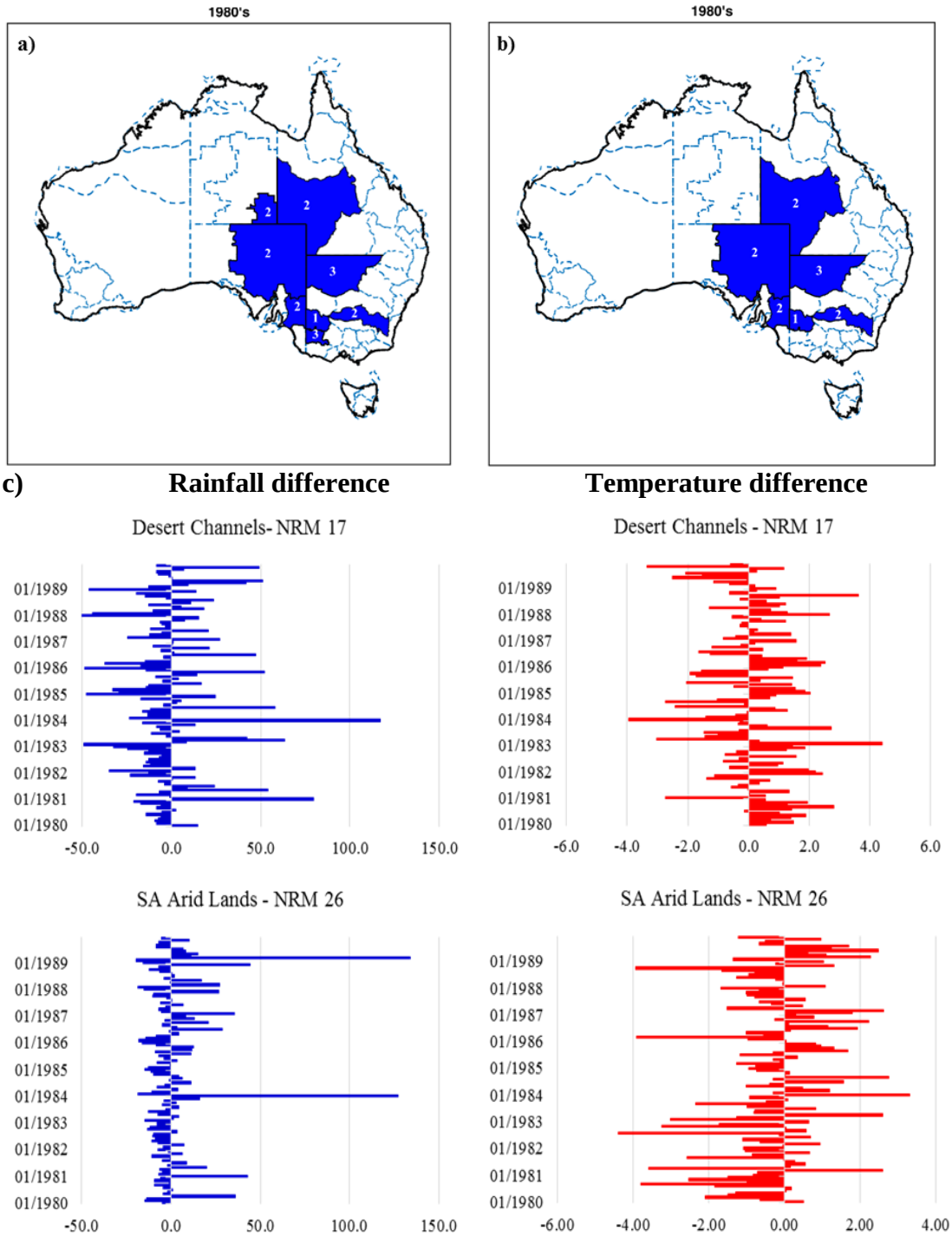

Figure 3.12: Decadal maps (1980 – 1989) showing NRM regions with a) the number of noted dust events, b) the number of documented dust events in dust source areas, and c) the difference from the long-term average rainfall (mm) and temperature (ºC) data for the dust source areas. Figure continues over next page.

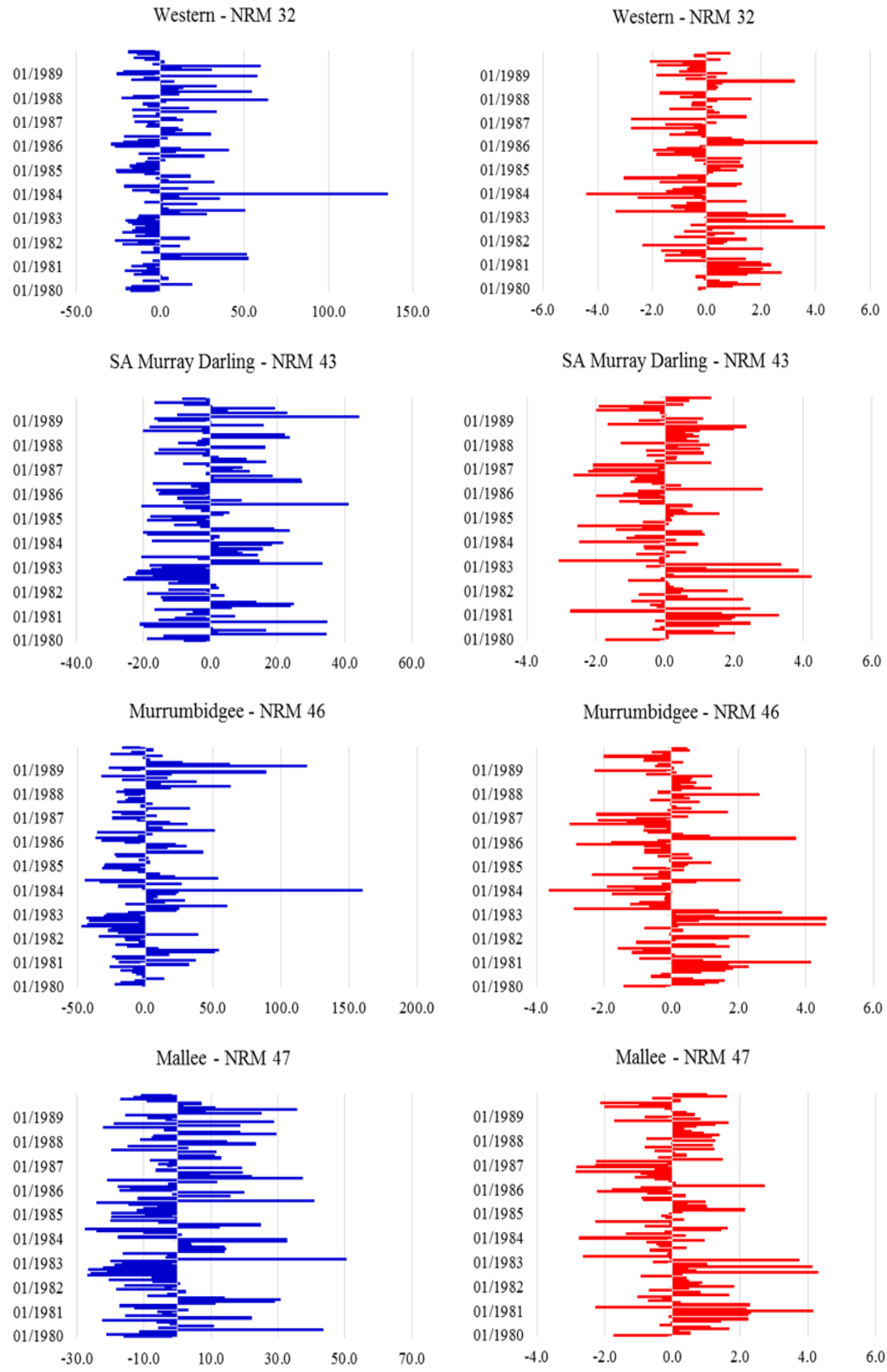

Figure 3.12: Decadal maps (1980 – 1989) showing NRM regions with a) the number of noted dust events, b) the number of documented dust events in dust source areas, and c) the difference from the long-term average rainfall (mm) and temperature (ºC) data for the dust source areas.

Table 3.27: The percentage of months when rainfall was below the long-term average in the NRM dust source regions during 1980 – 1989.

1980 – 1989	17	26	32	43	46	47
% of months below average Rainfall	64	64	58	58	57	61

Table 3.28: The percentage of months when temperatures were above the long-term average in the NRM dust source regions during 1980 – 1989.

1980 – 1989	17	26	32	43	46	47
% of months above average Temperature	56	42	47	53	51	52

The documented dust storm records in the HDED for the 1990 – 1999 decade indicate that 1994 was the only active dust storm year with 14 events in six NRM wind erosion regions. From the 24 – 25 May 1994, six events were documented and another eight between the 6 – 7 November 1994 (Table 3.29, Figure 3.13). SA Arid Lands region (4) had the highest number of events with all other regions reporting two each.

The decadal rainfall graphs for 1990 – 1999 (Figure 3.13) show that a number of NRM regions (Desert Channels, Western, Murrumbidgee) received well above long-term average rainfall in the first few months of 1990. Overall, rainfall fluctuated between above to below average throughout the decade. The temperature of the individual NRM regions followed the expected trend; when rainfall is above average, temperature is usually below. Over the entire decade, rainfall was below the long-term average between 54 – 60% of the months in the six NRM regions (Table 3.30). Temperatures varied between 47 – 64% above the long-term average (Table 3.31).

The sudden intensity of dust storm activity during May and November 1994 may be attributed to the El Niño episodes in the years leading up to 1994 (Figure 3.3). The first El Niño (1991 – 1992) had a strong influence on QLD and the northern part of NSW. A second longer El Niño followed in 1993 – 1995. Temperatures were for a large number of months up to 2 – 3 ºC above the long-term average (Figure 3.13). The influence of the consecutive El Niño events which were broken up with very short periods of above average rainfall in some areas, may explain the occurrence of dust storm events in 1994.

Table 3.29: NRM wind erosion regions showing recorded dust events 1990 – 1999.

No	NRM Regions	1990	1991	1992	1993	1994	1995	1996	1997	1998	1999	Total
17	Desert Channel					2						**2**
26	SA Arid Lands					4						**4**
32	Western Murray Darling Basin					2						**2**
43	SA Murray Darling Basin					2						**2**
46	Murrumbidgee					2						**2**
47	Mallee					2						**2**

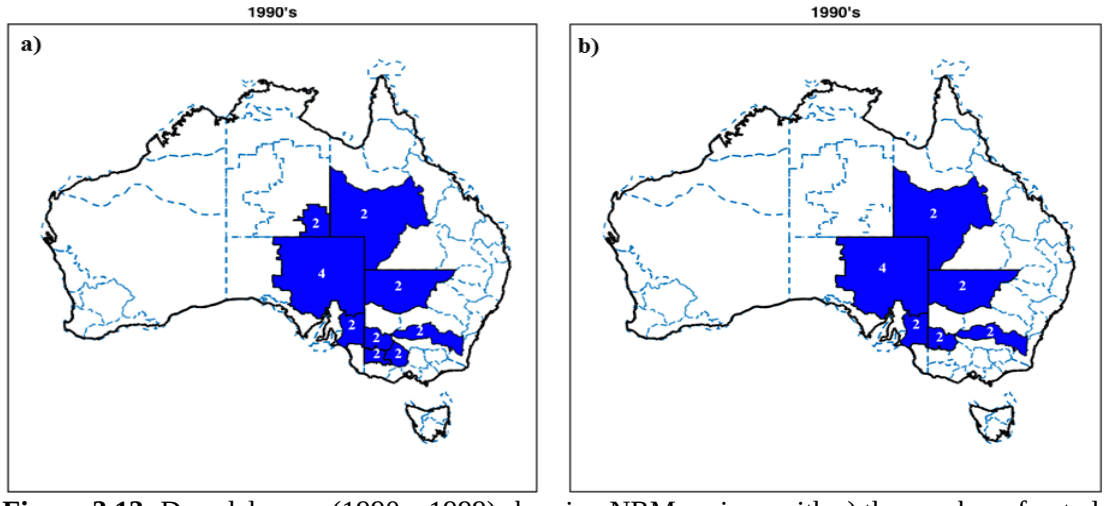

Figure 3.13: Decadal maps (1990 – 1999) showing NRM regions with a) the number of noted dust events, b) the number of documented dust events in dust source areas, and c) the difference from the long-term average rainfall (mm) and temperature (ºC) data for the dust source areas. Figure continues over next page.

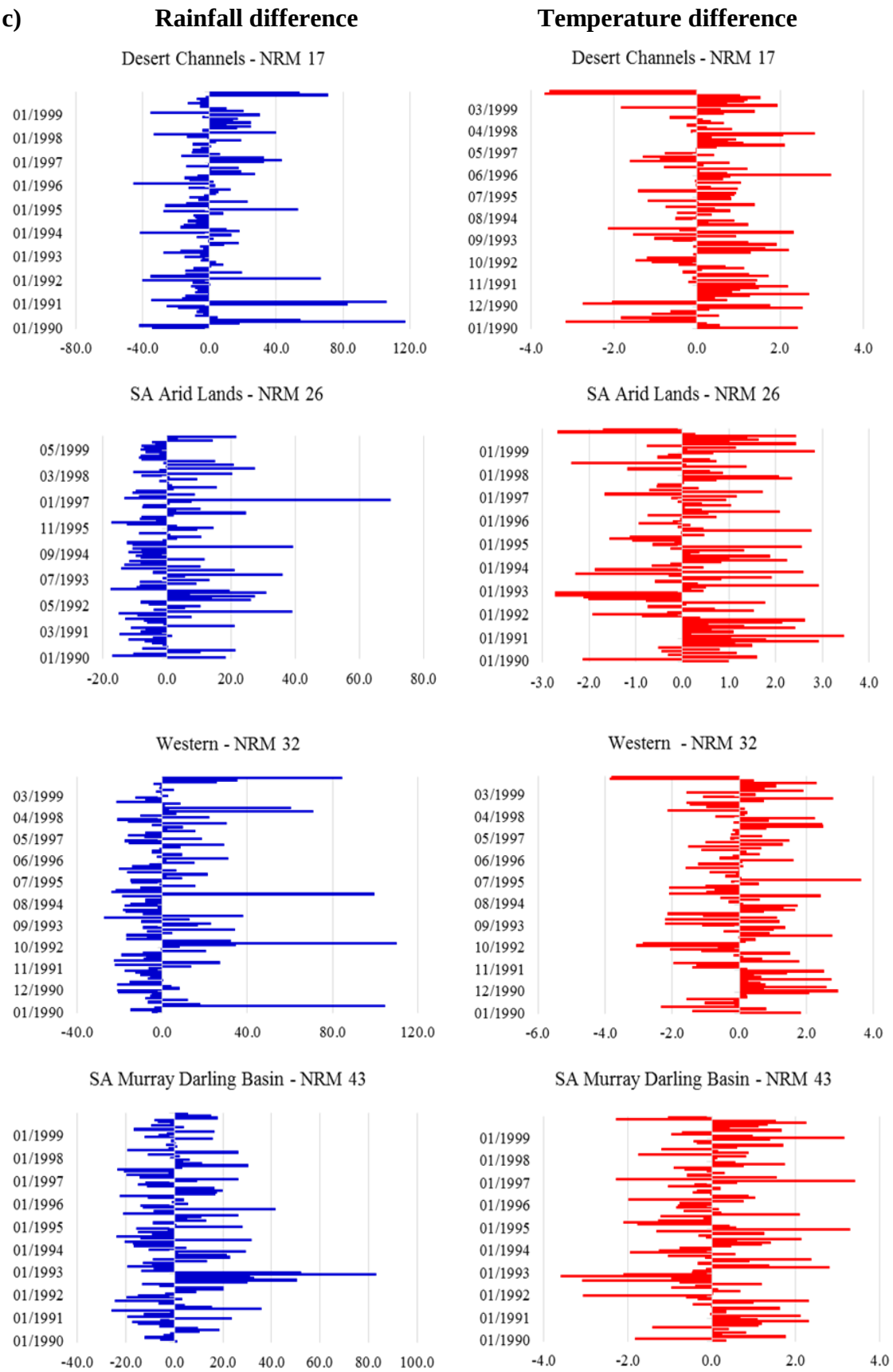

Figure 3.13: Decadal maps (1990 – 1999) showing NRM regions with a) the number of noted dust events, b) the number of documented dust events in dust source areas, and c) the difference from the long-term average rainfall (mm) and temperature (ºC) data for the dust source areas. Figure continues over next page

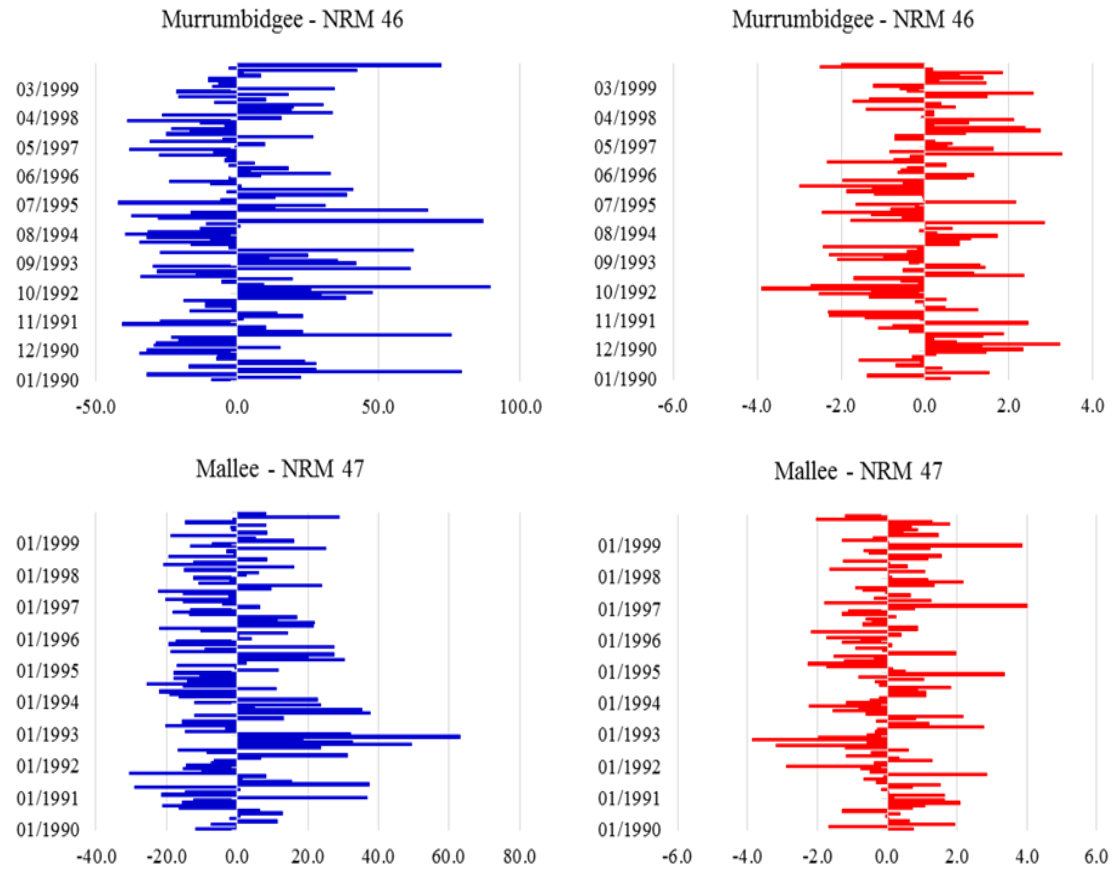

Figure 3.13: Decadal maps (1990 – 1999) showing NRM regions with a) the number of noted dust events, b) the number of documented dust events in dust source areas, and c) the difference from the long-term average rainfall (mm) and temperature (ºC) data for the dust source areas.

Table 3.30: The percentage of months when rainfall was below the long-term average in the NRM dust source regions during 1990 – 1999.

1990 - 1999	17	26	32	43	46	47
% of months below average Rainfall	59	57	60	54	55	57

Table 3.31: The percentage of months when temperatures were above the long-term average in the NRM dust source regions during 1990 – 1999.

1990 - 1999	17	26	32	43	46	47
% of months above average Temperature	64	63	54	54	47	49

The HDED for the 2000 – 2010 decade shows that eight out of the nine NRM regions which are susceptible to wind erosion, were experiencing a total of 150 dust storm events during the 11 years (Table 3.32, Figure 3.14). Nine events were recorded in 2002. In 2009 the dust storm season for this decade peaked with 83 additional events

followed by another 32 dust events in 2010. The Western (22), SA Arid Lands (19), Lower Murray Darling (16) and Desert Channels (10) NRM regions were particularly active in 2009 (Table 3.32). A slightly less active season followed in 2010 in SA Arid Lands (9), Western (7) and Lower Murray Darling (7).

The large numbers of dust storms were the result of the long lasting "Millennium Drought" starting in mid-1990s and ended mid-2010. The drought had a profound impact on southeast Australia with periods of well below long-term average rainfall and temperatures reaching between 2 – 4 ºC above the 103 year long-term average for many months during this decade. The severe rainfall deficiencies and higher than normal temperatures are displayed in Figure 3.14 and were the direct result of a number of El Niños in this decade and are briefly summarised here.

The first El Niño started in March 2002 – January 2003 (Figure 3.3) and virtually affected the entire continent. The situation was exacerbated due to several preceding years of dry conditions. The extreme dryness coincided with maximum temperatures reaching new levels in autumn, winter and spring. The onset of above to very much above average falls in February 2003 (Figure 3.14) provided a very short relief until the return of another El Niño in May 2006 – January 2007, influencing most parts of Australia. The situation improved with a return to more favourable conditions in January 2007 – February 2008 with the onset of a La Niña, affecting most areas except central to southeastern Australia. This period was followed by a second short La Niña in August 2008 – April 2009, with the greatest impact across northern Australia while the southeast experienced very much below average rainfall. The May 2009 – March 2010 El Niño was exceptionally dry over much of the continent resulting in the very severe "Red Dawn" dust storm on the 22nd – 25th October 2009 which made world headlines.

The 2000 decade reported temperatures well above the long-term average (Figure 3.14) and the trend appears to continue into the next decade with recent reports of February and March 2016 temperatures exceeding very much above average and highest on record mean daily minimum temperatures across all States and Territories (Bureau of Meteorology 2016). During 2000 – 2010, the eight NRM regions experienced between 51 – 62% of the time rainfall below the long-term average (Table

3.33) and between 68 – 79% of the time temperatures were above the long-term average (Table 3.34).

The drought conditions which produced well below average rainfalls and above average temperatures for most of the decade resulting in a large dieback of vegetation cover and therefore increased the potential for wind erosion activity. The effect is particular noticeable in 2009 with 83 reported dust events (Table 3.32). The results show that the collated records in the HDED reflect the quantitative climate data for this period.

Table 3.32: NRM wind erosion regions showing recorded dust events 2000 – 2010.

No	NRM Regions	2000	2001	2002	2003	2004	2005	2006	2007	2008	2009	2010	Total
13	NT Arid Centre							1	2	1	1		**5**
17	Desert Channels			3			2	2	2	1	10	1	**21**
26	SA Arid Lands			3	1	1	2	2	2	1	19	9	**40**
32	Western			3			2	2		1	22	7	**37**
40	Lower Murray Darling				1						16	7	**24**
42	Lachlan										7	3	**10**
46	Murrumbidgee										5	2	**7**
47	Mallee										3	3	**6**

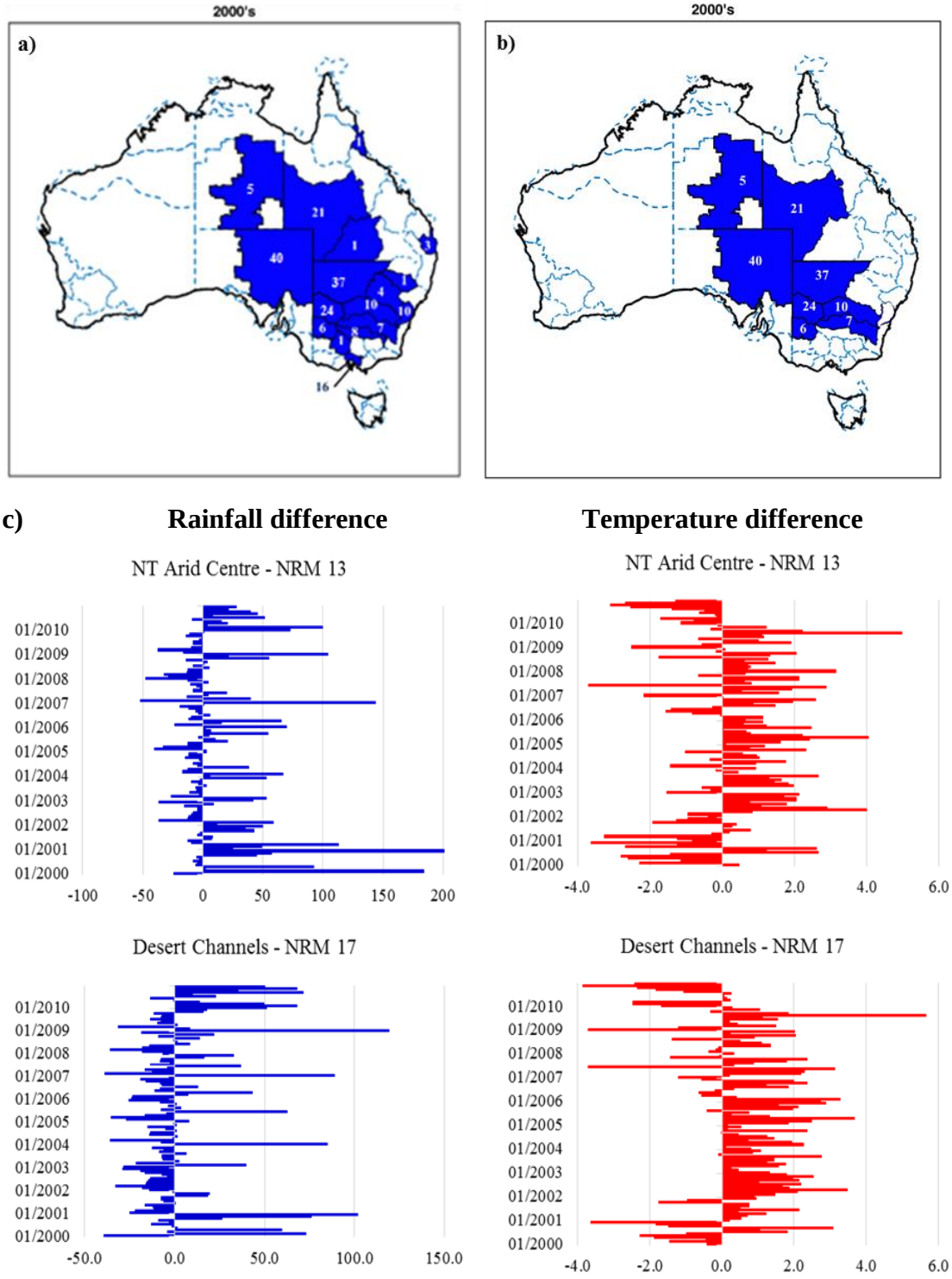

Figure 3.14: Decadal maps (2000 – 2010) showing NRM regions with a) the number of noted dust events, b) the number of documented dust events in dust source areas, and c) the difference from the long-term average rainfall (mm) and temperature (ºC) data for the dust source areas. Figure continues over next page.

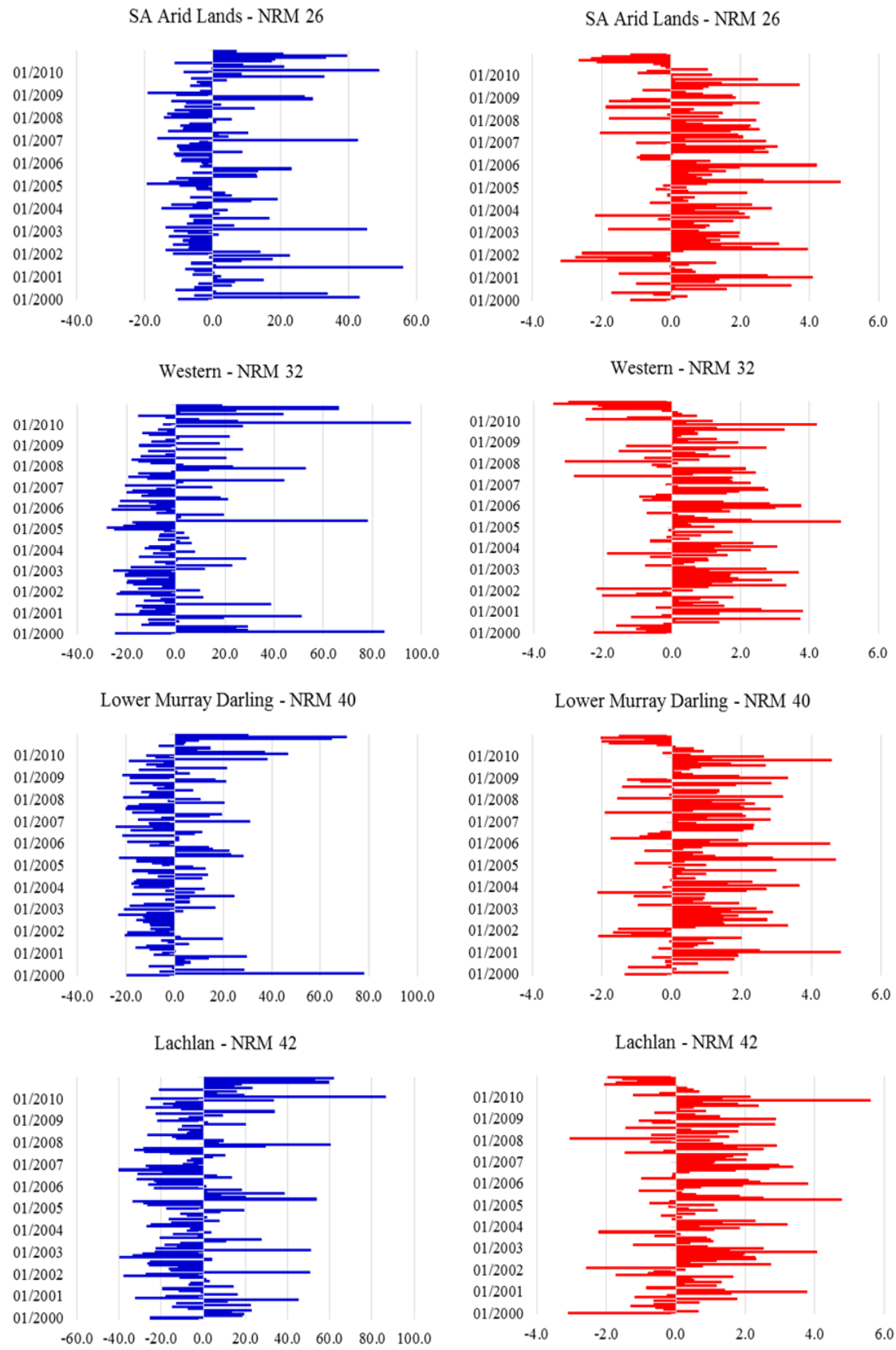

Figure 3.14: Decadal maps (2000 – 2010) showing NRM regions with a) the number of noted dust events, b) the number of documented dust events in dust source areas, and c) the difference from the long-term average rainfall (mm) and temperature (ºC) data for the dust source areas. Figure continues over next page.

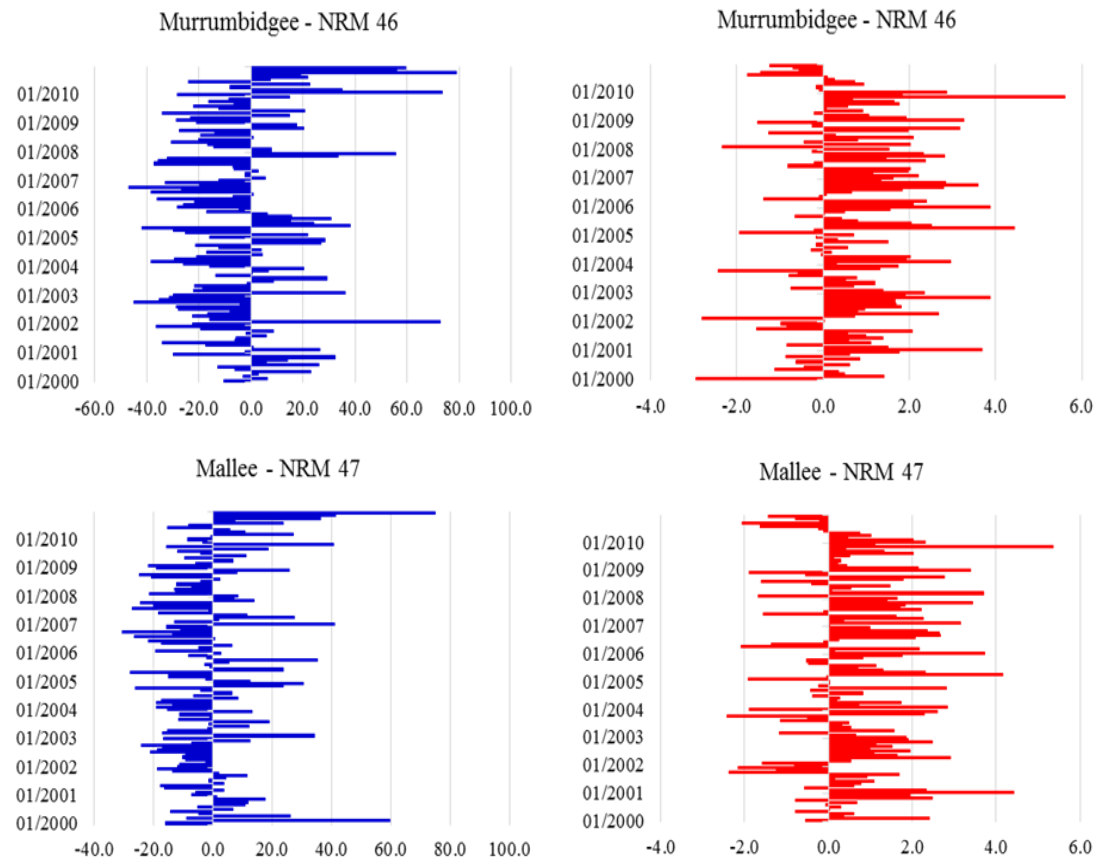

Figure 3.14: Decadal maps (2000 – 2010) showing NRM regions with a) the number of noted dust events, b) the number of documented dust events in dust source areas, and c) the difference from the long-term average rainfall (mm) and temperature (ºC) data for the dust source areas.

Table 3.33: The percentage of months when rainfall was below the long-term average in the NRM dust source regions during 2000 – 2010.

2000 - 2010	**13**	**17**	**26**	**32**	**40**	**42**	**46**	**47**
% of months below average Rainfall	51	62	56	59	55	58	58	58

Table 3.34: The percentage of months when temperatures were above the long-term average in the NRM dust source regions during 2000 – 2010.

2000 - 2010	**13**	**17**	**26**	**32**	**40**	**42**	**46**	**47**
% of months above average Temperature	68	79	78	77	79	76	78	78

The decadal rainfall and temperature history data as outlined in this Section indicates that the occurrence of dust storms and wind erosion events are closely linked to climatic conditions. In turn climate directly impacts on vegetation cover which is one of the key factors driving the frequency, intensity and spatial distribution of dust

events. The anecdotal dust event history database (HDED), covering more than 100 years, describes the spatial and temporal distribution of wind erosion events but the data does not provide any information of the degree of vegetation cover which protects the soil surface from wind erosion.

Chapter 4: Climate Aridity Vegetation Index

Vegetation cover is a key factor influencing the frequency, intensity and spatial distribution of wind erosion events (Shao 2008). In Section 3.2 it was shown that there is a strong link between wind erosion activity and climatic conditions. This chapter details the development of a new vegetation index as outlined in objectives two and three in Section 1.6. Section 4.1 outlines the rationale for the development of the Climate Aridity Vegetation Index (*CAVI*). Section 4.2 focuses on the development of a simple broad scale *CAVI* for Australia, based on rainfall and temperature data. To test the accuracy of the index a statistical comparison between *CAVI* and fractional cover data is provided in Section 4.3. The results are discussed in Section 4.4 and Section 4.5 investigates if reliable spatial and temporal vegetation cover maps can be produced based on the *CAVI* without modelling individual vegetation type responses, seasonality and land-use.

Vegetation cover information can currently be estimated via satellite remote sensing data or vegetation-type modelling methods which also rely, to a large extent, on satellite data. The availability of remote sensing information is a fairly recent technology. For periods prior to the 1990, when no satellite records are available, there is currently no simple, broadly applicable modelling method or index to produce good representative estimates and spatial maps of vegetation cover levels during the spring – summer seasons in Australia. This includes any historical periods and any future forecasting. Vegetation cover information is useful in a wide range of applications and is of particular interest and value in areas of environmental, ecological and land-use modelling. Without remote sensed vegetation cover estimates (Malthus et al. 2013), integrated wind erosion modelling systems (Shao et al. 2007) cannot confidently be used to estimate wind erosion rates.

4.1 Rational for the development of the Climate Aridity Vegetation Index

Satellite remote sensing data captures the combined effect of both climate and land management practices and records any alive or dead vegetation cover as viewed vertically from above. It can be used to estimate fractional vegetation cover, which

divides cover into three components: green or photosynthetic vegetation (f_{PV}), non-photosynthetic vegetation or stubble, senescent herbage, leaf litter and wood (f_{NPV}) and bare soil/rock (f_{BS}). Areas that have been burnt resulting in ash/blackened soil are considered as a bare soil cover type. The relationship between the three components is $f_{PV} + f_{NPV} + f_{BS} = 1$ (Guerschman et al. 2009).

As mentioned previously (Section 1.4) reliable satellite remote sensing data only became available in 1992, whereas the Australian Bureau of Meteorology (ABoM) started monitoring meteorological conditions across Australia in 1910. Gridded rainfall and temperature data are readily available from this time onwards. Rainfall (precipitation) and temperature (evaporation) provide an indication of soil moisture potentially available for plant growth. The Climate Aridity Vegetation Index (*CAVI*) developed in this research and discussed in this Chapter, is based on freely available rainfall and temperature data, and aims to predict broad-scale spatial variation in vegetation cover. Although the performance of the *CAVI* has been tested Australia wide and across all seasons (Pudmenzky, King & Butler 2015), the main area of interest and focus is on the performance within the typical wind erosion season through Spring and Summer (September to February) in arid to semi-arid areas were the landscape is most prone to wind erosion and dust transportation events (McTainsh & Boughton 1993; Strong et al. 2011).

Fractional cover values derived from remote sensing data were used to validate the *CAVI* estimates. Although lateral (standing) vegetation cover would be preferred for wind erosion since vegetation height has an influence on the wind velocity profile (roughness height), shown in Figure 4.1 (Chepil & Woodruff 1963), currently there is no reliable, long-term records of lateral cover available (Chappell 2013). Fractional cover data was chosen over the Normalized Difference Vegetation Index (NDVI) (which is a measure of the greenness of vegetation and is also derived from spectrographic data) as it has been more extensively ground-truthed in Australia. Fractional cover data is used in climate and ecological research including regional and global carbon modelling, ecological assessment, agricultural monitoring and wind erosion research conducted by Australian Bureau of Agricultural and Resource Economics and Sciences (ABARES) (Guerschman et al. 2012), Shao et al. (2007) and DustWatch (Gill, Heidenreich & Guerschman 2014).

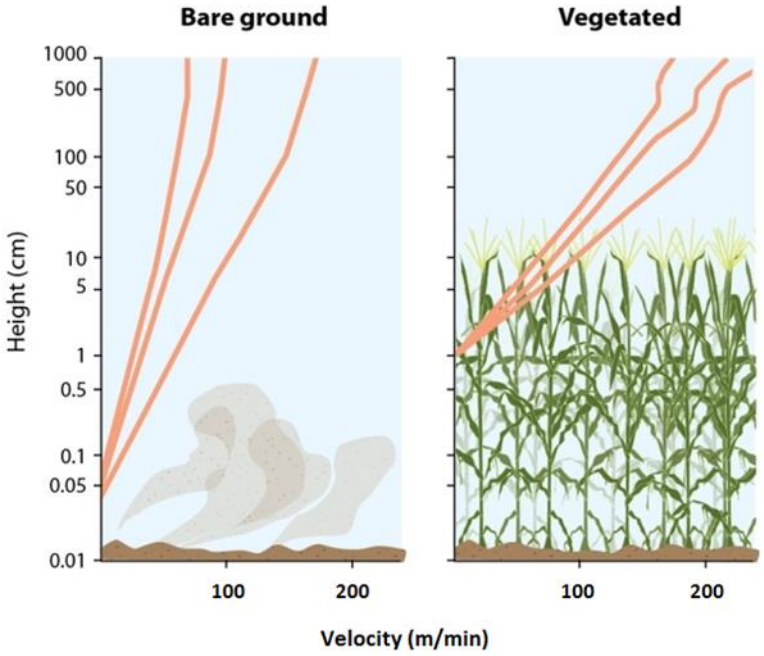

Figure 4.1: Wind velocity profile and roughness height in the absence/presence of vegetation. Modified from Chepil and Woodruff (1963).

Monthly remote sensed fractional cover data for both the photosynthetically active vegetation (green) fraction (f_{PV}) and the bare soil fraction (f_{BS}) (Guerschman et al. 2009) were used to validate the performance of the *CAVI* in this study. The potential for wind erosion can be mitigated by total cover (f_{TC}) where $f_{TC} = f_{PV} + f_{NPV} = 1 - f_{BS}$. Since f_{PV} is more dynamically responsive to changes in rainfall and temperature than f_{NPV}, it therefore has the potential to be more strongly related to the *CAVI*. As the f_{BS} indicates a soil surface without any vegetation cover and therefore highly susceptible to wind erosion, the f_{PV} and f_{BS} estimates represent the two extremes in the remote sensing colour spectrum and were used to help identify the fraction to which the *CAVI* is most closely correlated.

4.2 Climate Aridity Vegetation Index Development

The development of the *CAVI* is based on the De Martonne (1926) Aridity Index (AI). The AI is defined as a ratio of rainfall (mm) and corrected temperature (°C + 10) for temperatures greater than -9.9 °C for the target month. For months where there is no rainfall within a given month, this index fails (returns a zero value). As more than 78% of the Australian continent is classified as arid to semi-arid (Figure 1.3) many months

record zero rainfall and the AI generally performs unsatisfactorily. The AI provides a history snapshot but it does not give any details of how severe the dry period is. The longer the dry period, the less the cover. However, its simplicity and reliance on only rainfall and temperature data provided a template for development of an index appropriate to Australian conditions.

In arid to semi-arid zones vegetation has evolved to survive long periods without rainfall. Consequently, vegetation cover is generally influenced by rainfall and temperature over several months leading up to the target month, rather than the rainfall and temperature of the target month itself (Klein & Roehrig 2006; Donohue, McVicar & Roderick 2009). Rainfall of the previous 12 months has an impact on soil moisture and vegetation. Therefore, the *CAVI* for a target month was developed to incorporate the preceding 12 months weighted rainfall and temperature to allow for a lag time between the occurrence of climatic conditions and an observable vegetation response. For example, the *CAVI* for July 2012 would be based on rainfall and temperature data from July 2011 (lowest weighting) to June 2012 (highest weighting). The *CAVI* is defined as follows:

$$CAVI_m = \frac{\sum_{i=1}^{12} w_i \left(\frac{P_i}{T_i + 10} \right)}{12} \quad , \tag{1}$$

where P_i is the total monthly rainfall (mm); T_i is the mean monthly maximum temperature (ºC); m is the target month; i is the i^{th} contributing month preceding m; and the weighting w_i is determined by:

$$w_i = \frac{(13 - i) \cdot w_f}{12} \quad , \tag{2}$$

where w_f is an additional weighting factor that influences the rate of change w_i for each contributing month.

When $w_f = 1$ the weighting w_i decreases by a factor of 12 for each month preceding the target month. This acts to reduce the influence of rainfall and temperature in months most distant from the target month. When $w_f < 1$ the weighting w_i (i.e. the influence of rainfall and temperature) decreases more quickly across the preceding 12 months. Initially, the w_f value was set to 1 and the performance of the *CAVI* assessed.

As these results showed potential, alternate values of w_f were also investigated. The *CAVI* was calculated based on Equation (1) for all months from February 2000 to December 2012, for every grid point across the spatial domain of 110.00 to 155.00º E and -10.00 to -45.00º N and a spatial resolution of 5 km.

The *CAVI* calculated in this way has no natural upper boundary. The maximum *CAVI* value recorded was 8.5. However, comparison of the *CAVI* values to remote sensed f_{PV} showed that a *CAVI* of 1.5 was indicative of 100% green vegetation cover. Hence, the *CAVI* was restricted as follows:

$$CAVI = \begin{cases} CAVI, & \text{if } CAVI < 1.5, \\ 1.5, & \text{if } CAVI \geq 1.5. \end{cases} \quad (3)$$

To enable direct comparison of the *CAVI* estimates with f_{PV} and f_{BS} percent values, the *CAVI* was then rescaled so that a maximum value of 1 was assumed as equivalent to 100% green cover. The *CAVI*, in this simple form, includes no corrections for individual vegetation types, seasonality or land use (e.g. clearing, overgrazing).

4.3 Statistical comparison

A random selection of 1 500 grid points from the spatial domain was extracted from the f_{PV}, f_{BS} and *CAVI* grids. A linear regression analysis was performed to examine the relationship between the extracted remote sensed values and the *CAVI* values. The R^2 (coefficient of determination) was used to estimate the percentage variation in f_{PV} or f_{BS} values explained by the *CAVI* for all months between February 2000 and December 2012. A strong relationship between *CAVI* estimates and remote sensed data indicated that the *CAVI* was successfully reproducing remote sensed ground cover. The results indicated that there was a stronger relationship between f_{PV} values explained by the *CAVI* than there was for the f_{BS} values (Figure 4.2). The *CAVI* predictions always performed better during the Spring and Summer months (September – February) within each year. Two exception to this were January 2002 & February 2003 and are marked with red ovals in Figure 4.2. Various reasons for this will be discussed further in Section 4.5.4. Based on these results further evaluation of the *CAVI* performance focused on the relationship between green fraction vegetation cover (f_{PV}) and the *CAVI* estimates. The results for three exemplar months (November 2002, November 2005

and November 2009) are presented to demonstrate the overall performance. The month of November was selected as it falls within the spring-summer seasons when wind erosion events are most likely to occur. The three years, 2002, 2005 and 2009 were chosen as they provide examples of the *CAVI* performance under very different climatic conditions in the 12 months preceding the target month. The underperformance of the *CAVI* in some of the months within the wind erosion season (September – February) was also investigated.

The percentage of grid points where the absolute difference between f_{PV} and the *CAVI* values, $\left(\left| f_{PV} - CAVI \right|\right)$, was within 0.1 was calculated (Note: that this is not a 0.1 interval around the regression line). Points outside this interval were considered noteworthy over- or under-estimations of vegetation cover and were further explored. A 0.1 interval represents a maximum 10% over- or under-estimation in green fraction vegetation cover by the *CAVI* and was considered to be a tolerable difference.

4.4 Results

The overall performance of the *CAVI* as a predictor of vegetation cover was evaluated by graphing the R^2 value derived from each regression analysis for all months between February 2000 and December 2012. The results indicated that 0.9 was the best performing weighting factor and will be discussed later in this Section. The plot of R^2 values based on the *CAVI* estimates using w_f = 0.9 and all grid points is shown in Figure 4.2. Across the 155 months (February 2000 – December 2012) a similar pattern of performance was seen for the *CAVI*:f_{PV} and the *CAVI*:f_{BS} comparisons. The *CAVI* predictions always performed better during the Spring to Summer months (September – February) within each year, and during these months the *CAVI* consistently showed a stronger relationship with f_{PV} than with f_{BS}. The *CAVI*:f_{PV} R^2 values during the summer months were generally greater than 0.7 and as high as 0.81 in 2008 indicating that the *CAVI* explained approximately 70 – 81% of the variability in green vegetation cover (f_{PV}) observed across the continent. The greater overall variance in the *CAVI*:f_{PV} relationship (greater range in R^2 values) also meant that during periods when the *CAVI* underperformed it tended to have a weaker relationship with f_{PV} than with f_{BS} but this only occurred on a few occasions and outside the wind erosion season. As particular interest was in the September – February period when wind erosion is most prevalent

in arid to semi-arid regions, further results presented here focus on the *CAVI*:f_{PV} relationship. The performance of *CAVI* during the 2010/2011 extreme flood event is also considered.

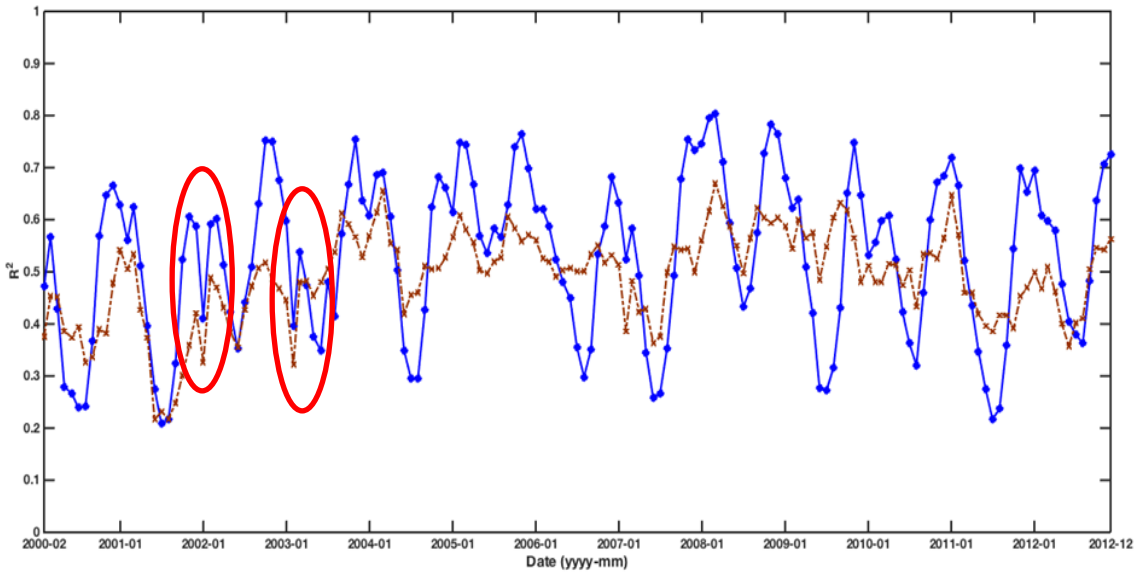

Figure 4.2: R^2 values for f_{PV} (blue '*' symbol and solid line) and f_{BS} (brown 'x' symbol and dashed line) with *CAVI* weighting w_f = 0.9 for all months from February 2000 – December 2012. (Pudmenzky, King & Butler 2015)

Table 4.1 summarises the effect of changing the *CAVI* weighting factor (w_f) from 1 to 0.9 on the R^2 values and on the percentage of points under- and over-estimating the f_{PV} for the three exemplar months within a typical wind erosion season: November 2002, November 2005 and November 2009.

When w_f = 1, the R^2 values ranged from 0.73 to 0.78 for all grid points and from 0.84 to 0.90 within the $\left|f_{PV} - CAVI\right| \leq 0.1$ interval. The number of grid points that met the $\left|f_{PV} - CAVI\right| \leq 0.1$ interval criterion was promising in November 2002 (78.9%), but less promising in November 2005 (45.5%) and 2009 (52.5%). In all exemplar months, the percentage of grid points over-estimating vegetation cover far exceeded the percentage under-estimating.

When the w_f = 0.9 weighting was applied, the R^2 values for all grid points and for grid points within the $\left|f_{PV} - CAVI\right| \leq 0.1$ interval remained similar to those found when applying a weighting of w_f = 1. However, the percentage of points falling within the 0.1 interval increased, ranging from 55.9 – 81.5% (Table 4.1). The percentage of over-

estimated points decreased notably compared to the $w_f = 1$ results, while the percentage of under-estimated points only slightly increased. In November 2005, the worst performing exemplar month, the change in the w_f resulted in a greater percentage of points falling within the 0.1 interval (55.9%) than outside it (44.1%).

Table 4.1: Summary of results for November exemplar months with w_f = 1 and w_f = 0.9. (Pudmenzky, King & Butler 2015)

Date	w_f	*N* Points	R^2 of all Points	Interval: $\lvert f_{PV} - CAVI \rvert \leq 0.1$			
				% Points	R^2	% Points Over-estimated	% Points Under-estimated
2002	1.0	1150	0.7463	78.9	0.8417	17.3	3.8
2002	0.9	1150	0.7381	81.5	0.8400	12.7	5.8
2005	1.0	1146	0.7768	45.5	0.9040	52.4	2.1
2005	0.9	1146	0.7705	55.9	0.9117	40.7	3.4
2009	1.0	1149	0.7293	52.5	0.9008	46.0	1.5
2009	0.9	1149	0.7344	60.0	0.8959	37.9	2.2

The effect of changing the *CAVI* weighting factor to w_f values of 0.8 and 0.7 were also tested and results are shown in Table 4.2. When the w_f = 0.8 and 0.7 weighting was applied, the R^2 values for all grid points and for grid points within the $\left| f_{PV} - CAVI \right| \leq 0.1$ interval remained similar to those found when applying a weighting of w_f = 1 and 0.9. However, the percentage of points falling within the 0.1 interval increased, ranging from 66.0 – 84.8%. The percentage of over-estimated points decreased compared to the $w_f = 1$ and 0.9 results, while the percentage of under-estimated points increased. Results of the analysis based on alternative w_f values of 0.8 and 0.7 continued to decrease the number of over-estimating grid points, however the number of under-estimating points increased substantially, outweighing any advantage. For example, in November 2009, the worst performing exemplar month, the change in the w_f resulted in a decrease percentage of over-estimated points from 30.4 – 4.9% but the number of under-estimating points increased substantially from 3.7 – 22.0%. Further analysis presented focuses on w_f = 0.9 weighting.

Table 4.2: Summary of results for November exemplar months with w_f = 0.8 and w_f = 0.7.

Date	w_f	*N* Points	R^2 of all Points	Interval: $\lvert f_{PV} - CAVI \rvert \leq 0.1$			
				% Points	R^2	% Points Over-estimated	% Points Under-estimated
2002	0.8	1150	0.7270	83.6	0.8366	8.3	8.1
2002	0.7	1150	0.7148	84.8	0.8017	10.6	4.6
2005	0.8	1146	0.7586	66.5	0.9010	27.9	5.6
2005	0.7	1146	0.7429	71.9	0.8698	9.6	18.5
2009	0.8	1149	0.7344	66.0	0.8873	30.4	3.7

2009	0.7	1149	0.7293	73.0	0.8679	4.9	22.0

A visual comparison of the *CAVI* (w_f = 0.9) based vegetation coverage maps and those based on satellite remote sensed f_{PV} can be seen in Figure 4.3. These maps indicate that the *CAVI* predictions broadly reflect the same spatial changes in the colour spectrum as suggested by the f_{PV} vegetation cover maps.

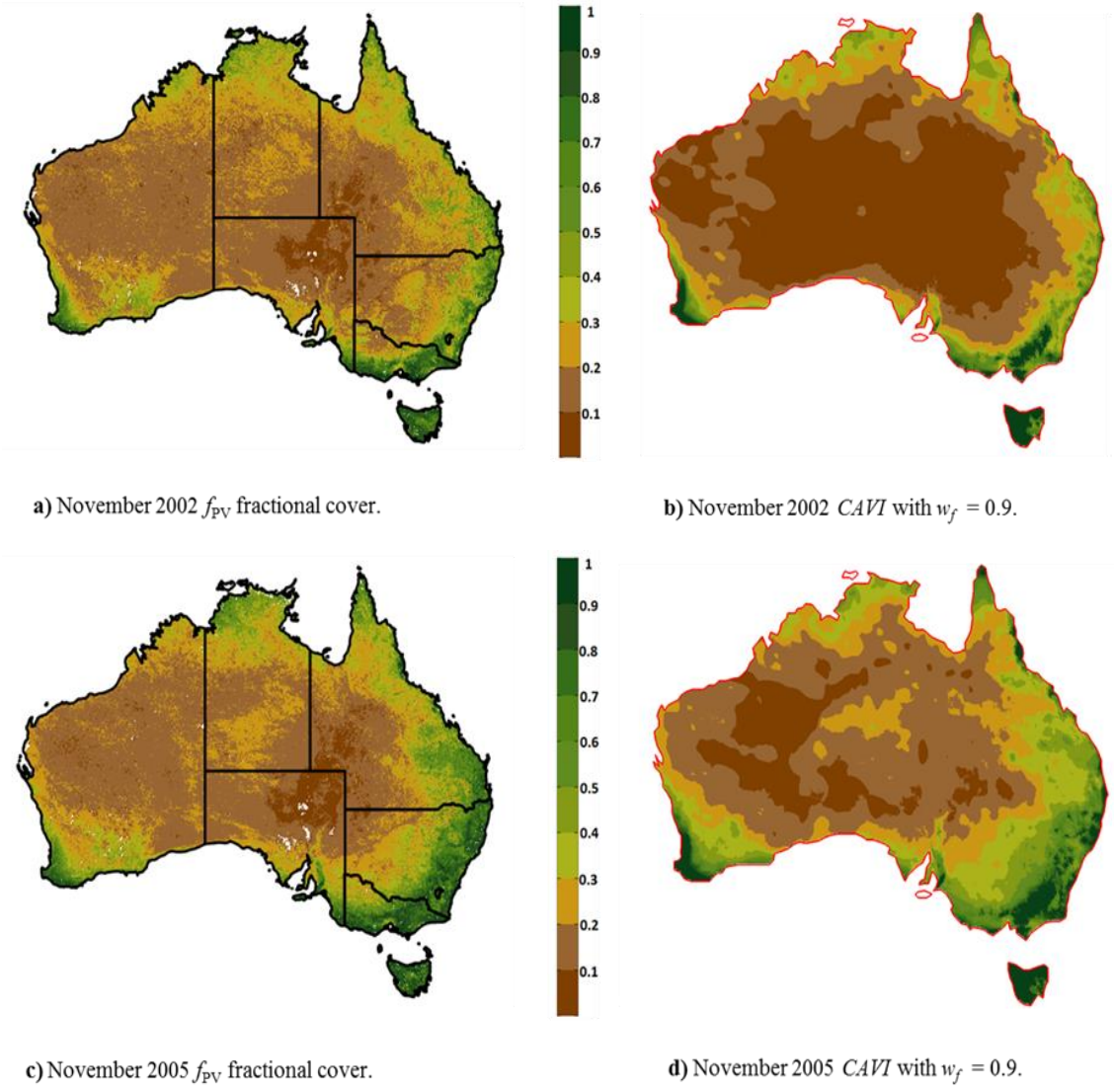

a) November 2002 f_{PV} fractional cover.

b) November 2002 *CAVI* with w_f = 0.9.

c) November 2005 f_{PV} fractional cover.

d) November 2005 *CAVI* with w_f = 0.9.

Figure 4.3: Comparison between fractional cover f_{PV} maps (a, c, e) and the *CAVI* (b, d, f) with w_f = 0.9 maps. (Pudmenzky, King & Butler 2015). Figure continues over next page.

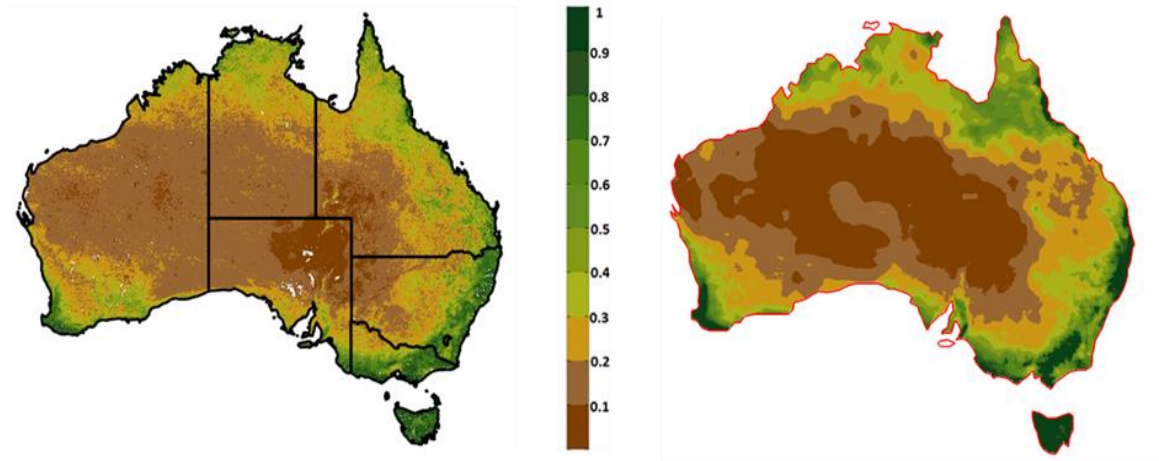

e) November 2009 f_{PV} fractional cover.

f) November 2009 *CAVI* with $w_f = 0.9$.

Figure 4.4: Comparison between fractional cover f_{PV} maps (a, c, e) and the *CAVI* (b, d, f) with $w_f = 0.9$ maps. (Pudmenzky, King & Butler 2015)

Figure 4.4 illustrates the relationship between f_{PV} and the *CAVI* values for all grid points falling under, within and over the 0.1 interval. The slope of the regression lines for all grid points in Figures 4.4a, Figure 4.4c and Figure 4.4e ranged from 0.68 – 0.82. A slope of 1 would indicate a direct mapping of the *CAVI* to the f_{PV}. Values of less than 1 reflect the general tendency of the *CAVI* to overestimate vegetation cover when compared to f_{PV} estimates. Figures 4.4b, Figure 4.4d and Figure 4.4f display the spatial distribution of grid points and highlight that under and over estimations by the *CAVI* mostly occurred in coastal areas or areas outside the arid to semi-arid zone.

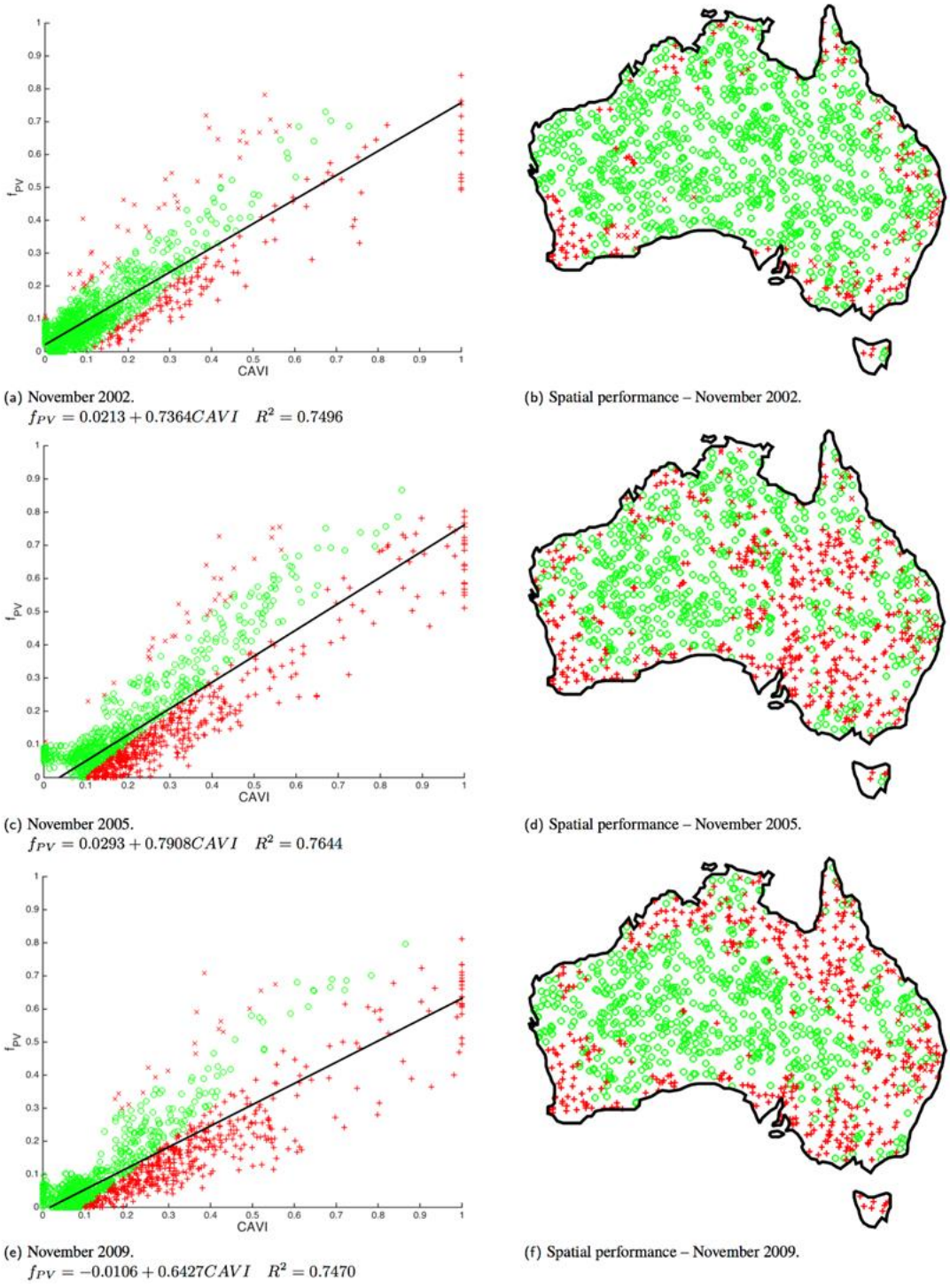

Figure 4.5: Regression analyses (a, c and e) showing the relationship between f_{PV} and *CAVI* (w_f = 0.9) and corresponding *CAVI* spatial performance maps (b, d and f). On all figures, points within the 0.10 interval are shown with a green 'o', grid points over-estimating vegetation cover (below the interval) are shown with a red '+' and grid points under-estimating vegetation cover (above the interval) are shown with red 'x'. (Pudmenzky, King & Butler 2015)

January 2002 and February 2003 were the only months within the wind erosion session (September – February) were the *CAVI* did not perform as well as expected (Figure 4.2). These months will be discussed in more detail in Section 4.5.4.

4.5 Seasonal and regional performance of the *CAVI*

Between 1997 and 2009 Australia was in the grip of the "Millennium drought", with below average rainfall for south-eastern Australia (South Eastern Australian Climate Initiative 2011). Areas of north-western NSW, south western QLD and north-eastern SA were particularly affected. Similar drought events are not uncommon in Australia and have been well documented in historical accounts since early settlement (Nicholls 1988).

The overall performance of the *CAVI* was very promising, particularly in arid to semi-arid regions during the Spring to Summer wind erosion season. The *CAVI* estimates were used to create vegetation cover maps which accurately reproduced broad scale colour/vegetation cover changes seen in f_{PV} maps such as those shown in Figure 4.2. However, the *CAVI* as currently specified was found to exhibit some temporal and spatial variability in its performance and utility. Two main factors have been considered when interpreting the *CAVI* performance: the effect of seasonality (time of year of the target and/or contributing months) and the effect of regionality (location of the target grid point). Both seasonality and regionality directly influence rainfall and temperature which in-turn affect vegetation growth and levels of cover.

The *CAVI* showed a general tendency to overestimate green vegetation cover (f_{PV}) (Table 4.1 and Figure 4.2), particularly in those regions outside the arid to semi-arid zone that receive more regular rainfall. The *CAVI*:f_{PV} relationship was consistently stronger (higher R^2 values) during the Spring to Summer (September to February) seasons when most plant growth occurs, and a consistently weaker (lower R^2 values) during Autumn and Winter (March to August) seasons (Figure 4.2).

These results indicate that the inclusion of the preceding 12 months rainfall and temperature data for the calculation of any target month the *CAVI* is, as hoped, effectively overcoming the problems encountered by the original AI (De Martonne 1926) in areas where rainfall is generally low and infrequent i.e. within arid and semi-

arid zones. However, where the AI had no lower threshold (and incorrectly estimated no vegetation cover if there were no rainfall in the single target month), the *CAVI* is currently assuming no upper threshold and is over-emphasising the influence of regular rainfall in the preceding 12 months. Over-estimation for many grid points was reduced when the weighting factor w_f was set to $w_f = 0.9$ which more quickly reduced the contribution of each subsequent contributing month over the preceding 12 months (as shown for the three exemplar months in Table 4.1). This blanket approach, in effect, reduced the total amount of rainfall included in the calculation of the *CAVI* regardless of the season of the target month or the region of the target grid point. However, further reductions in the value of w_f led to an undesired counter increase in the number of grid-points under–estimating vegetation cover (Table 4.2) and therefore this would be an ineffective method of further moderating the influence of rainfall in the *CAVI* calculation.

Three November months in 2002, 2005 and 2009 were specifically chosen as exemplar months based on their differing climatic conditions across the spatial domain during the 12 months leading up to the target month. These differences may help to explain the current variability in the performance of the *CAVI* and suggest future work needed to improve the index while retaining its minimalist data requirements for calculation and broad scale applicability.

4.5.1 November 2002

Of the three exemplar months the *CAVI* generally performed best for November 2002. The R^2 value between f_{PV} and the *CAVI* grid points was 0.74 and approximately 82% of all grid points were within the 0.1 interval. Only 13% of grid points over-estimated and 6% under-estimated vegetation cover (Table 4.1; Figure 4.4a). The promising performance of the *CAVI* in this month may be driven by the low variability in rainfall that occurred during the 12 months of data included in the index calculations.

Throughout 2002 – 2003, a weak to moderate El Niño developed and six months prior to November 2002 most of the continent was extremely dry with ‘very much below average’ rainfall (as defined by the ABoM) for most of QLD, NSW, VIC, north-eastern SA and parts of WA. These conditions occurred directly following several years of dry conditions. For a more detailed discussion see Section 3.2. This extreme dryness coincided with exceptionally warm conditions with maximum temperatures reaching

new records for the Autumn, Winter and Spring season, March – November (Bureau of Meteorology 2014). As a consequence, vegetation cover was extremely low in those areas that had recorded 'very much below average' rainfall (Figure 4.3a & Figure 4.3b).

Overall, due to these conditions, November 2002 represented the 'driest' of the exemplar months. The *CAVI* performed very well in the arid to semi-arid zones of the continent, with the vast majority of grid points falling within the 0.1 interval. The *CAVI* tendency for over-estimation of vegetation cover was confined to coastal areas of QLD, NSW, VIC and parts of WA that were less affected by reduced rainfall (Figure 4.4b). The weighting of rainfall and temperature may, therefore, need to be adjusted for particular climatic regions if the *CAVI* were to be used for continent wide vegetation cover estimation. Figure 4.4b shows that the *CAVI* performed well in the primary area of interest, with the majority of grid points falling within the 0.1 interval across the arid and semi-arid regions of the continent.

4.5.2 November 2005

November 2005 was the worst performing exemplar month. The R^2 value between f_{PV} and the *CAVI* grid points was 0.77 and only 56% of all grid points were within the 0.1 interval. A high percentage of grid points, 41%, over-estimated, while only 3% under-estimated vegetation cover (Table 4.1; Figure 4.4c). The underperformance of the *CAVI* in some parts of the Australian continent in this month maybe explained by the vastly different climatic conditions influencing the index compared to those that occurred for November 2002.

During the 2004 – 2005 period parts of WA, NT, SA and QLD received 'below average' to 'very well below average' rainfall due to a weak El Niño phase (Bureau of Meteorology 2014). However, halfway through 2005 ENSO Neutral conditions set in and most parts of the NT, NSW, parts of western QLD, SA and WA received 'very much above average' rainfall for the six months preceding November 2005. The 'above average' rainfall that fell over a significant portion of Australia during this Spring season (September – November) included many areas within the arid to semi-arid zone. The rainfall relieved the dry conditions that had dominated the first half of the year (Shein 2006) and led to an increase in actual green vegetation cover (f_{PV}) (Figure 4.3c). However, in the *CAVI* calculation these high levels of rainfall resulted

in over-estimation of vegetation cover at a large number of grid points in areas of western QLD, NSW, north-eastern SA and along the coastline of WA (Figure 4.4d). Some of these regions are within the wind erosion zone and would affect the performance of the *CAVI*.

These results, along with those related to November 2002, highlight that the *CAVI* performs better in regions of low rainfall and illustrates that problems of over-estimation extend into arid and semi-arid areas when rainfall in the preceding months has been high in those regions. These results contrast those of De Martonne (1926), which performed well in regions, and during seasons, of regular rainfall (e.g. in the Mediterranean) and failed in areas and seasons of little to no rainfall. Climatic conditions like those experienced during the six months prior to November 2005 are regular, if not frequent, occurrences in Australia. As these conditions directly impacted the regions of primary interest in this study (i.e. arid to semi-arid zones), the sensitivity of the *CAVI* to high rainfall will need to be explored further. However, *CAVI* still provides a reasonable estimation for the purpose of this study in the absence of other information.

4.5.3 November 2009

In November 2009, the performance of the *CAVI* was intermediary between that of November 2002 and 2005. The R^2 value between f_{PV} and the *CAVI* grid points was 0.73 and 60% of all grid points were within the 0.1 interval. A high percentage of grid points, 38%, over-estimated vegetation cover while only 2% under-estimated cover (Table 4.2; Figure 4.4e) for this target month. Although these values are similar to those of November 2005, the percentage of grid points for which the *CAVI* over-estimated vegetation cover are relatively confined to coastal areas with only slight encroachment (few grid points) into arid and semi-arid areas (Figure 4.4f). Over-estimation of vegetation cover using the *CAVI* primarily occurred in some parts of western QLD, western NSW and VIC, and along the coastline of WA (Figure 4.4f). The majority of these regions are either outside the main arid to semi-arid wind erosion zone, or are regions that only experience wind erosion in extreme conditions.

The September 2009 ‘Red Dawn’ dust storm event was associated with a transition period between a La Niña and an El Niño event. A La Niña phase was in effect prior to mid-2009 which led to ‘very much above average’ to ‘highest on record’ rainfall in

areas of northern Australia including the NT, WA and QLD (Bureau of Meteorology 2014). At the same time much of southern Australia was experiencing very dry conditions, with VIC and SA having 94% and 65% of their area recording 'very much below average' rainfall, respectively. As a result of the strong La Niña in northern Australia, sediment rich flood waters from the Cooper Creek, Diamantina and Georgina Rivers reached the Lake Eyre Basin in central Australia during May 2009 (Arthur 2009). These sediment rich flood waters resulted in an increase in newly deposited sediments available for mobilisation and increased vegetation cover along the flood plains of these rivers across large areas of central Australia and the Lake Eyre Basin. However, in mid-2009 an El Niño started to affect Australia by reducing rainfall 'below' to 'very much below average' for large areas of QLD, the NT and WA, eastern VIC and most parts of NSW. With a lack of follow up rain, vegetation died back and actual green vegetation cover was drastically reduced (Figure 4.3e).

The pattern of rainfall seen in this month was, in part, the reverse of that observed in November 2005 which was preceded by six months of dry conditions followed by six months of high rainfall directly prior to the target month. In contrast, November 2009 was preceded by six months of high rainfall in northern Australia followed by six months of very dry conditions immediately prior to the target month. As both of these exemplar months performed less promisingly than November 2002 this suggests that it is the distribution of rainfall across the whole 12 months that is influencing the over-estimations of the *CAVI*. However, given that 2009 performed better than 2005 this further suggests that the immediately preceding six months may be more influential than the earlier six months.

4.5.4 January 2002 and February 2003

The Time Series of R^2 values for the *CAVI*:f_{PV} and the *CAVI*:f_{BS} comparisons shows a periodic pattern with an annual cycle for the period from February 2000 to December 2012 (Figure 4.2). The R^2 values for January 2002 and February 2003 for the *CAVI*:f_{PV} (green cover) and the *CAVI*:f_{BS} (bare soil) are unusually low for a typical wind erosion season (September to February) compared to other years in this time series. The January 2002 values were $f_{PV} = 0.41$, $f_{BS} = 0.33$ and $f_{PV} = 0.40$, $f_{BS} = 0.32$ for February 2003. Whereas the f_{PV} and f_{BS} values two months before and after January 2002 and February 2003 were considerably higher (Figure 4.2). A sudden drop occurred in January 2002 and February 2003. A visual comparison of the *CAVI* ($w_f = 0.9$) based

vegetation cover maps and those based on satellite remote sensed f_{PV} can be seen in Figure 4.5. This visual comparison indicate that the *CAVI* broadly predicts similar spatial pattern in the colour spectrum as suggested by the f_{PV} vegetation cover maps. However, some areas on the *CAVI* maps show an overestimation of vegetation cover which is reflected in the lower R^2 values for those months.

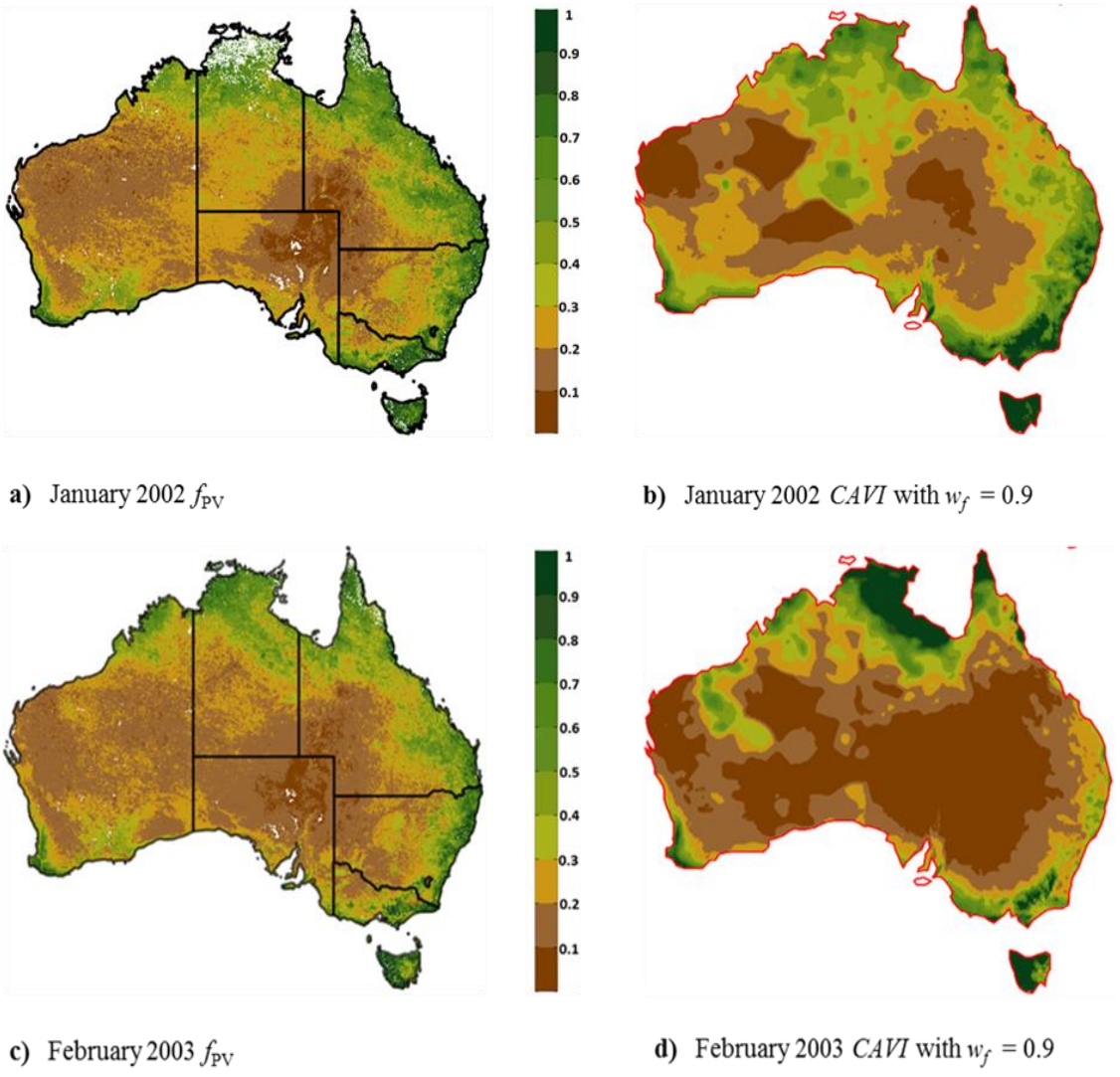

Figure 4.6: Comparison between fractional cover f_{PV} maps (a, c) and the *CAVI* (b, d) with w_f = 0.9 maps.

The relationship between f_{PV} and *CAVI* values for all grid points falling under, within and over the 0.1 interval for February 2002 and January 2003 is shown in Figure 4.6. The slope of the regression lines for all grid points in Figures 4.6a, and Figure 4.6c are 0.54 and 0.46 respectively. The spatial distribution of grid points is displayed in Figures 4.6b and Figure 4.6d. Points falling within the 0.1 interval are shown with a green 'o', grid points over-estimating vegetation cover (below the interval) are shown

with a red '+' and grid points under-estimating vegetation cover (above the interval) are shown with red 'x'. *CAVI* over-estimated (red '+') vegetation cover in arid and semi-arid areas during January 2002 (Figure 4.6b) whereas in February 2003, *CAVI* under and over-estimated vegetation cover mostly in coastal areas or areas outside the arid to semi-arid zone (Figure 4.6d).

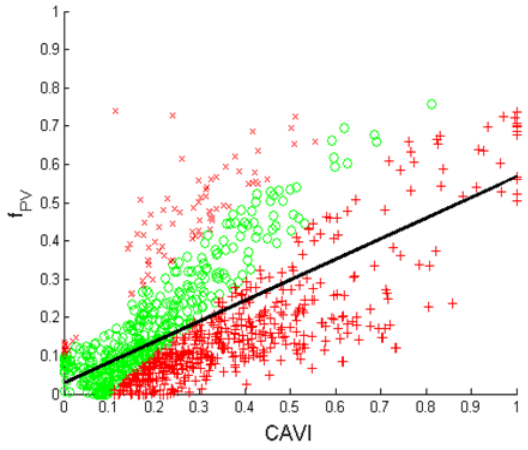

a) January 2002
$f_{PV} = 0.0290 + 0.5381 CAVI \quad R^2 = 0.4108$

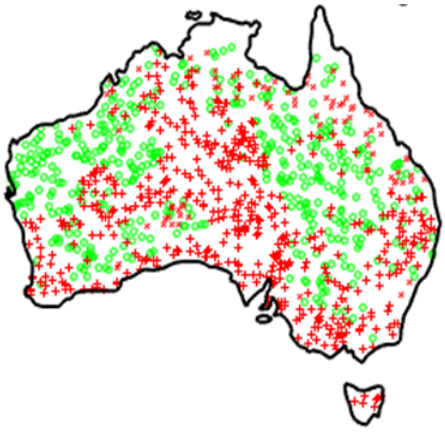

b) Spatial performance – January 2002

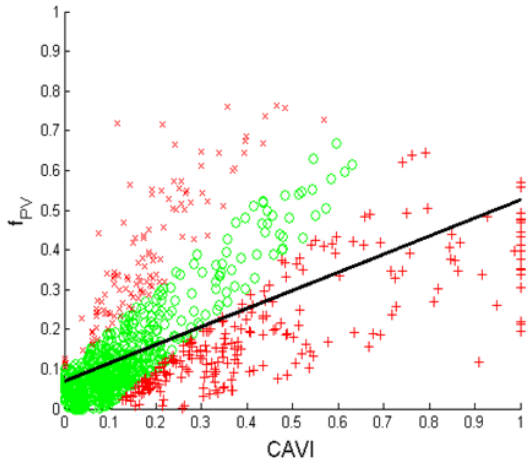

c) February 2003
$f_{PV} = 0.0698 + 0.4560 CAVI \quad R^2 = 0.3964$

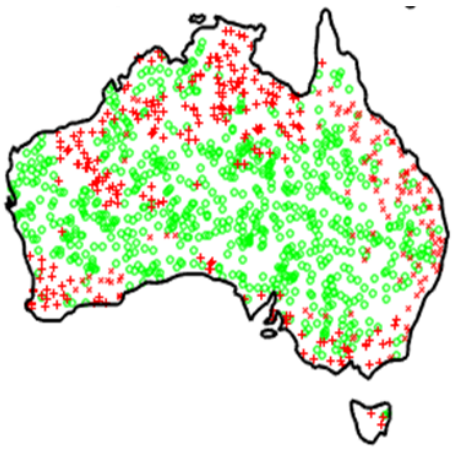

d) Spatial performance – February 2003

Figure 4.7: Regression analyses (a and c) showing the relationship between f_{PV} and *CAVI* (w_f = 0.9) and corresponding *CAVI* spatial performance maps (b and d). On all figures, points within the 0.10 interval are shown with a green 'o', grid points over-estimating vegetation cover (below the interval) are shown with a red '+' and grid points under-estimating vegetation cover (above the interval) are shown with red 'x'.

The overestimation of vegetation cover in January 2002 can be linked in one part to the above average rainfall activity in some areas (e. g. the Northern Territory Arid

Centre and South Australian Arid Lands NRM regions) a few months before January 2002 (Section 3.2, Figure 3.14) but also to the fact that in the months leading up to January 2002 and February 2003, Australia experienced a long continuous period of very much below average rainfall and higher than average temperatures (Section 3.2, Figure 3.14). This resulted in an extremely large number of bushfires. The Rapid Response fire maps produced from the Moderate Resolution Imaging Spectroradiometer (MODIS) data captured on board the Terra (launched 1999) and Aqua (launched 2002) satellites provide evidence of the scale of bushfires during the months prior to January 2002 and February 2003 (Figure 4.7a & Figure 4.7b). MODIS has the capability to detect "hotspots" instantly whereas 10-day bushfire products (e.g. maps) have been post-processed. (Giglio et al. 2003; Davies, Kumar & Desclorites 2004). During bushfires any vegetation cover was removed and this effect was captured in the f_{PV} and f_{BS} values. The *CAVI* estimates based only on rainfall and temperature data did not incorporate the effects of fires and therefore overestimated vegetation cover at these times. This explains the lower values in both green cover and bare soil data in January 2002 (f_{PV} = 0.41, f_{BS} = 0.33) and February 2003 (f_{PV} = 0.40, f_{BS} = 0.32) and that large areas of the continent were covered with non-photosynthetic dead vegetation (f_{NPV}). These land areas affected by bush fires often have been stripped of their protective vegetation cover and can potentially become sources of dust (Strong et al. 2010). This is a process that is random in nature and difficult to capture. However, this issue needs to be further explored.

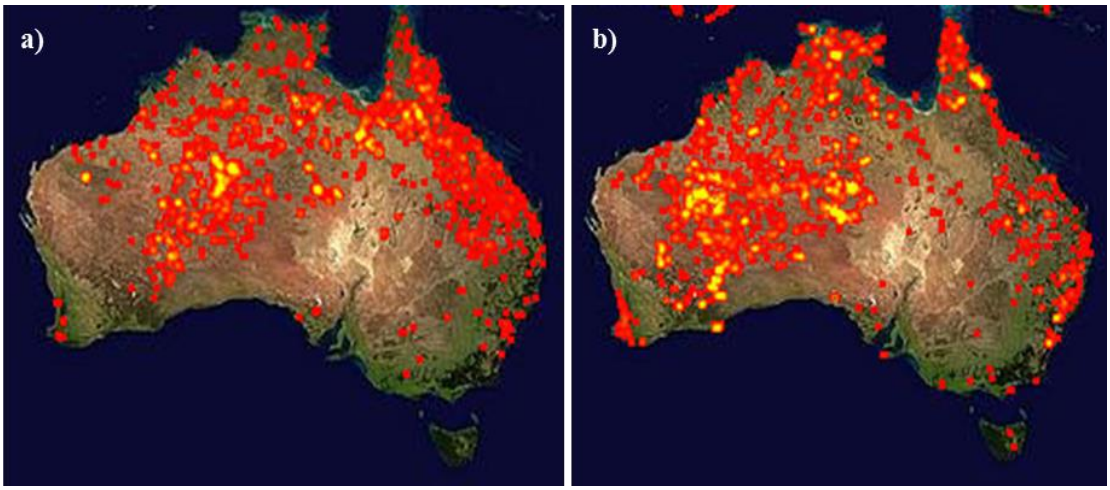

Figure 4.8: Rapid Response Fire maps (a) 27 Nov – 6 Dec 2001 and (b) 7 Nov – 16 Nov 2002. (Giglio et al. 2003; Davies, Kumar & Desclorites 2004)

4.5.5 January 2011 flood

The performance of the *CAVI* was also tested during severe wet conditions. A strong La Niña resulting in widespread severe flooding between September 2010 and March 2011. The continent experienced well above average rainfall and below average temperatures during the months leading up to January 2011 (Section 3.2, Figure 3.14). During the 2010/2011 flood *CAVI* showed a strong relationship with f_{PV} and f_{BS} (Figure 4.2). The January 2011 *CAVI*:f_{PV} R^2 value was 0.72 and 0.65 for *CAVI*:f_{BS}. A visual comparison of the *CAVI* (w_f = 0.9) based vegetation cover map and satellite remote sensed f_{PV} map can be seen in Figure 4.8 and indicates that the *CAVI* generally overestimated vegetation cover in this month during the flooding season. The overestimation of vegetation cover can be expected since the *CAVI* is based on 12 months weighted rainfall with the months closer to the target month influencing the *CAVI* more due to the intense rainfall leading up to January 2011.

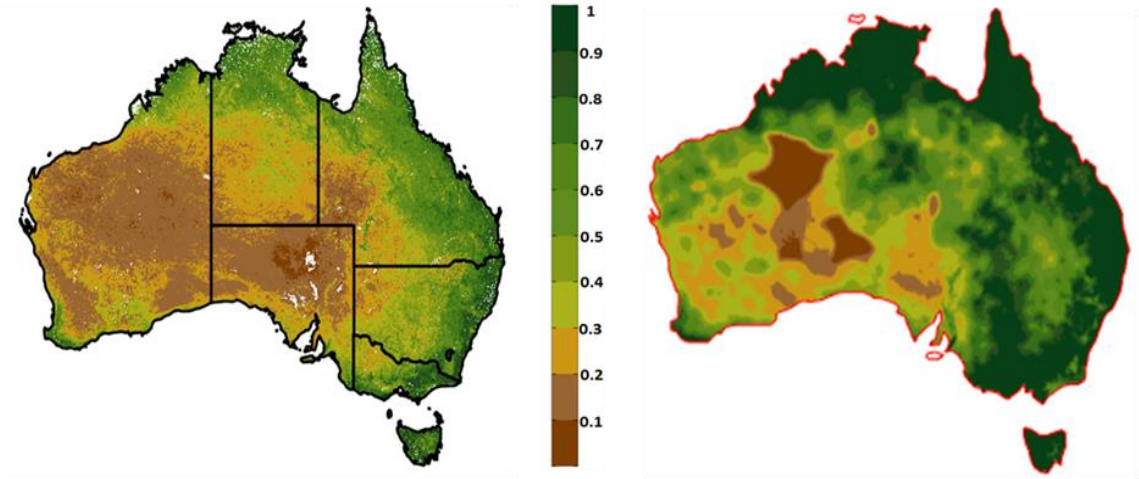

a) January 2011 f_{PV} fractional cover. **b)** January 2011 *CAVI* with w_f = 0.9.

Figure 4.9: Comparison between fractional cover f_{PV} map (a) and the *CAVI* (b) with w_f = 0.9 map.

The overall results of the *CAVI* indicate that the extension of De Martonne's Aridity Index to include 12 months weighted rainfall and temperature data to model vegetation cover on a broad geographical scale has been positive. This particularly applies to the arid to semi-arid regions of Australia which have generally lower annual rainfall and experience higher temperatures during the Spring - Summer months which coincides with the wind erosion season. The *CAVI* is a particularly good estimation of vegetation cover during the Spring - Summer season. The *CAVI* in the current development stage

has the tendency to over emphasise the relationships between rainfall, temperature and vegetation/green cover. A limiting or threshold factor that constrains the influence of extended periods of rainfall and which is applied with a degree of seasonal and regional variability in its moderating effect may be needed to improve overall performance and extend the application of the *CAVI*. The inclusion of a correction for different types of vegetation cover across Australia may also improve the overall performance of the *CAVI*. These improvements are considered and are part of further research.

The prediction of future conditions, using rainfall and temperature data to calculate the *CAVI*, will facilitate the development of seasonal forecasts and providing an additional planning tool for environmental, ecological and land-use agencies. The development of a workable index allows for the modelling of vegetation cover where rainfall and temperature data is available but satellite data is not. Of particular interest is the 1940 and 1960 period which were active dust storm seasons (Chapter 2, Figure 2.2). The *CAVI* is next tested in the Computational Environmental Management System (CEMSYS) wind erosion model which calculates the extent and severity of wind erosion across Australia. The index has been used as a surrogate for the Fractional Cover vegetation component of the GIS model component of CEMSYS which is discussed in Chapter 5.

Chapter 5: Wind Erosion Modelling using *CAVI*

In Australia, wind erosion monitoring occurs at a variety of spatial and temporal scales as discussed in Section 1.4. The Computational Environmental Management System (CEMSYS) is an integrated processed-based physical wind erosion model that can be used to estimate the extent and severity of wind erosion across the Australian continent. This chapter addresses the fourth key research objective as outlined in Section 1.6. The aim is to investigate if *CAVI* estimates of vegetation cover can be successfully used as a surrogate for remote sensed vegetation cover in CEMSYS, and thus extend the utility of the CEMSYS model to periods where no satellite remote sensing data is available. Section 5.1 provides an overview of the individual components of the CEMSYS model. In Section 5.2 CEMSYS estimated dust loads based on *CAVI* and photosynthetically active fractional cover (f_{PV}) are compared for two dust storm events. The results of this comparison are discussed in Section 5.2.1. Section 5.2.2 focuses on the modelling of known historical wind erosion periods using *CAVI*, identified in Chapter 3 where rainfall and temperature data is available but satellite based vegetation data is not readily available.

5.1 The Computational Environmental Management System model

The Computational Environmental Management System (CEMSYS) is a physically based process model of wind erosion which can be used to quantify the extent of source areas, and magnitude of dust storms events as mentioned in Section 1.4. As illustrated in Figure 5.1, CEMSYS couples an atmospheric model, a land surface scheme, a wind erosion scheme, a transport and deposition scheme, and a Geographic Information System (GIS) database, for the modelling of dust storm events. The atmospheric model includes the treatments for atmospheric dynamic and physical processes, including radiation, clouds, advection, convection, turbulent diffusion, and the atmospheric boundary layer (Leslie & Wightwick 1995). The atmospheric model interacts with the other three system components. The land surface model simulates energy, momentum, and mass exchanges between the atmosphere, soil, and vegetation and produces friction velocity and soil moisture as outputs. The wind erosion scheme obtains friction velocity from the atmospheric model, soil moisture from the land surface scheme and

other spatially distributed parameters such as vegetation and soil texture data from the GIS database. To predict dust movement, the transport and deposition scheme obtains wind fields, turbulent diffusivities and precipitation from the atmospheric model, and dust emission rate and particle size information from the wind erosion scheme. Using CEMSYS it is possible to model dust storm events and identify the regions of dust emission and deposition, estimate the strengths of the dust sources and sinks, simulate dust plume size and transport pathways, and gain a better understanding of the climate systems that generate these dust storms (Butler et al. 2007; Leys et al. 2010; Gabric et al. 2015). The model produces maps, time series and statistics for the following wind erosion variables:

- Sand flux (erosion rate),
- Dust flux (dust emission),
- Deposition,
- Net soil loss,
- Dust load, and
- Dust concentration.

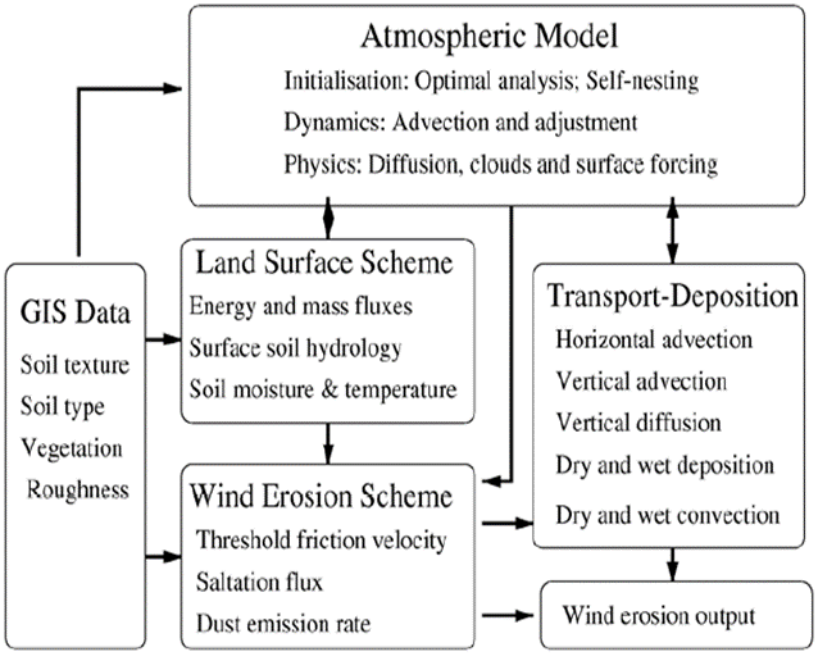

Figure 5.1: The structure of the integrated wind erosion modelling system. The system consists of an atmospheric model, a land surface scheme, a wind erosion scheme, a transport and deposition scheme and a GIS database.

5.2 Using *CAVI* as a surrogate for Fractional Cover in the CEMSYS model

This section is divided into two parts. Section 5.2.1, the feasibility of using *CAVI* as a surrogate for vegetation cover in the CEMSYS model is tested by running CEMSYS with both f_{PV} and *CAVI* vegetation cover input data and comparing the results. In Section 5.2.2, *CAVI* vegetation cover input data together with historical atmospheric data is used to model historical dust event periods. This has previously never been possible since satellite derived f_{PV} vegetation cover does not date back past 2000.

5.2.1 Validation of *CAVI* as a surrogate for f_{PV} in wind erosion modelling

In this research, CEMSYS has been used to model wind erosion events over the Australian continent at 50 km scale resolution in hourly time steps over the domain (110.00º to 155.00° E and -10.00º to -45.00° N). The test period of the *CAVI* is restricted from February 2000 – December 2012 since reliable satellite derived monthly photosynthetically active fractional vegetation cover (f_{PV}) data only became available from the CSIRO from February 2000. A 'proof of concept' approach was chosen to test if *CAVI* estimates of vegetation cover can produce similar daily dust load maps as f_{PV}. The CEMSYS model was run with f_{PV} and *CAVI* vegetation cover input data for the two large scale dust storm events in this period (September 2009 and October 2002). These two months had particularly active wind erosion season which were reported by the ABoM, NOAA and other agencies, and have been extensively covered and discussed in the literature and media. Every individual day in September 2009 and October 2002 was modelled in CEMSYS with both vegetation covers. The results for the dust storm events on the 22nd – 25th September 2009 and 22nd – 25th October 2002 based on *CAVI* and f_{PV} vegetation covers were compared in regards to the areas which were eroded and the amount of dust removed as a result of wind erosion. The setup of the modelling runs are shown in Figure 5.2.

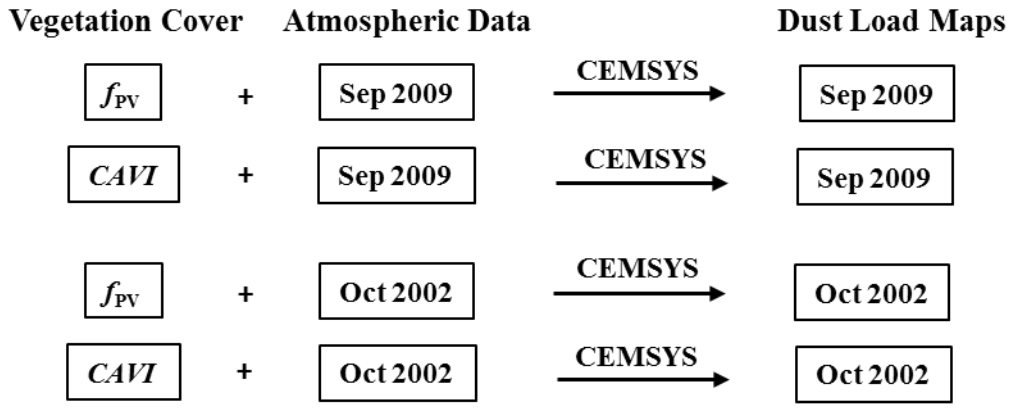

Figure 5.2: CEMSYS modelling setup to test the performance of *CAVI.*

The CEMSYS model has been extensively tested with remote sensing data (f_{PV}) and is known to perform well (Leys et al. 2011a). In order to establish a base line as a comparison for the performance of *CAVI,* September 2009 was modelled using f_{PV} data to represent the vegetation cover in the model together with the September 2009 atmospheric input data (Figure 5.2). The September 2009 model runs were then repeated but f_{PV} was replaced with the September 2009 *CAVI* estimates of vegetation cover information. The same modelling setup was used to test the performance of *CAVI* for October 2002 as outlined in Figure 5.2. All available wind erosion properties mentioned in Section 5.1 were calculated but only the average daily dust load results are reported here.

The satellite derived f_{PV} vegetation map for September 2009 (Figure 5.3a) shows the severity of the 'Millennium' drought. Eastern Australia, in particular the lower Lake Eyre Basin, north west NSW, the Channel Country in QLD, parts of the NT and WA were severely affected by a long lasting drought with well below average rainfall and higher than average temperatures (Leys et al. 2011b). These areas are shaded in light to dark brown colours in Figure 5.3a & 5.3b. Between May 2009 – March 2010 (Figure 3.3), Australia was under the influence of an exceptionally dry El Niño which affected much of the continent. During these dry conditions the very severe 'Red Dawn' dust storm occurred on the 22 – 25 September 2009 (Leys et al. 2011b). The climatic conditions associated with the dust storm event have been discussed in Section 3.2. The *CAVI* based vegetation cover map for the same month (Figure 5.3b) shows a very similar spatial distribution of vegetation and broadly reflects the same spatial changes as suggested by the f_{PV} vegetation cover map.

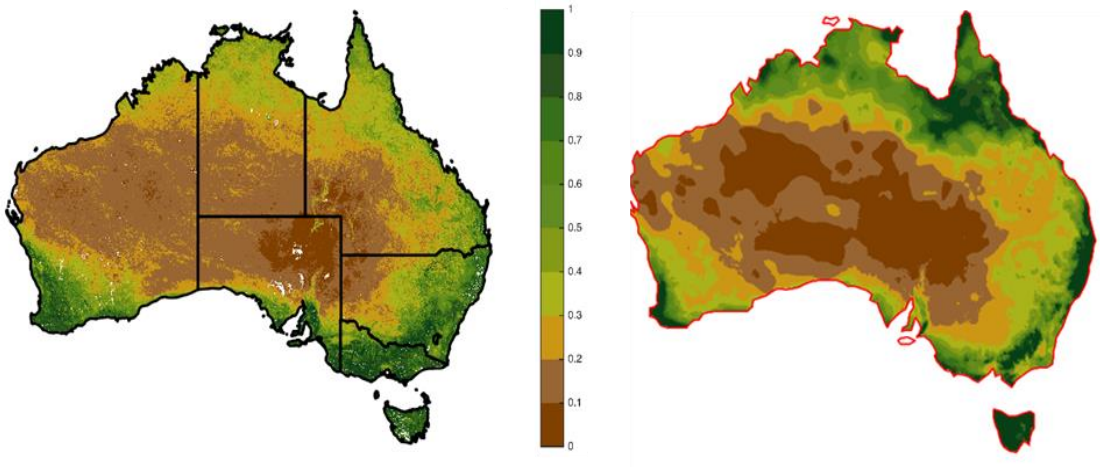

a) September 2009 f_{PV} fractional cover map b) September 2009 *CAVI* map

Figure 5.3: Comparison between f_{PV} map (a) and *CAVI* map (b) of September 2009.

Starting on 22nd – 23rd September 2009 and 25th September 2009, were some of the most severe dust storm events Australia experienced since the 1940s (Leys et al. 2011b). To compare the dust load estimate of the event, the three days have been modelled with f_{PV} and *CAVI* vegetation cover. The average daily dust load results of f_{PV} and *CAVI* are compared and shown in Figure 5.4a – Figure 5.4f. The difference of the maximum daily average dust load produced with *CAVI* vegetation cover is compared to the f_{PV} maximum daily average dust load and listed in Table 5.1.

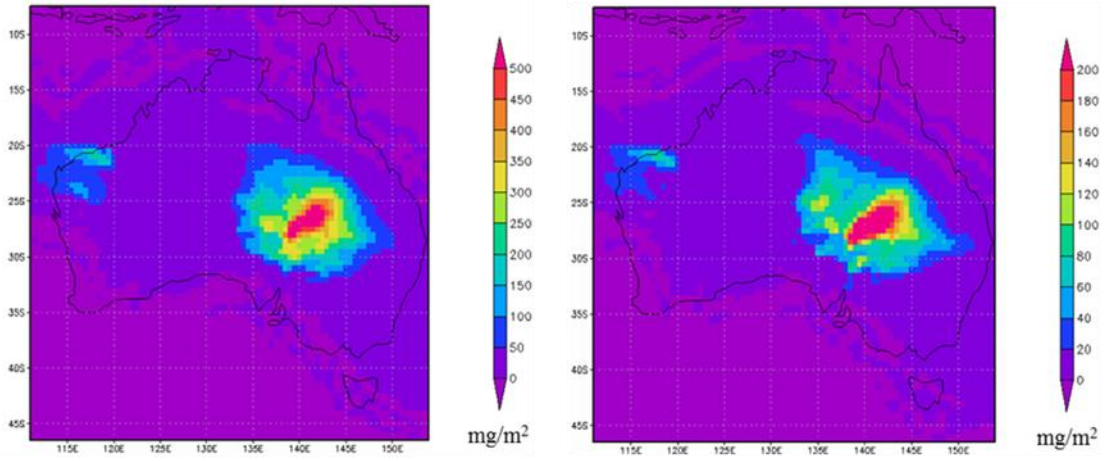

a) Predicted dust load for f_{PV} 22nd September 2009 with a maximum daily average dust load of 687 mg/m².

b) Predicted dust load for *CAVI* 22nd September 2009 with a maximum daily average dust load of 401 mg/m².

Figure 5.4a – 5.4f: Spatial distribution of the dust plume across the continent for 22nd – 23rd September and 25th September 2009 based on f_{PV} and *CAVI*, and the difference of the maximum daily average dust load produced with *CAVI* vegetation cover compared to the f_{PV} maximum daily average dust load. Figure continues over next page.

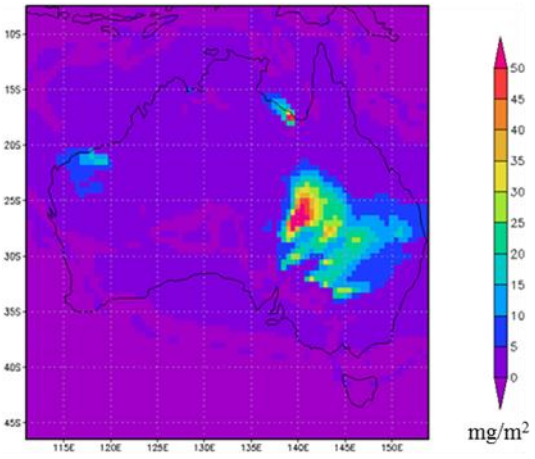

c) Predicted dust load for f_{PV} 23rd September 2009 with a maximum daily average dust load of 70 mg/m^2.

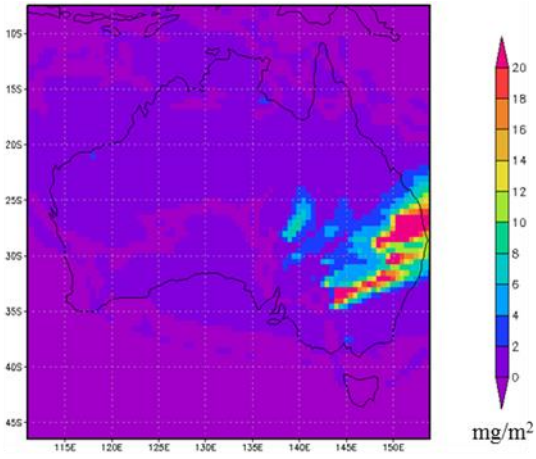

d) Predicted dust load for *CAVI* 23rd September 2009 with a maximum daily average dust load of 45 mg/m^2.

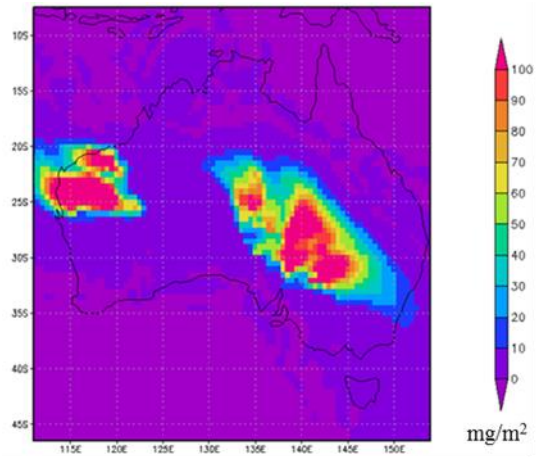

e) Predicted dust load for f_{PV} and 25th September 2009 with a maximum daily average dust load of 399 mg/m^2.

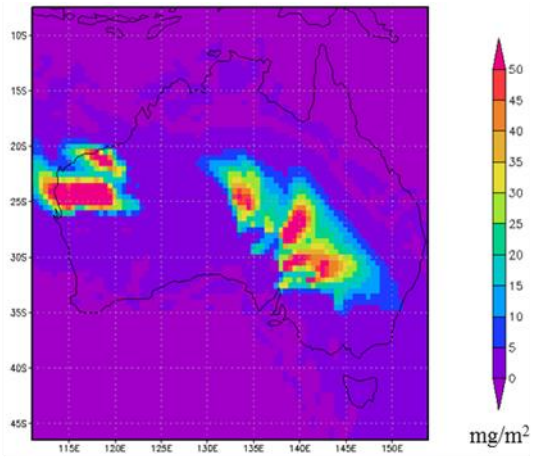

f) Predicted dust load for *CAVI* 25th September 2009 with a maximum daily average dust load of 175 mg/m^2.

Figure 5.5a – 5.4f: Spatial distribution of the dust plume across the continent for 22nd – 23rd September and 25th September 2009 based on f_{PV} and *CAVI*, and the difference of the maximum daily average dust load produced with *CAVI* vegetation cover compared to the f_{PV} maximum daily average dust load.

Table 5.1: Maximum daily average dust load comparison between September 2009 f_{PV} and September 2009 *CAVI*, and the percentage of dust produced with *CAVI* vegetation cover compared to the f_{PV} dust load.

Day	**Sep 2009 f_{PV}**	**Sep 2009 *CAVI***	***CAVI* dust in % to f_{PV}**
22nd	687 mg/m^2	401 mg/m^2	59%
23rd	70 mg/m^2	45 mg/m^2	64%
25th	399 mg/m^2	175 mg/m^2	44%

Previous research has identified the red sandplains of western NSW, riverine channels and lakes of the lower Lake Eyre Basin and the Channel Country of western QLD as the dust source areas for the September 2009 'Red Dawn' event (DustWatch 2011a;

Leys et al. 2011b). The dust load maps from the CEMSYS results using f_{PV} shown in Figures 5.4a indicate that the dust storm started in the Lake Eyre Basin. The peak of the storm occurred on the 22nd September 2009 which was also reflected in the high maximum daily average dust load of 682 mg/m^2 (Table 5.1). This was followed by a less active day on the 23rd September 2009 (Figure 5.4c) with a reduced dust load of 70 mg/m^2 (Table 5.1). An increase in dust storm activity can be observed in Figure 5.4e when the maximum daily average dust load increased to 399 mg/m^2 on the 25th September 2009 (Table 5.1). O'Loingsigh et al. (2015) also reported that the peak of the 'Red Dawn' event occurred in the late afternoon and evening of 22nd September 2009. The study was based on a time integrated approach and observed data, where the dust flux is calculated through a distance perpendicular to the wind direction each hour for 24 hrs to calculate the dust concentration.

The dust load modelling results based on *CAVI* for 22nd – 23rd September 2009 and 25th September 2009 are shown in Figure 5.4b, 5.4d, 5.4f and Table 5.1. The estimated maximum daily average dust load for the most active day during the 'Red Dawn' event was calculated to have reached 401 mg/m^2 on the 22nd September 2009 (Figure 5.4b). This is 58% of the f_{PV} maximum daily average dust load for the same day (Table 5.1). On the 23rd September 2009, the dust plume had advanced further eastwards and started to move off the coast and the maximum daily average dust load was reduced to 45 mg/m^2, 64% of f_{PV} (Figure 5.4d & Table 5.1). By the 25th September 2009, the dust storm had intensified again resulting in an increase in maximum daily average dust load to 175 mg/m^2 which is 44% of the f_{PV} maximum daily average dust load (Figure 5.4f & Table 5.1).

The dust load maps based on *CAVI* as a replacement of f_{PV} produced similar spatial distributions of the dust plume for the active days but was different on the 23rd September 2009 (Figure 5.4a – 5.4f). The two models indicate that soil was eroded from approximately the same locations (spatial distribution) but at lower concentration levels. The difference in dust load concentration is to be expected since both f_{PV} and *CAVI* are not a direct measure of the vegetation cover. The *CAVI* based dust estimates for the three dust storm days in September 2009 ranged between 44 – 64% of the dust load predicted when using f_{PV} estimates of vegetation cover (Table 5.1). The underestimated dust loads were expected due to the weaker correlation ($R^2 = 0.45$) of *CAVI* with f_{PV} vegetation cover during September 2009 (Figure 4.2). This indicates

that CAVI is over-estimating vegetation cover. The *CAVI* with f_{PV} correlation tends to be weaker during the first month of the wind erosion season (September – February). In the months leading up to the September dust storm event, Australia experienced above average rainfall in some parts of the continent due to a La Niña which finished in mid-2009. Since *CAVI* is based on weighted rainfall and temperatures data the index over-estimated vegetation cover. The correlation between *CAVI* and f_{PV} over the period 2000 – 2012 has been discussed in detail in Section 4.5.

The difference in dust load concentration levels can also be the result of a number factors. Firstly, the *CAVI* as currently being defined exhibits some temporal and spatial variability in its performance and effectiveness. The index performs particularly well in arid to semi-arid regions of Australia which have generally lower rainfall levels all year and experience high temperatures during the wind erosion season (Spring – Summer) but underperforms in the autumn and winter months. Both seasonality and regionality directly influence rainfall and temperature which in-turn affect vegetation growth and levels of cover. The *CAVI* as it has been used in this study does not include any corrections for individual vegetation types, seasonality or land use. The *CAVI* has a general tendency to overestimate green vegetation cover (Pudmenzky, King & Butler 2015), particularly in those regions outside the arid to semi-arid zone that receive more regular rainfall.

The second factor to consider is that satellite derived vegetation indices have certain limitations in arid to semi-arid regions due to their low sensitivity to low vegetation cover (Wu 2014). The f_{PV} index was first developed by Guerschman et al. (2009) based on MODIS satellite reflectance information to monitor the northern tropical savanna region in the Northern Territory and was proposed to be used across Australia (Stewart et al. 2009). However, the Australian continent encompasses a great diversity of climate, soils, and vegetation types other than the northern savanna (Government of South Australia 2007; Lawley, Lewis & Ostendorf 2015). It has been established that fractional cover data derived from satellite data has a tendency to underestimate non-photosynthetic vegetation and overestimate bare soil (Guerschman et al. 2012). Considering these two facts, it is likely that f_{PV} based CEMSYS results overestimate (Leys et al. 2011a) the amount of eroded soil in arid and semi-arid areas and the *CAVI* overestimates vegetation cover in these regions.

Thirdly, possible sources of modelling/computational errors also needs to be taken into account. Wind erosion models are only approximations to a set of complex processes. Even if these processes were accurately represented in the models, model simulations may still deviate from reality due to inaccuracies in initial conditions and errors in model parameters and forcing data, and the propagation of errors during the modelling process. This can occur because the models are non-linear and sensitive to minute changes in initial conditions and parameters (Shao 2008). In summary, it is likely that errors may arise from modelled and observed data and therefore the results are difficult to compare (Steyn & McKendry 1988).

Considering the three possible 'errors sources' mentioned in the paragraphs above it can be expected that each approach to ascertain the impact of wind erosion has its own weaknesses. The September 2009 results are spatially similar but with a lower intensity. The results obtained based on f_{PV}, the *CAVI* and the CEMSYS model provide useful estimates of the wind erosion activity in Australia. However, the intensity levels each of these models produce needs to be used with caution.

Following the encouraging results of September 2009, similar comparison tests of f_{PV} versus the *CAVI* were performed for October 2002, which was in the middle of the Millennium drought and also had a severe dust storm event. Between March 2002 – January 2003 (Figure 3.3), a strong El Niño affected the entire continent. In the six months leading up the event, Australia was under the influence of a severe drought with below average rainfall and above maximum temperatures (Figure 3.14). The climatic conditions are described in more detail in Section 3.2. The satellite based f_{PV} vegetation map for October 2002 (Figure 5.5a) illustrates the impact of the drought in QLD, NSW, SA, and parts of VIC and WA. The corresponding *CAVI* vegetation map (Figure 5.5b) based on weighted rainfall and temperature for October 2002 repeats the same trend and indicated these areas had minimal vegetation cover.

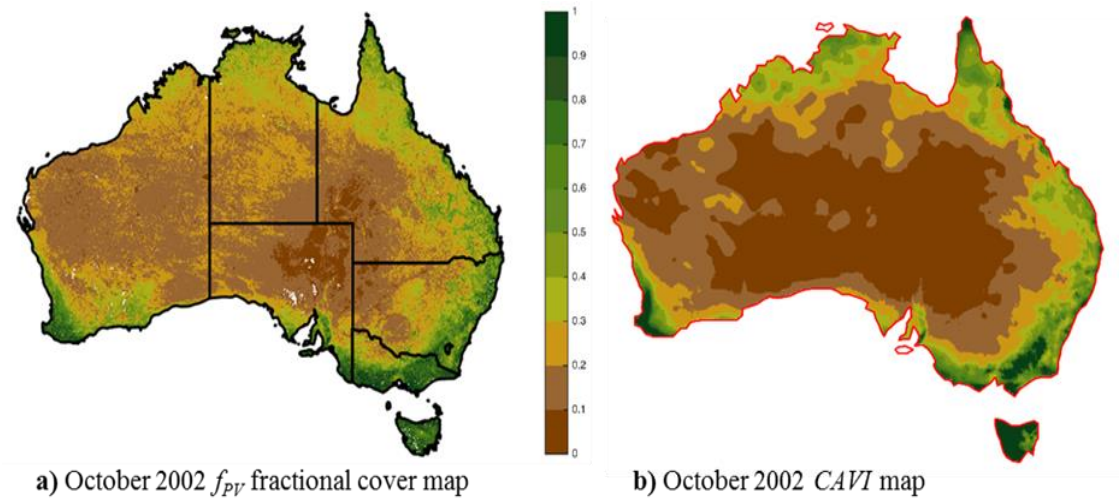

Figure 5.6: Comparison between f_{PV} map (a) and *CAVI* map (b) of October 2002.

The dust storm in October 2002 covered most parts of eastern Australia and lasted from the 22nd – 23rd October 2002 and 25th October 2002. The dust source areas were the southern parts of SA, the grazing lands of north-western NSW, the farm lands in western NSW, and the Channel Country in western QLD (McTainsh et al. 2005; Shao et al. 2007; DustWatch 2011b). The daily average dust load modelling results using f_{PV} as vegetation cover information are shown in Figure 5.6a, 5.6c, 5.6e and Table 5.2. The peak of the dust storm occurred on the 22nd and 23rd October 2002. The 22nd October 2002 saw the onset of the event and the modelling results based on f_{PV} vegetation cover estimated a maximum daily average dust load of 160 mg/m^2 (Figure 5.6a & Table 5.2). On the 23rd October 2002 the dust plume had moved in north easterly direction and the modelling results showed a small increase in maximum daily average dust load to 177 mg/m^2 (Figure 5.6c & Table 5.2). The dust storm activity was very much reduced on the 24th October 2002 but pick up again on the 25th October 2002 with a maximum daily average dust load of 98 mg/m^2 (Figure 5.6e & Table 5.2). The modelling results are comparable to Shao et al. (2007) study.

The same dust event was modelled with *CAVI* vegetation cover data as a replacement for f_{PV} and results are shown in Figure 5.6b, 5.6d, 5.6f and Table 5.2. The progression of the dust plume based on *CAVI* follows the same trend as the f_{PV}. The image in Figure 5.6b, based on the *CAVI* for 22nd October 2002 looks nearly identical to the image based on the f_{PV} and also includes a very similar maximum daily average dust concentration level of 145 mg/m^2 which is 91% of the f_{PV} maximum daily average dust load (Table 5.2). On the 23rd October 2002, the maximum daily average dust load

increased to 189 mg/m^2 which is 108% of the f_{PV} maximum daily average dust load (Table 5.2). The same 'butterfly' shaped dust plume can be observed in Figure 5.6c based on f_{PV} as in Figure 5.6d based on the *CAVI* but the dust concentration was not as high in the left part of the *CAVI* 'wing' over central Australia. The dust activity decreased considerably on the 24th October 2002 but intensified again on the 25th October 2002 reaching a maximum level of 86 mg/m^2 which is 86% of the f_{PV} maximum daily average dust load predicted for the day (Figure 5.6f & Table 5.2).

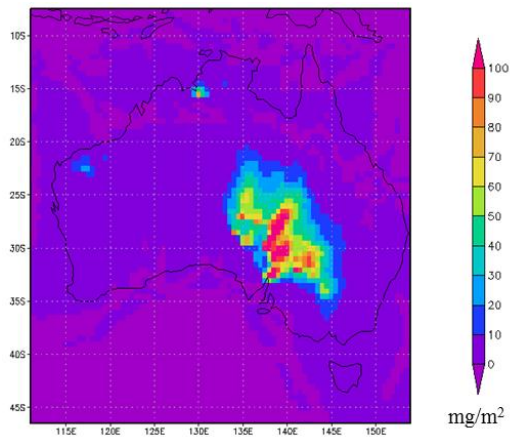

a) Predicted dust load for f_{PV} 22nd October 2002 with a maximum daily average dust load of 160 mg/m^2.

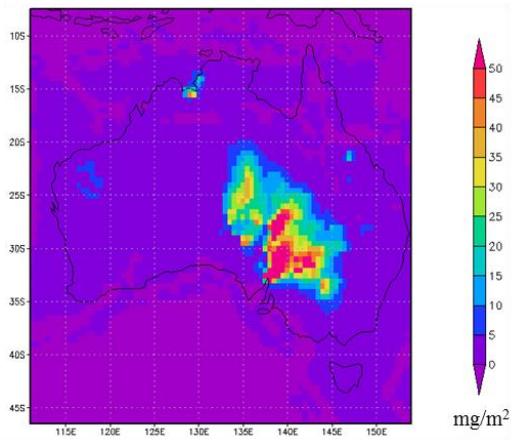

b) Predicted dust load for *CAVI* 22nd October 2002 with a maximum daily average dust load of 145 mg/m^2.

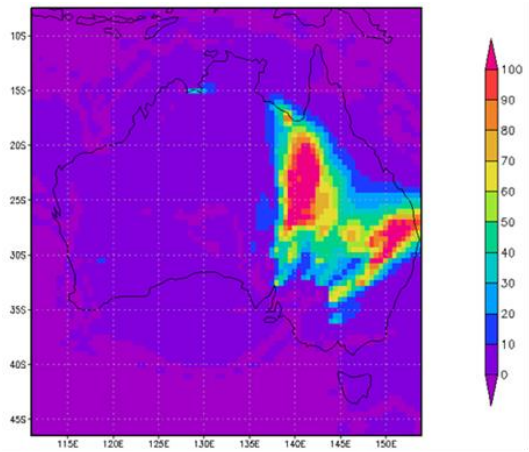

c) Predicted dust load for f_{PV} 23rd October 2002 with a maximum daily average dust load of 177 mg/m^2.

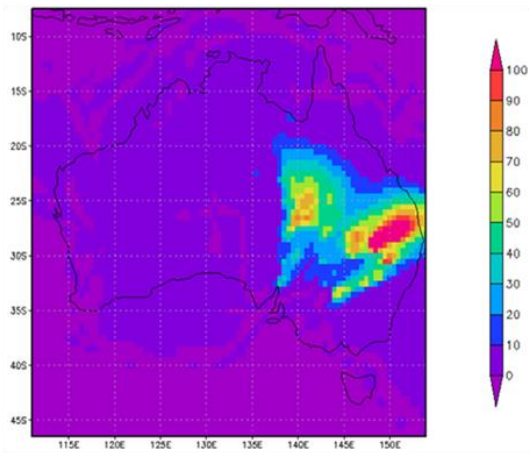

d) Predicted dust load for *CAVI* 23rd October 2002 with a maximum daily average dust load of 189 mg/m^2.

Figure 5.7: Spatial distribution of the dust plume across the continent for 22nd – 23rd October and 25th October 2002 based on f_{PV} and *CAVI*, and the difference of the maximum daily average dust load produced with *CAVI* vegetation cover compared to the f_{PV} maximum daily average dust load. Figure continues over next page.

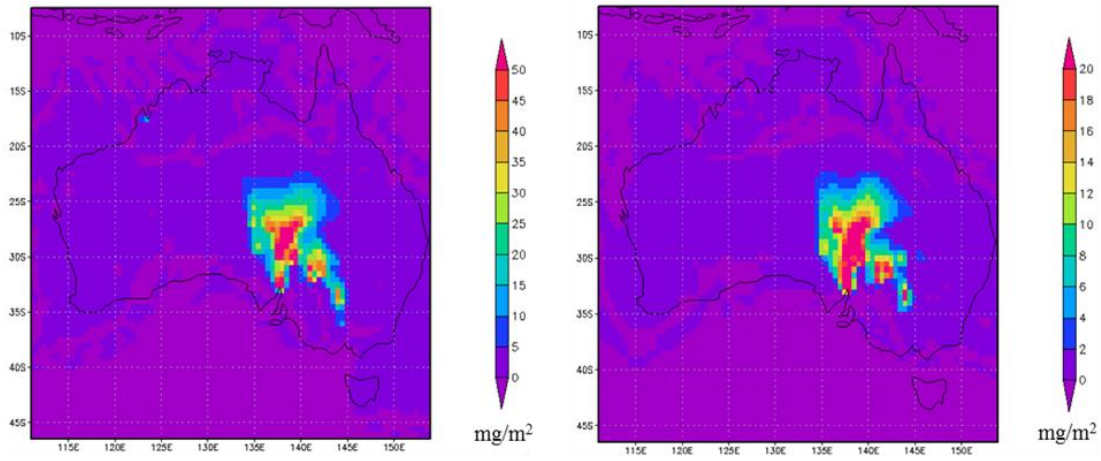

e) Predicted dust load for f_{PV} 25th October 2002 with a maximum daily average dust load of 98 mg/m^2.

f) Predicted dust load for *CAVI* 25th October 2002 with a maximum daily average dust load of 86 mg/m^2.

Figure 5.8: Spatial distribution of the dust plume across the continent for 22nd – 23rd October and 25th October 2002 based on f_{PV} and *CAVI*, and the difference of the maximum daily average dust load produced with *CAVI* vegetation cover compared to the f_{PV} maximum daily average dust load.

Table 5.2: Maximum daily average dust load comparison between October 2002 f_{PV} and October 2002 *CAVI*, and the percentage of dust produced with *CAVI* vegetation cover compared to the f_{PV} dust load.

Day	Oct 2002 f_{PV}	Oct 2002 *CAVI*	*CAVI* dust in % to f_{PV}
22nd	160 mg/m^2	145 mg/m^2	91%
23rd	177 mg/m^2	189 mg/m^2	107%
25th	98 mg/m^2	86 mg/m^2	88%

Both the f_{PV} and *CAVI* based CEMSYS modelling results show similar spatial patterns of wind erosion. The October 2002 f_{PV} and *CAVI* based dust concentrations estimates are relatively comparable over the three modelled days (Figure 5.6a – 5.6f). Overall, *CAVI* performed very well in October 2002 with maximum daily average dust load estimates ranging from 88 – 107% compared to f_{PV} estimates. The very good performance of *CAVI* in the CEMSYS model is linked to the strong correlation to f_{PV} ($R^2 = 0.72$) vegetation cover in October 2002, whereas September 2009 had a weaker correlation to f_{PV}. The good performance of the *CAVI* in this month is related to the low variability in rainfall that occurred during the 12 months prior. The correlation between *CAVI* and f_{PV} vegetation cover is discussed in more detail in Section 4.4 and shown in Figure 4.2.

5.2.2 Applying historical atmospherics together with *CAVI* to historic dust storm periods

Since the use of *CAVI* as a surrogate for f_{PV} in September 2009 and October 2002 CEMSYS modelling results were encouraging (although with some caveats relating to the performance of the index) the focus of Section 5.2.2 is to apply historical atmospheric conditions together with the *CAVI* vegetation cover to model historic dust storm periods. The experimental setup is shown in in Figure 5.7.

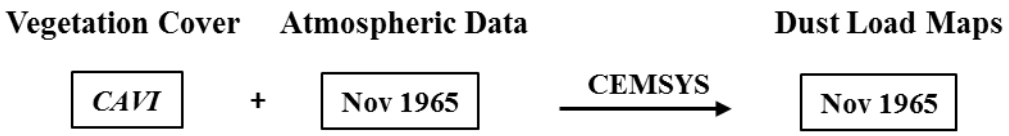

Figure 5.9: Modelling of historical dust storm events in November 1965 with *CAVI* vegetation cover.

Climate is the dominate driver of wind erosion as discussed in Section 1.1, but land management can either moderate or accelerate wind erosion rates. The 1940s, 1960s and 2000s experienced extreme drought conditions with an increase in wind erosion activity and large dust storms. The question remains to whether the 1940s and 1960s experienced more or less wind erosion activity than the 2000s, and whether human activities, such as the land clearing, cultivation practices, stocking (both domestic and feral), overgrazing and the activities during WWII may have played a role. Earlier work based on the HDED suggets that since the early 1900s the same source areas have been active and that during the 1960s simular areas have been active as noted by DustWatch (2011c). With the development of the *CAVI* it is now possible to model any time period of interest including the 1940s and 1960s. From previous reports (DustWatch 2011c) and collated records in the HDED (Chapter 2) it was known that November 1965 was extremly dry and experienced a number of dust storm events. To develop a better understanding whether land management practices have contributed to the increase in dust storm activity, November 1965 has been modelled with the use of *CAVI*. Since *CAVI* assumes current land management practices, the model results will provide an idea of what dust events should be like. November 1944 was also a month of interest but as mentioned previously in Section 2.4, NCEP/NCAR Reanalysis data, which feeds into CEMSYS model, has a global grid size resolution of 2.5 degree but only started in 1948. Any years prior to 1948 need to be modelled with a 2.0 degree

resolution data set and that requires the modification of some CEMSYS codes which was outside the scope of this study but is planned for the near future.

Beginning in 1958, Australia experienced 10 years of drought, which was extremely widespread and severe, covering central Australia and vast areas of adjacent QLD, SA, WA, NSW, and northern Australia. Prior to the large dust storm event in November 1965, Australia was under the influence of an El Niño with very much below average rainfall and above average temperatures. The five NRM regions received 53 – 72% of the time below the long-term average rainfall (Table 3.21) and temperatures were between 37 – 50% of the months above the long-term average (Table 3.22). As a consequence vegetation cover was reduced leaving the soil surface exposed. The climatic conditions for this period have been discussed in more detail in Setion 3.2. The November 1965 *CAVI* based vegetation cover maps in Figure 5.8 illustrations the severity of the drought with large areas of Australia exhibiting minimal vegetation cover as a consequence of very much below average rainfall.

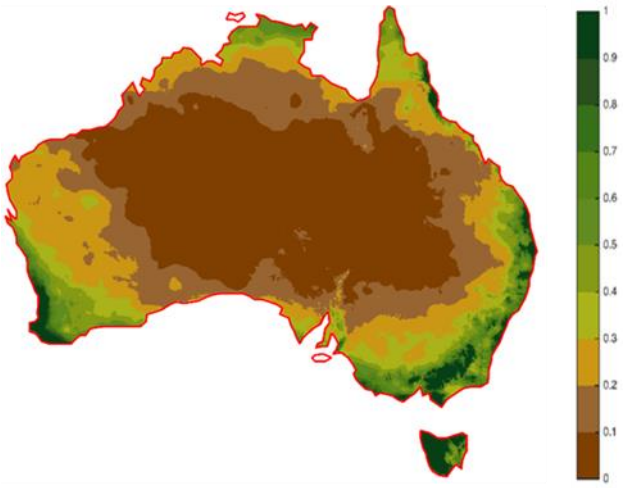

Figure 5.10: *CAVI* map of November 1965.

During November 1965, a number of severe dust storms occurred across Australia but until now it has not been possible to model the impact of these events or the areas affected. One of these dust storms has been documented in the DustWatch (2011c) report, which is based on ABoM visibility data. The dust storm event started on the 23rd November 1965. Wind speeds associated with the pre frontal northerlies entrained dust from the Lake Eyre region, Strzelecki Lakes in SA, and the central NSW and transported the dust towards the central coast. As the low and front moved eastward,

the post frontal southerlies entrained dust in western QLD, north western NSW and NT. The orientation of the cold front also resulted in a strong southerly wind, moving the dust northwards towards the Gulf of Carpentaria.

The days from the 22nd – 25th November 1965 were modelled with *CAVI* vegetation cover and November 1965 atmospheric data and the maximum daily average dust load results are summarised in Table 5.3. These days have been selected since the Historical Dust Event (HDE) database showed an increased number of dust storm recordings on the 22nd – 25th November 1965. The model run on the 22nd November 1965 produced a low maximum daily average dust load of 19 mg/m^2 (Table 5.3) with minimal erosion. On the 23rd November the estimated dust loads reached 57 mg/m^2 (Table 5.3). On the 24th November 1965 the dust storm activity increased which was also reported in DustWatch (2011c), reaching a maximum daily average dust load of 145 mg/m^2. The Lake Eyre Basin in SA, central parts of NSW, the Channel Country in western QLD, and areas in the NT and WA were affected (Figure 5.9a & Table 5.3). The same pattern has been reported in DustWatch (2011c) which is based on visibility data from the ABoM. By the 25th November 1965, the dust plume had moved eastwards (DustWatch 2011c) and started to move offshore. The modelled maximum daily average dust load estimate reached 122 mg/m^2 (Table 5.3) and Figure 5.9b confirms the location of the dust plume.

Table 5.3: *CAVI* based modelled maximum daily average dust load estimates for dust storm days in November 1965.

Day	Nov 1965 *CAVI*
1st	82 mg/m^2
9th	103 mg/m^2
10th	103 mg/m^2
11th	199 mg/m^2
16th	124 mg/m^2
17th	132 mg/m^2
22nd	19 mg/m^2
23rd	57 mg/m^2
24th	145 mg/m^2
25th	122 mg/m^2

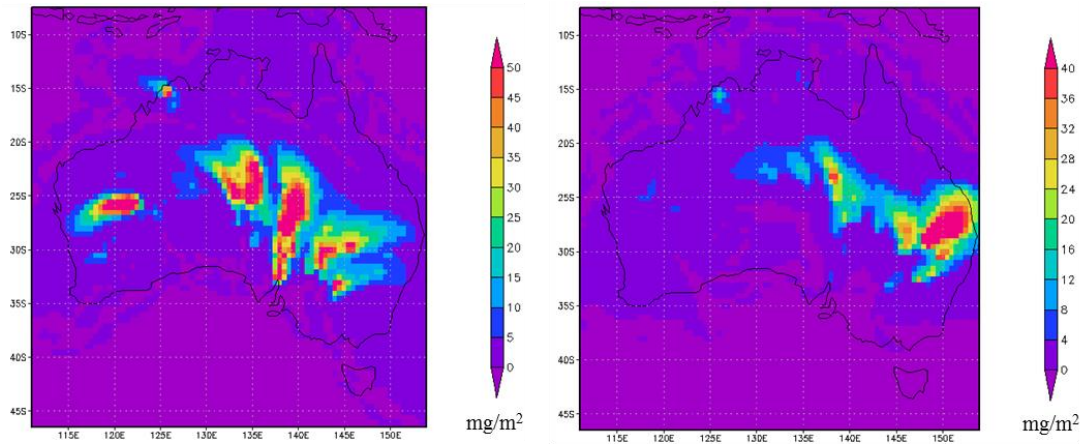

a) Predicted dust load for *CAVI* 24st November 1965 with maximum dust load of 145 mg/m^2.

b) Predicted dust load for *CAVI* 25st November 1965 with maximum dust load of 122 mg/m^2.

Figure 5.11: Spatial distribution and maximum daily average dust load of modelled dust storm events based on *CAVI* during the 24th – 25th November 1965.

The existence of other dust storm events in November 1965 have been identified through the HDED and the modelling of each individual day of this month. Previously, the occurrence and magnitude of these events were unknown but with the development of *CAVI* it is now possible to estimate historic vegetation cover for use in CEMSYS and hence model every day of interest as long as there is rainfall and temperature data available. Figure 5.10a – 5.10f illustrates the spatial patterns of the wind erosion activity for this period together with the estimated maximum daily average dust load in Table 5.3.

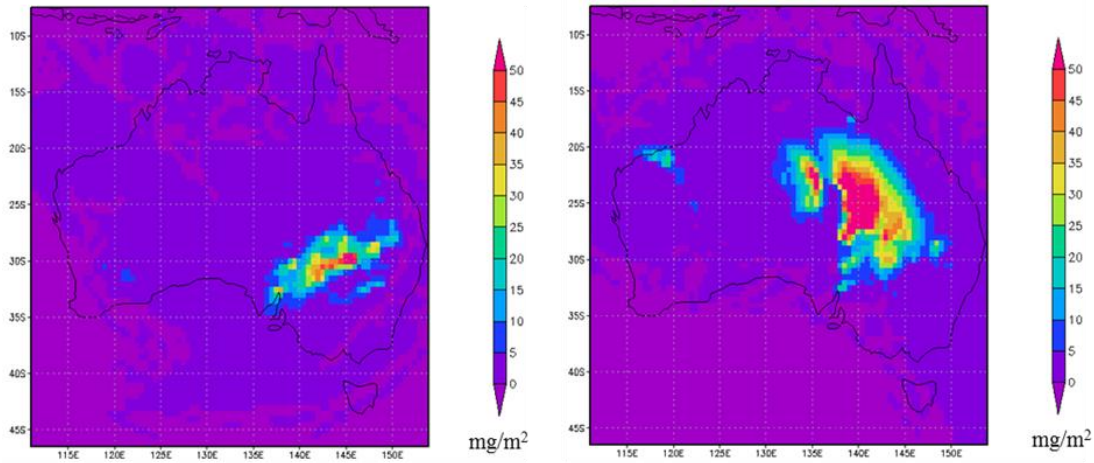

a) Predicted dust load for *CAVI* 1st November 1965 with maximum daily average dust load of 82 mg/m^2.

b) Predicted dust load for *CAVI* 9th November 1965 with maximum daily average dust load of 103 mg/m^2.

Figure 5.12: Spatial distribution and maximum daily average dust load of modelled dust storm events based on *CAVI* on the 1st, 9th – 11th, 16th – 17th November 1965. Figure continues over next page.

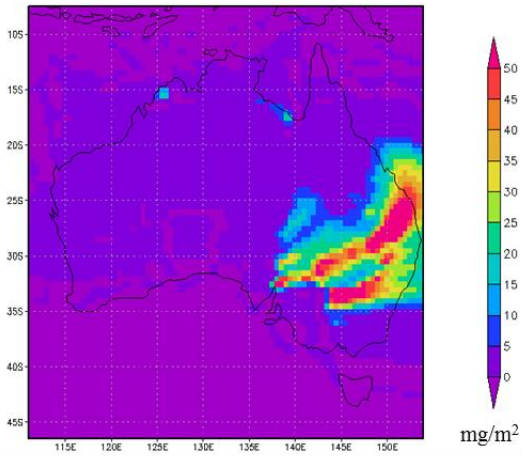

c) Predicted dust load for *CAVI* 10th November 1965 with maximum daily average dust load of 103 mg/m^2.

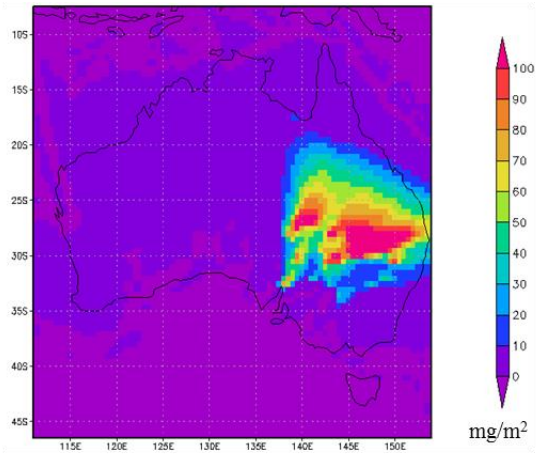

d) Predicted dust load for *CAVI* 11th November 1965 with maximum daily average dust load of 199 mg/m^2.

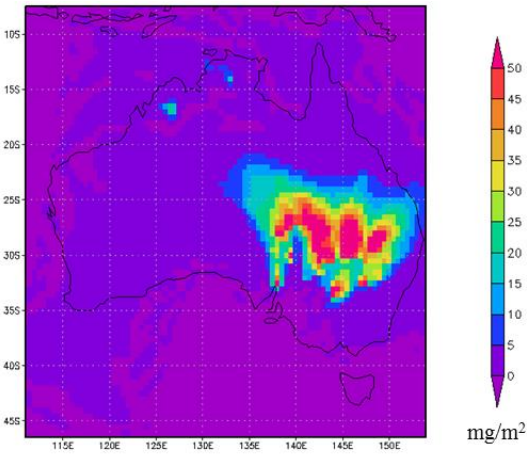

e) Predicted dust load for *CAVI* 16th November 1965 with maximum daily average dust load of 124 mg/m^2.

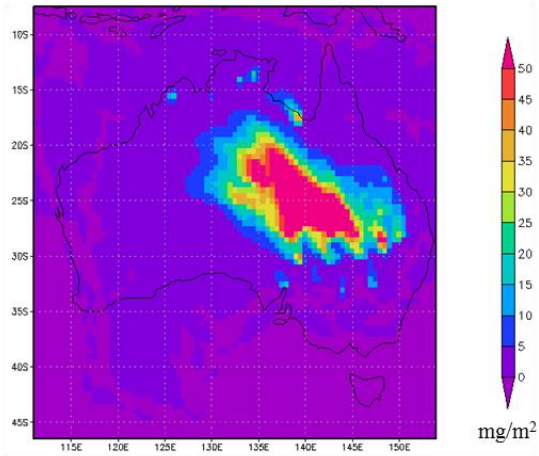

f) Predicted dust load for *CAVI* 17th November 1965 with maximum daily average dust load of 132 mg/m^2.

Figure 5.13: Spatial distribution and maximum daily average dust load of modelled dust storm events based on *CAVI* on the 1st, 9th – 11th, 16th – 17th November 1965.

A comparison of the modelled estimated maximum daily average dust load for November 1965 indicates that the dust storm on 11th November 1965 was more severe than on the 24th November 1965 (Table 5.3). The dust storm event on the 24th November seems to have originated from a number of dust source areas and was more widespread (Figure 5.9a), whereas the event on the 11th November 1965 was more concentrated in QLD, NSW and parts of SA regions (Figure 5.10d). A comparison of the *CAVI* based modelled maximum daily average dust load estimates of November 1965 (Table 5.3) with the September 2009 (Table 5.1) and October 2002 (Table 5.2) indicates that November 1965 and October 2002 were similar in magnitude in dust concentrations.

Both the HDED and DustWatch (2011d) reported a dust storm event during February 1983 which also has been modelled with *CAVI* but the modelled dust storm activity was not in the expected location in the *CAVI* simulation. Further investigation revealed that a frontal westerly weather system was present at 135° E but failed to move further east and instead was stationary for the entire three day period. Additional investigation into the 1983 atmospherics data and comparison of NECP/NCAR to 20th Century Reanalysis data revealed that the 1979 – 1992 sea level pressure data the ABoM supplied to NCEP/NCAR were incorrect and all other climate variables which are calculated based on the pressure data were therefore incorrect as well (Kalnay 1996; NOAA Research 2012). This mistake has been rectified but unfortunately the NCEP/NCAR reanalysis data set which is used in CEMSYS was not rerun with the corrected NCEP/NCAR sea level pressure data. The modified sea pressure data set has now been included in the NCEP/DOE Reanalysis II which has a 2.0 degree global resolution. The inclusion of finer resolution input data into the current structure of CEMSYS requires a modification of the code which was not possible at this point in time but is planned for the future.

The aim of Section 5.2 was to evaluate if it is feasible to substitute satellite based f_{PV} vegetation cover data with the *CAVI* as a surrogate for vegetation cover. The results from the study indicate that there is potential for *CAVI* to be used as a surrogate for f_{PV}. Similar spatial erosion characteristics have been observed but occasionally *CAVI* produces poor estimates and therefore it is likely that the dust intensity is underestimated. The difference in the modelled results is due to a number of factors as discussed in Section 5.2.1. Firstly, the *CAVI* index performs particularly well in arid to semi-arid regions of Australia which have generally lower rainfall levels all year and experience high temperatures during the wind erosion season (Spring – Summer) but underperforms in the autumn and winter months. The index has a tendency to overestimate green vegetation cover, predominantly in regions outside the arid and semi-arid zone that receive more regular rainfall. Secondly, satellite derived vegetation indices have certain limitation in arid to semi-arid regions due to their low sensitivity to low vegetation cover. Satellite data has a tendency to underestimate non-photosynthetic vegetation and overestimate bare soil. Therefore it is possible that f_{PV} based CEMSYS results overestimate the amount of eroded soil in arid and semi-arid areas and *CAVI* can overestimate vegetation cover in these regions. And thirdly, it is

likely that errors may arise from modelled and observed data and therefore the results are difficult to compare.

Chapter 6: Thesis Summary and Future Directions

6.1 Summary of Research Outcomes

In this chapter the main findings of each of the preceding chapters is summarised and areas of future work and development of these findings are suggested. There is a potential for increased frequency and intensity of wind erosion and dust storms causing serious land degradation in arid and semi-arid regions of Australia due to climate change. In this context the relationships between climate factors and vegetation cover are of great interest. Broad-scale estimation of spatial changes in vegetation cover is of value in many areas of research and land-use management.

The aim of this research was to investigate the historic relationship between climatic conditions and recorded dust storm events across Australia. This study also explored the relationship between climate variables and vegetation cover, in particular the potential for using long-term climate information to predict broad scale vegetation cover. As part of the research a vegetation cover index was developed and the validity of using this index as a surrogate for integrated wind erosion modelling was tested.

The five research objectives and the outcomes achieved in this research are itemized below:

1. To establish a Historical Dust Event Database (HDED) from a wide number of sources including personal experiences, diaries, book excerpts, newspaper clippings, journal articles, reports and others.
    - An extensive HDED has been established starting in 1852, spanning over 16 decades and documenting 587 dust storm events in Australia. The HDED will be made available on request. If funding comes available the HDED will be published online.
    - The number of documented historical dust storm sightings in the HDED indicate that the 1900s, 1940s, 1960s and 2000s were the most active wind erosion periods.
    - The actual number of dust storm events is likely to be higher as many may have past unnoticed and/or been unrecorded due to the sparse population in arid and semi-arid areas. Others might have been written down in diaries, letters etc. but have not been archived in museums or libraries (i.e. lost in the annals of time).

2. To compare the HDED to the climatic history of ENSO, rainfall and temperature to establish if dust event records match climate records.
    - Rainfall and temperature are closely linked to the ENSO cycle and directly impact on the vegetation cover which is a key factor driving the frequency, intensity and spatial distribution of dust events.
    - The HDED showed that an increased number of dust storm events were documented during years of intense droughts (1900s, 1940s, 1960s and 2000s) when rainfall was below average and temperatures above average for extended periods of time.

3. To develop a simple broad scale Climate Aridity Vegetation Index (*CAVI*) for the arid to semi-arid regions in Australia based solely on rainfall and temperature data. Secondly, to investigate if reliable spatial and temporal vegetation cover maps can be produced based on the *CAVI* without modelling individual vegetation type responses, seasonality and land-use.
    - The simple broad scale *CAVI* was developed based on weighted rainfall and temperature data.
    - Monthly remote sensed fractional cover data for both the photosynthetically active vegetation (green) fraction (f_{PV}) and the bare soil fraction (f_{BS}) were used to validate the performance of the *CAVI* from 2000 – 2012.
    - The index produced particularly good spatial and temporal vegetation cover maps across arid and semi-arid regions of Australia during the Spring – Summer wind erosion season.
    - The *CAVI* with f_{PV} correlation tends to be weaker during the first month of the wind erosion season (September – February).
    - The *CAVI* in the current development state has the tendency to over emphasise the relationship between rainfall, temperature and vegetation/green cover when increased rainfall occurs close to the month of interest and outside the arid and semi-arid regions.

4. To investigate and validate if the *CAVI* can be used as a surrogate for vegetation cover for integrated wind erosion modelling where no satellite remote sensing data is available.
    - The results from the study indicate that there is potential for *CAVI* to be used as a surrogate for f_{PV} or remotely sensed vegetation data.
    - Both the f_{PV} and *CAVI* based CEMSYS modelling results show similar spatial erosion characteristics but occasionally *CAVI* produces reduced estimates and therefore it is likely that the dust intensity is underestimated than results based on f_{PV}.
    - *CAVI* vegetation cover input data together with historical atmospheric data can be used to model any historical dust event periods of interest (i.e. 1940s & 1960s). This has previously never been possible since satellite derived f_{PV} vegetation cover data does not go back past 2000.
    - The *CAVI* performs particularly well in arid and semi-arid regions of Australia which have generally lower rainfall levels all year around and experience high temperatures during the wind erosion season (Spring – Summer) but underperforms in the autumn and winter months.

5. To discusses the usefulness of the *CAVI* and suggests possible improvements to the effectiveness of the index to allow for the modelling and mapping of vegetation cover for periods where rainfall and temperature data is available but satellite data and fine scale remote sensing data are not.
    - Vegetation cover information has a wide range of applications and is of particular interest and value in areas of environmental, ecological and land-use modelling.
    - The development of *CAVI* allows forecasting of vegetation cover into the future using modelled precipitation and temperature data.
    - The development of *CAVI* allows for modelling and mapping of vegetation cover where rainfall and temperature data is available but satellite data and fine scale environmental data are not.
    - With the development of *CAVI* it is now possible to model historical dust storm periods which has previously never been possible. The *CAVI* vegetation cover

information can be used to estimate the impact of past events and approximate the potential wind erosion risk in the future.

- The overall aim is to develop a *CAVI* that can be used universally without making it too complex. This could be achieved by firstly, including a correction factor for different types of vegetation cover across Australia.
- Secondly, a geographical correction for north – south or east – west across the continent might also improve the performance of *CAVI*.
- Thirdly, a correction for the different climate and/or vegetation zones in Australia may also improve the performance of *CAVI*.
- Fourthly, a sensitive analysis into the weighting factor applied to rainfall data to calculate the *CAVI* could improve the performance.
- Fifthly, a limiting or threshold factor that constrains the influence of extended periods of rainfall.

6.2 Future Research Directions

Vegetation cover information is valuable in climate and ecological research including regional and global carbon modelling, ecological assessment, and agricultural monitoring and wind erosion research. But since remote sensing information is a fairly recent technology and there is currently no simple, broadly applicable modelling method or index to realistically estimate and map vegetation cover levels in Australia, the following recommendations may increase the possible application and capability of *CAVI* to predict vegetation cover more accurately:

- Continue to update the HDED with additional dust storm records as they become available.
- The overall performance of *CAVI* may be improved by implementing the suggestions outlined in Point 5 above.
- Compare the performance of *CAVI* and CEMSYS with field data (e.g. DustWatch nodes, roadside survey observations etc.).
- The NCEP/NCAR Reanalysis data, which feeds into CEMSYS model, has a global grid size resolution of 2.5 degree but only started in 1948. Any years prior to 1948 need to be modelled with a 2.0 degree resolution data set and that requires the modification of some parts of the CEMSYS wind erosion modelling codes.

References

Advocate 1937, 'Miss Batten Held Up: Dust Storm delays Record Attempt', *Advocate*, Advocate.

Allan, R 1983, 'Monsoon and teleconnection variability over Australasia during the southern hemisphere summers of 1973-77', *American Meteorological Society*, vol. 111, no. 1, pp. 113-42.

Allan, R & D'Arrigo, R 1999, 'Persistent' ENSO Sequences: How unusual was the recent El Nino?', *The Holocene*, vol. 9, pp. 101-18.

Allan, R, Lindesay, J & Parker, D 1996, *El Niño Southern Oscillation & Climatic Variability*, CSIRO, Collingwood, Vic., Australia, 405.

Allan, R, Chambers, D, Drosdowsky, W, Hendon, H, Latif, M, Nicholls, N, Smith, I, Stone, R & Tourre, Y 2001, 'Is there an Indian Ocean dipole, and is it independent of the El Niño - Southern Oscillation?', *CLIVAR Exchanges*, vol. 6, no. 3, pp. 18-22.

Allan, R, Endfield, G, Damodaran, V, Adamson, G, Hannaford, M, Carroll, F, Macdonald, N, Groom, N, Jones, JW, Williamson, F, Hendy, E, Holper, P, Arroyo-Mora, JP, Hughes, L, Bickers, R & Bliuc, A 2016, 'Toward integrated historical climate research: the example of Atmospheric Circulation Reconstructions over the Earth', *Wiley Interdisciplinary Reviews: Climate Change*, 10.1002/wcc.379.

Arthur, C 2009, *Outback seagulls a long way from home*, 12 May 2014, <http://www.abc.net.au/news/2009-05-28/outback-seagulls-a-long-way-from-home/1696710>.

Aryal, R, Kandel, D, Acharya, D, Chong, MN & Beecham, S 2012, 'Unusual Sydney dust storm and its mineralogical and organic characteristics', *Environmental Chemistry*, vol. 9, no. 6, p. 537, 10.1071/en12131.

Aubault, H, Webb, NP, Strong, CL, McTainsh, GH, Leys, JF & Scanlan, JC 2015, 'Grazing impacts on the susceptibility of rangelands to wind erosion: The effects of stocking rate, stocking strategy and land condition', *Aeolian Research*, vol. 17, pp. 89-99, 10.1016/j.aeolia.2014.12.005.

AusCover 2012, *AVHRR NDVI (BoM) v2*, 3 March 2016, <www.auscover.org.au/xwiki/bin/view/.../AVHRR+NDVI+(BoM)+v2>.

Australasian Sketcher 1882, 'A Great Dust Storm', Argus Melbourne.

Australian Bureau of Statistics 1988, *Drought in Australia*, 18 February 2015, <http://www.abs.gov.au/AUSSTATS/abs@.nsf/lookup/1301.0Feature%20Article151988>.

Australian Bureau of Statistics 2011, *Australian National Accounts, National Income, Expenditure and Product*, Cat. Nos. 5204.0 and 5206.0,Australian Bureau of Statistics, Canberra.

Australian Government Land and Coasts 2010, *Monitoring and reporting on wind erosion fact sheet*, 2, Department of Environment , Water, Heritage and the Arts, Canberra, ACT.

Australian Weather News 2002, *Worst dust storm in decades sweeps across four states*, <http://www.australianweathernews.com/news/2002/10/20021023.htm>.

Bagnold, RA 1941, *The Physics of Blown Sand and Desert Dunes*, William Morrow & Company, New York.

Baltas, E 2007, 'Spatial distribution of climatic indices in northern Greece', *Meteorological Applications*, vol. 14, no. 1, pp. 69-78, 10.1002/met.7.

Barrier Miner 1895, 'A Melbourne Duststorm', Broken Hill, N.S.W.

Barrier Miner 1924, 'Monday's duststorm', Broken Hill, N.S.W.

Barrier Miner 1953, 'Red dust storm covers city', Broken Hill, N.S.W.

Barrier Miner 1954, 'Duststorm sweeps city; 15 pts. of rain', Broken Hill, N.S.W.

Barson, M & Leys, J 2009, 'Ground cover inputs for wind and water monitoring and modelling', in Ground cover monitoring for Australia - establishing a nationally coordinated approach to ground cover mapping: *Proceedings of theGround cover monitoring for Australia - establishing a nationally coordinated approach to ground cover mapping*, JB Stewart, et al. (eds.), Canberra, p. 48.

Bauer, E & Ganopolski, A 2014, 'Sensitivity simulations with direct shortwave radiative forcing by aeolian dust during glacial cycles', *Climate of the Past*, vol. 10, no. 4, pp. 1333-48, 10.5194/cp-10-1333-2014.

Belnap, J & Gillette, D 1998, 'Vulnerability of desert biological soil crusts to wind erosion: the influences of crust development, soil texture, and disturbance', *Journal of Arid Environments*, vol. 39, pp. 133-42.

Ben-Dor, E, Irons, J & Epema, G 1999, 'Soil reflectance', in A Renzc (ed.), *Remote sensing for Earth Sciences*, Wiley, New York, vol. 3, pp. 111-88.

Borrelli, P, Ballabio, C, Panagos, P & Montanarella, L 2014, 'Wind erosion susceptibility of European soils', *Geoderma*, vol. 232-234, pp. 471-8, 10.1016/j.geoderma.2014.06.008.

Bowler, J 1976, 'Aridity in Australia: Age, Origins and Expressipon in Aeolian Landforms and Sediments', *Earth Science Reviews*, vol. 12, pp. 279-310.

Bowman, A & Scott, B 2009, 'Managing ground cover in the cropping zone of southern NSW', *Primefacts*, vol. 957.

Boyd, PW, McTainsh, G, Sherlock, V, Richardson, K, Nichol, S, Ellwood, M & Frew, R 2004, 'Episodic enhancement of phytoplankton stocks in New Zealand subantarctic waters: Contribution of atmospheric and oceanic iron supply', *Global Biogeochemical Cycles*, vol. 18, no. 1, pp. n/a-n/a, 10.1029/2002gb002020.

Bullard, JE, McTainsh, GH & Pudmenzky, C 2004, 'Aeolian abrasion and modes of fine particle production from natural red dune sands: an experimental study', *Sedimentology*, vol. 51, no. 5, pp. 1103-25, 10.1111/j.1365-3091.2004.00662.x.

Bullard, JE, McTainsh, GH & Pudmenzky, C 2007, 'Factors affecting the nature and rate of dust production from natural dune sands', *Sedimentology*, vol. 54, no. 1, pp. 169-82, 10.1111/j.1365-3091.2006.00827.x.

Bureau of Meteorology 2006, *About Dust*, 5 February 2014, <http://www.bom.gov.au/nsw/sevwx/facts/dust.shtml>.

Bureau of Meteorology 2014, *ENSO Wrap-Up*, 8/04/2014, <http://www.bom.gov.au/climate/enso/index.shtml>.

Bureau of Meteorology 2015, *Tropical Cyclone Alby: 4 April 1978*, 2 August 2015, <http://www.bom.gov.au/cyclone/history/wa/alby.shtml>.

Bureau of Meteorology 2016, *Australia in March 2016*, 4 April 2016, <http://www.bom.gov.au/climate/current/month/aus/summary.shtml>.

Bureau of Meteorology & CSIRO 2012, *State of the Climate 2012*, 12, Commonwealth of Australia.

Bureau of Meteorology & CSIRO 2014, *State of the Climate 2014*, Commonwealth of Australia.

Burgess, R, McTainsh, G & Pitblado, J 1989, 'An index of wind erosion in Australia', *Australian Geographical Studies*, vol. 27, no. 1, pp. 98-110.

Butler, HJ, Shao, Y., Leys, JF & McTainsh, GH 2007, *Modelling Wind Erosion at National & Regional Scale using the CEMSYS Model*, 1-38, National Land & Water Resources Audit, Canberra.

Cai, W, van Rensch, P, Cowan, T & Sullivan, A 2010, 'Asymmetry in ENSO Teleconnection with Regional Rainfall, Its Multidecadal Variability, and Impact', *Journal of Climate*, vol. 23, no. 18, pp. 4944-55, 10.1175/2010jcli3501.1.

Cai, W, Purich, A, Cowan, T, van Rensch, P & Weller, E 2014, 'Did Climate Change–Induced Rainfall Trends Contribute to the Australian Millennium Drought?', *Journal of Climate*, vol. 27, no. 9, pp. 3145-68, 10.1175/jcli-d-13-00322.1.

Cairns Post 1951, 'New planes land in dust storm - Disaster averted', News Limited, Cairns.

Carter, JO, Hall, W, Brook, KD, McKeon, G, Day, KA & Paull, CJ 2000, 'Aussie GRASS: Australian grassland and rangeland assessment by spatial simulation', in G Hammer, et al. (eds), *The Australian Experience*, Kluwer Academic, Netherlands, pp. 329-49.

Chan, Y, McTainsh, G, Leys, J & McGowan, H 2005, 'Influence of the 23 October 2002 Dust Storm on the Air Quality of Four Australian Cities', *Water, Air, and Soil Pollution*, vol. 164, pp. 329-48.

Chapman, F & Grayson, HJ 1903, 'On red rain with special reference to its occurrence in Victoria. With a note on Melbourne dust', *The Victorian Naturalist*, vol. 20, pp. 17-32.

Chappell, A 2013, 'Improving the spatio-temporal erodibility of dust emission models using MODIS data', in AGU Fall Meeting: *Proceedings of the AGU Fall Meeting* San Francisco, p. 1.

Chappell, A, Webb, NP, Butler, HJ, Strong, CL, McTainsh, GH, Leys, JF & Viscarra Rossel, RA 2013, 'Soil organic carbon dust emission: an omitted global source of atmospheric CO2', *Global Change Biology*, vol. 19, no. 10, pp. 3238-44, 10.1111/gcb.12305.

Chepil, W 1965, 'Transport of soil and snow by wind', *Meteorological Monographs*, vol. 6, no. 28, pp. 123-32.

Chepil, W & Woodruff, R 1963, 'The physics of wind erosion and its control', *Advances in Agronomy*, vol. 19, pp. 211-302.

Choobari, OA, Zawar-Reza, P & Sturman, A 2014, 'The global distribution of mineral dust and its impacts on the climate system: A review', *Atmospheric Research*, vol. 138, pp. 152-65, 10.1016/j.atmosres.2013.11.007.

Clacey, C 1853, *A Lady's Visit to the Gold Diggings of Australia in 1852-53*, Hurst and Blackett, London, 134.

Compo, GP & Sardeshmukh, PD 2010, 'Removing ENSO-Related Variations from the Climate Record', *Journal of Climate*, vol. 23, no. 8, pp. 1957-78, 10.1175/2009jcli2735.1.

Cork, S, Eadie, L, Mele, P, Price, R & Yule, D 2012, *The relationships between land management practices and soil condition and the quality of ecosystem services delivered from agricultural land in Australia*, 128, Kiri-ganai Research Pty Ltd, Canberra.

Cropp, RA, Gabric, AJ, Levasseur, M, McTainsh, G, Bowie, A, Hassler, C, Law, C, McGowan, H, Tindale, N & Viscarra Rossel, R 2013, 'The likelihood of observing dust-stimulated phytoplankton growth in waters proximal to the Australian continent', *Journal of Marine Systems*, vol. 117-118, pp. 43-52.

CSIRO 2011, *Climate change : Science and Solutions for Australia*, CSIRO Publishing, Melbourne.

Darwin, C 1839, *The Voyage of the Beagle*, Wordsworth, Hertfordshire, Great Britain, 481.

Davies, D, Kumar, S & Desclorites, J 2004, 'Global fire monitoring using MODIS near-real-time satellite data', *GIM International*, vol. 18, no. 4, pp. 41-3.

De Deckker, P, Norman, M, Goodwin, ID, Wain, A & Gingele, FX 2010, 'Lead isotopic evidence for an Australian source of aeolian dust to Antarctica at times over the last 170,000years', *Palaeogeography, Palaeoclimatology, Palaeoecology*, vol. 285, no. 3-4, pp. 205-23, 10.1016/j.palaeo.2009.11.013.

De Martonne, E 1926, 'Aréisme et indice artidite', *Comptes Rendus de L'Acad Sci*, vol. 182, pp. 1395-8.

Deloitte Access Economics 2014, *Scoping Study on a Cost Benefit Analysis of Bushfire Mitigation*, 65, Australian Forest Products Association, Sydney.

Delworth, TL & Zeng, F 2014, 'Regional rainfall decline in Australia attributed to anthropogenic greenhouse gases and ozone levels', *Nature Geoscience*, vol. 7, no. 8, pp. 583-7, 10.1038/ngeo2201.

Dineley, J 2013, 'On this day: Melbourne's monster dust storm', *Australian Geographic*, vol. 112.

Dommenget, D, Semenov, V & Latif, M 2006, 'Impacts of the tropical Indian and Atlantic Oceans on ENSO', *Geophysical Research Letters*, vol. 33, no. 11, 10.1029/2006gl025871.

Donohue, RJ, McVicar, TR & Roderick, ML 2009, 'Climate-related trends in Australian vegetation cover as inferred from satellite observations, 1981-2006', *Global Change Biology*, vol. 15, no. 4, pp. 1025-39, 10.1111/j.1365-2486.2008.01746.x.

Downs, N, Butler, H & Parisi, A 2016, 'Solar ultraviolet attenuation during the Australian (Red Dawn) dust event of 23 September 2009', *Bulletin of the American Meteorological Society*, vol. in Press, 10.1175/BAMS-D-15-00053.1.

Durdin, J 2010, *Mary Jacob's Diary May 1866 - March 1867*, 17.

DustWatch 2011a, *DustWatch Australia, Dust Storm File: 23 September 2009*.

DustWatch 2011b, *DustWatch Australia, Dust Storm File: 23 October 2002*.

DustWatch 2011c, *DustWatch Australia, Dust Storm File: 25 November 1965*.

DustWatch 2011d, *DustWatch Australia, Dust Storm File: 8 February 1983*.

Edwards, B, Gray, B & Hunter, B 2008, *Social and economic impacts of drought on farm families and rural communities*, 27, Submission to the Productivity Commission's Inquiry into Government Drought SupportAustralian Institute of Family Studies, Melbourne, Vic.

Ekström, M, McTainsh, GH & Chappell, A 2004, 'Australian dust storms: temporal trends and relationships with synoptic pressure distributions (1960-99)', *International Journal of Climatology*, vol. 24, no. 12, pp. 1581-99, 10.1002/joc.1072.

Eldridge, D 2003, 'Exploring some relationships between biological soil crusts, soil aggregation and wind erosion', *Journal of Arid Environments*, vol. 53, no. 4, pp. 457-66, 10.1006/jare.2002.1068.

Evans, J & Allan, R 1992, 'El Nino/southern oscillation modification to the structure of the monsoon and tropical cyclone activity in the Australasian region', *International Journal of Climatology*, vol. 12, no. 6, pp. 611-23.

Frauen, C & Dommenget, D 2012, 'Influences of the tropical Indian and Atlantic Oceans on the predictability of ENSO', *Geophysical Research Letters*, vol. 39, no. 2, p. 6, 10.1029/2011gl050520.

Gabric, AJ, Cropp, R, McTainsh, G, Butler, H, Johnston, BM, O'Loingsigh, T & Van Tran, D 2015, 'Tasman Sea biological response to dust storm events during the austral spring of 2009', *Marine and Freshwater Research*, vol. 67, no. 8, pp. 1090 - 102, 10.1071/mf14321.

Gallant, A, Hennessy, K & Risbey, J 2007, 'Trends in rainfall indices for six Australian regions: 1910-2005', *Australian Meteorological Magazine*, vol. 56, pp. 223-39.

Gergis, J, Karoly, D & Allan, R 2009, 'A climate reconstruction of Sydney Cove, New South Wales, using weather journal and documentary data, 1788–1791', *Australian Meteorological and Oceanographic Journal*, vol. 58, pp. 83-98.

Gergis, J, Brohan, P & Allan, R 2010, 'The weather of the First Fleet voyage to Botany Bay, 1787–1788', *Royal Meteorological Society*, vol. 65, no. 12, pp. 315-9.

Gergis, JL & Fowler, AM 2009, 'A history of ENSO events since A.D. 1525: implications for future climate change', *Climatic Change*, vol. 92, no. 3-4, pp. 343-87, 10.1007/s10584-008-9476-z.

Giglio, L, Desclorites, J, Justice, C & Kaufman, YJ 2003, 'An enhanced contextual fire detection algorithm for MODIS', *Remote Sensing of Environment*, vol. 87, pp. 273-82.

Gill, T, Heidenreich, S & Guerschman, JP 2014, *MODIS Monthly Fractional Cover*, 10, Joint Remote Sensing Research Program Publication Series.

Goudie, AS 2009, 'Dust storms: Recent developments', *J Environ Manage*, vol. 90, no. 1, pp. 89-94, item: 18783869, 10.1016/j.jenvman.2008.07.007.

Government of South Australia 2007, *Atlas of South Australia*, 27 November 2015, <http://www.atlas.sa.gov.au/go/resources/environments-of-south-australia>.

Guerschman, JP, Hill, MJ, Renzullo, LJ, Barrett, DJ, Marks, AS & Botha, EJ 2009, 'Estimating fractional cover of photosynthetic vegetation, non-photosynthetic vegetation and bare soil in the Australian tropical savanna region upscaling the EO-1 Hyperion and MODIS sensors', *Remote Sensing of Environment*, vol. 113, no. 5, pp. 928-45, 10.1016/j.rse.2009.01.006.

Guerschman, JP, Oyarzábal, M, Malthus, TJ, McVicar, TR, Byrne, G, Randall, LA & Stewart, JB 2012, *Evaluation of the MODIS-based vegetation fractional cover product*, 40, National Research Flagships Sustainable Agriculture CSIROAustralian Government, Department of Agriculture, Fisheries and Forestry, ABARES, Canberra.

Hagen, LJ 1991, 'A wind erosion prediction system to meet user needs', *Journal of Soil and Water Conservation*, vol. 46, pp. 106-11.

Harris, M 1956, *Darbys Falls - Margaret Harris' Diary 1934-1956*, 14 August 2013, <http://www.frankmurray.com.au/?page_id=4368>.

Harrison, S, Kohfeld, K, Roelandt, C & Claquin, T 2001, 'The role of dust in climate changes today, at the last glacial maximum and in the future', *Earth Science Reviews*, vol. 54, pp. 43-80.

Hesse, P & McTainsh, G 2003, 'Australian dust deposits: modern processes and the Quaternary record', *Quaternary Science Reviews*, vol. 22, no. 18-19, pp. 2007-35, 10.1016/s0277-3791(03)00164-1.

Hui, WJ, Cook, BI, Ravi, S, Fuentes, JD & D'Odorico, P 2008, 'Dust-rainfall feedbacks in the West African Sahel', *Water Resources Research*, vol. 44, no. 5, 10.1029/2008wr006885.

IPCC 2001, *Climate Change 2001: The Scientific Basis. Contribution of Working Group I to the Third Assessment Report of the Intergovernmental Panel on Climate Change*, 881, Cambridge, United Kingdom and New York, NY, USA.

IPCC 2013, *Summary for Policymakers*, Climate Change 2013: The Physical Science Basis. Contribution of Working Group I to the Fifth Assessment Report of the Intergovernmental Panel on Climate ChangeCambridge, United Kingdom and New York, NY, USA.

IPCC 2014, *Climate Change 2014: Impacts, Adaptation, and Vulnerability. Part A: Global and Sectoral Aspects. Contribution of Working Group II to the Fifth Assessment Report of the Intergovernmental Panel on Climate Change*, 1132, Cambridge, United Kingdom and New York, NY, USA.

Jaeger, K 1988, 'An Account of a Major Dust Storm in Inland Australia during November 1965', Honours thesis, Griffith University, Nathan, Brisbane.

Johnson, R & Burrows, W 1994, 'Acacia open-forests, woodlands and shrublands', in R Groves (ed.), *Australian Vegetation*, Cambridge University Press, Cambridge, vol. 2. Edition, pp. 257–90.

Journet, E, Balkanski, Y & Harrison, SP 2014, 'A new data set of soil mineralogy for dust-cycle modeling', *Atmospheric Chemistry and Physics*, vol. 14, no. 8, pp. 3801-16, 10.5194/acp-14-3801-2014.

Kalnay, E 1996, *The Problem with PAOBS*, 17 December 2015, <http://www.cpc.ncep.noaa.gov/products/wesley/paobs/paobs.html>.

Klein, D & Roehrig, J 2006, 'How does vegetation cover respond to rainfall variability in a semi-humid West African in comparison to a semi-arid East African environment?', in Proceedings of the 2nd Workshop of the EARSeL SIG on Land Use and Land Cover: *Proceedings of theProceedings of the 2nd Workshop of the EARSeL SIG on Land Use and Land Cover* Bonn, Germany, pp. 149-56.

Knight, A, McTainsh, G & Simpson, R 1995, 'Sediment loads in an Australian dust storm: implications for present and past dust processes', *Catena*, vol. 24, pp. 195-213.

Kok, JF, Parteli, E, Michaels, T & Bou Karam, D 2012, 'The physics of windblown sand and dust', *Reports on Progress in Physics*, vol. 75, p. 119.

Lamb, PJ, Leslie, LM, Timmer, RP & Speer, MS 2009, 'Multidecadal variability of Eastern Australian dust and Northern New Zealand sunshine: Associations with Pacific climate system', *Journal of Geophysical Research*, vol. 114, no. D9, p. 12, 10.1029/2008jd011184.

Lawley, E, Lewis, M & Ostendorf, B 2015, 'Evaluating MODIS soil fractional cover for arid regions, using albedo from high-spatial resolution satellite imagery', *International Journal of Remote Sensing*, vol. 35, no. 6, pp. 2028-46, 10.1080/01431161.2014.885150.

Leslie, L & Wightwick, G 1995, 'A new limited-area numerical weather prediction model for operations and research: formulation and assessment', *Monthly Weather Reviews*, vol. 123, pp. 1759-75.

Leys, J 2003, *Farming Ahead - Cropping Wind erosion: Prevent valuable soil from blowing away*, 4, Department Infrastructure, Planning and Natural Resources.

Leys, J & Raupach, M 1991, 'Soil flux measurements using a portable wind erosion tunnel', *Australian Journal of Soil Research*, vol. 29, no. 4, pp. 533-52.

Leys, J, McTainsh, G & Shao, Y 1999, 'Wind Erosion Monitoring and Modeling Techniques in Australia', in 10th International Soil Conservation Meeting: *Proceedings of the10th International Soil Conservation Meeting*, DE Stott, et al. (eds.), Purdue University and the USDA-ARS National Soil Erosion Reserach Laboratory, pp. 940-50.

Leys, J, Heidenreich, S & Case, M 2009, *DustWatch report for week ending 28 September 2009* 6.

Leys, J, Butler, H, Yang, X & Heidenreich, S 2010, *CEMSYS modelled wind erosion*, 91, NSW Department of Environment, Climate Change and Water, Sydney South, Australia.

Leys, J, Butler, H, Strong, C & McTainsh, G 2011a, *Caring For Our Country - Wind Erosion Extent And Severity Maps Of Australia (WEESMap) Milestone 4 Project Progress Report Friday 2 December, 2011*, 43, NSW Government Office of Environment & Heritage, Sydney, Australia.

Leys, J, McTainsh, G, Strong, C, Heidenreich, S & Biesaga, K 2008, 'DustWatch: using community networks to improve wind erosion monitoring in Australia', *Earth Surface Processes and Landforms*, vol. 33, no. 12, pp. 1912-26, 10.1002/esp.1733.

Leys, J, Heidenreich, S, Strong, CL, McTainsh, G & Quigley, S 2011b, 'PM10 concentrations and mass transport during "Red Dawn" – Sydney 23 September 2009', *Aeolian Research*, vol. 3, no. 3, pp. 327-42, 10.1016/j.aeolia.2011.06.003.

Leys, J, Smith, J, MacRae, C, Rickards, J, Yang, X, Randall, L, Hairsine, P, Dixon, J & McTainsh, G 2009, *Improving the capacity to monitor wind and water erosion: A Review*, 1-160, Australian Government Department of Agriculture, Fisheries and Forestry.

Liversidge, A 1902, 'Meteoric dusts, New South Wales', *Journal of the Proceedings of the Royal Society of NSW*, vol. 36, pp. 241-85.

Lopes dos Aantos, RA, De Deckker, P, Hopmans, E, Magee, J, Mets, A, Sinninghe Damsté, J & Schouten, L 2013, 'Abrupt vegetation change after the Late Quaternary megafaunal extinction in southeastern Australia', *Nature Geoscience*, vol. 6, pp. 627-31, 10.1038/ngeo1856.

Love, G 2005, 'Impacts of Climate Variability on Regional Australia', in ABARE Outlook Conference Proceedings (National Agricultural and Resources Outlook Conference Proceedings): *Proceedings of theABARE Outlook Conference Proceedings (National Agricultural and Resources Outlook Conference Proceedings)* Australian Government Department of Agriculture, Fisheries and Forestry, Canberra, pp. 10-9.

Macinnis-Ng, C & Eamus, D 2007, *The increasing density of shrubs and trees across a landscape*, 16, University of Technology Sydney.

Maliva, R & Missimer, T 2012, 'Aridity and Drought', in *Arid Lands Water Evaluation and Management*, Springer, Berlin Heidelberg, ch 2, pp. 21-39.

Malthus, TJ, Barry, S, Randall, L, McVicar, T, Bordas, VM, Stewart, JB, Guerschman, JP & Penrose, L 2013, *Ground cover monitoring for Australia: Sampling strategy and selection of ground cover control sites*, CSIRO, Australia.

Martin, HA 2006, 'Cenozoic climatic change and the development of the arid vegetation in Australia', *Journal of Arid Environments*, vol. 66, no. 3, pp. 533-63, 10.1016/j.jaridenv.2006.01.009.

Marx, SK, McGowan, HA & Kamber, BS 2009, 'Long-range dust transport from eastern Australia: A proxy for Holocene aridity and ENSO-type climate variability', *Earth and Planetary Science Letters*, vol. 282, no. 1-4, pp. 167-77, 10.1016/j.epsl.2009.03.013.

McGowan, H & Clark, A 2008, 'Identification of dust transport pathways from Lake Eyre, Australia using Hysplit', *Atmospheric Environment*, vol. 42, no. 29, pp. 6915-25, 10.1016/j.atmosenv.2008.05.053.

McGowan, H, McTainsh, G, Zawar-Reza, P & Sturman, P 2000, 'Identifying regional dust transport pathways: application of kinematic trajectory modelling to a trans-Tasman case', *Earth Surface Processes and Landforms*, vol. 25, pp. 633–47.

McTainsh, G 1985, 'Desertification and dust monitoring in West Africa', *Desertification Control Bulletin*, vol. 12, pp. 26-33.

McTainsh, G 1989, 'Quaternary aeolian dust processes and sediments in the Australian region', *Quaternary Science Reviews*, vol. 8, no. 3, pp. 235-53.

McTainsh, G & Pitbaldo, J 1987, 'Dust storms and related phenomena measured from meteorological records in Australia', *Earth Surface Processes and Landforms*, vol. 12, pp. 415-24.

McTainsh, G & Boughton, WC 1993, *Land Degradation Processes in Australia*, Longman Cheshire, Melbourne, Australia.

McTainsh, G & Tews, K 2007, *Soil erosion by wind - Dust Storm Index (DSI)*, 1-28, National Monitoring and Evaluation Framework, Griffith University.

McTainsh, G & Strong, C 2007, 'The role of aeolian dust in ecosystems', *Geomorphology*, vol. 89, no. 1-2, pp. 39-54, 10.1016/j.geomorph.2006.07.028.

McTainsh, G, Lynch, A & Tews, K 1998, 'Climatic controls upon dust storm occurrence in eastern Australia', *Journal of Arid Environments*, vol. 39, pp. 457-66.

McTainsh, G, Tews, K, Leys, J & Bastin, G 2007, *Spatial and temporal trends in wind erosion of Australian rangelands during 1960 to 2005 using the Dust Storm Index (DSI)*, 25, A Report for the Australian Collaborative Rangeland Information System [ACRIS]; Griffith University.

McTainsh, G, Leys, J, O'Loingsigh, T & Strong, C 2011, *Wind erosion and land management in Australia during 1940-1949 and 2000-2009*, 48, Report prepared for the Australian Government Department of Sustainability, Environment, Water, Population and Communities on behalf of the State of the Environment 2011 Committee; Canberra.

McTainsh, G, Chan, Y, McGowan, H, Leys, J & Tews, K 2005, 'The 23rd October 2002 dust storm in eastern Australia: characteristics and meteorological conditions', *Atmospheric Environment*, vol. 39, no. 7, pp. 1227-36, 10.1016/j.atmosenv.2004.10.016.

Mezösi, G & Szatmári, J 1998, 'Assessment of wind erosion risk on the agricultural area of the southern part of Hungary', *Journal of Hazardous Materials*, vol. 61, pp. 139-53.

Middleton, N 1984, 'Dust storms in Australia: frequency, distribution and seasonality', *Search*, vol. 15, pp. 46-7.

Miller, RL & Tegen, I 1998, 'Climate Response to Soil Dust Aerosols', *Journal of Climate*, vol. 11, pp. 3247-67.

Mills, M, Ridame, C & Davey, M 2004, 'Iron and phosphorus co-limit nitrogen fixation in the eastern tropical North Atlantic', *Nature*, vol. 429, pp. 292-4.

Mott, J & Groves, R 1994, 'Natural and derived grasslands', in R Groves (ed.), *Australian Vegetation*, Cambridge, Cambridge University Press, pp. 369–92.

Nicholls, N 1985, 'Towards the prediction of major Australian droughts', *Australian Meteorological Magazine*, vol. 33, no. 4, pp. 161-6.

Nicholls, N 1988, 'More on Early ENSOs: Evidence from Australian Documentary Sources', *American Meteorological Society*, vol. 69, no. 1, pp. 4-6.

Nicholls, N 2006, 'Detecting and attributing Australian climate change: a review', *Australian Meteorological Magazine*, vol. 55, no. 3, pp. 199-211.

Nicholls, N 2009, *Inquiry into Long-term Meteorological Forecasting in Australia*, 8, Submission to the House of Representatives Industry, Science and Innovation Committee, Clayton, VIC 3800.

Nicholls, N & Wong, K 1990, 'Dependence of Rainfall Variability on Mean Rainfall, Latitude, and the Southern Oscillation', *Journal of Climate*, vol. 3, no. 1, pp. 163-70.

NOAA Research 2012, *NCEP/NCAR Reanalysis Problems List*, 17 December 2015, <http://www.esrl.noaa.gov/psd/data/reanalysis/problems.shtml >.

NSW Department of Primary Industries 2013, *What are C3 and C4 Native Grass?*, 3 June 2015, <http://www.dpi.nsw.gov.au/agriculture/pastures/pastures-and-rangelands/native-pastures/what-are-c3-and-c4-native-grass>.

NSW Government Office of Environment and Heritage 2014, *Wind erosion*, 21 January 2015, <http://www.environment.nsw.gov.au/soildegradation/winder.htm>.

O'Loingsigh, McTainsh, G, Parsons, K, Strong, C, Shinkfield, P & Tapper, NJ 2015, 'Using meteorological observer data to compare wind erosion during two great droughts in eastern Australia; the World War II Drought (1937-1946) and the Millennium Drought (2001-2010)', *Earth Surface Processes and Landforms*, vol. 40, no. 1, pp. 123-30.

O'Loingsigh, T, McTainsh, GH, Tapper, NJ & Shinkfield, P 2010, 'Lost in code: A critical analysis of using meteorological data for wind erosion monitoring', *Aeolian Research*, vol. 2, no. 1, pp. 49-57, 10.1016/j.aeolia.2010.03.002.

O'Shaughnessy, T 1903, *The Diary of Thomas O'Shaughnessy, 1835-1903*, 14 August 2013, <http://www.frankmurray.com.au/?page_id=457>.

Paltineanu, C, Tanasescu, N, Chitu, E & Mihailescu, I 2007, 'Relationships between the De Martonne aridity index and water requirements of some representative crops: A case study from Romania', *International Agrophysics*, vol. 21, pp. 81-93.

Peel, P, Finlayson, B & McMahon, T 2007, 'Updated world map of the Köppen-Geiger climate classification', *Hydrology and Earth System Sciences*, vol. 11, pp. 1633-44.

Power, S 2014, 'Climate Science: Expulsion from history', *Nature*, vol. 511, no. 7507, pp. 38-9.

Power, S, Haylock, M, Colman, D & Wang, B 2006, 'The Predictability of Interdecadal Changes in ENSO Activity and ENSO Teleconnections', *Journal of Climate*, vol. 19, pp. 4755-71.

Power, SB & Smith, IN 2007, 'Weakening of the Walker Circulation and apparent dominance of El Niño both reach record levels, but has ENSO really changed?', *Geophysical Research Letters*, vol. 34, no. 18, pp. 945-51, 10.1029/2007gl030854.

Prospero, J, Ginoux, P & Torres, O 2002, 'Environmental characterization of global sources of atmospheric soil dust identified with the nimbus 7 total ozone mapping spectrometer (TOMS) absorbing aerosol product', *Reviews of Geophysics*, vol. 40, no. 1, pp. 1-31, 10.1029/2000RG000095.

Pudmenzky, C, King, R & Butler, H 2015, 'Broad scale mapping of vegetation cover across Australia from rainfall and temperature data', *Journal of Arid Environments*, vol. 120, pp. 55-62, 10.1016/j.jaridenv.2015.04.010.

Pulido-Villena, E, Rerolle, V & Guieu, C 2010, 'Transient fertilizing effect of dust in P-deficient LNLC surface ocean', *Geophysical Research Letters*, vol. 37, p. L01603.

Pye, K 1987, *Aeolian Dust and Dust Deposits*, Academic Press, Inc., London, 334.

Qin, Y & Mitchell, R 2009, 'Characterisation of episodic aerosol types over the Australian continent', *Atmospheric Chemistry and Physics*, vol. 9, pp. 1943-56.

Queensland Government Department of Agriculture and Fisheries 2015, *Drought declarations* 15 February 2016, <https://www.longpaddock.qld.gov.au/queenslanddroughtmonitor/queenslanddroughtreport/>.

Radhi, M, Box, GP, Mitchell, R, Cohen, DD, Stelcer, E & Keywood, M 2010, 'Optical, physical and chemical characteristics of Australian continental aerosols: results from a field experiment', *Atmospheric Chemistry and Physics*, vol. 10, pp. 5925-42, 10.5194/acp-10-5925-2010.

Raupach, M & Lu, H 2004, 'Representation of land-surface processes in aeolian transport models', *Environmental Modelling & Software*, vol. 19, no. 2, pp. 93-112, 10.1016/s1364-8152(03)00113-0.

Raupach, M, McTainsh, G & Leys, J 1994, 'Estimates of dust mass in recent major Australian dust storms', *Australian Journal of Soil and Water Conservation*, vol. 7, pp. 20-4.

Reason, CJC, Allan, R, Lindsay, J & Ansell, T 2000, 'ENSO and climate signals across the Indian Ocean Basin in the global context: Part 1, interannual composite patterns', *International Journal of Climatology*, vol. 20, pp. 1285-327.

Reeder, M & Smith, R 1998, 'Mesoscale Meteorology', in D Karoly & D Vincent (eds), *Meteorology of the Southern Hemisphere*, Springer, ch 5, pp. 201-41.

Revelrolland, M, De Deckker, P, Delmonte, B, Hesse, P, Magee, J, Basiledoelsch, I, Grousset, F & Bosch, D 2006, 'Eastern Australia: A possible source of dust in East Antarctica interglacial ice', *Earth and Planetary Science Letters*, vol. 249, no. 1-2, pp. 1-13, 10.1016/j.epsl.2006.06.028.

Reynolds, RL, Cattle, SR, Moskowitz, BM, Goldstein, HL, Yauk, K, Flagg, CB, Berquó, TS, Kokaly, RF, Morman, S & Breit, GN 2014, 'Iron oxide minerals in dust of the Red Dawn event in eastern Australia, September 2009', *Aeolian Research*, pp. 1-13, 10.1016/j.aeolia.2014.02.003.

Risbey, J, McIntosh, PC, Pook, MJ, Rashid, H & Hirst, AC 2011, 'Evaluation of rainfall drivers and teleconnections in an ACCESS AMIP run', *Australian Meteorological and Oceanographic Journal*, vol. 61, pp. 91-105.

Risbey, JS, Pook, MJ, McIntosh, PC, Wheeler, MC & Hendon, HH 2009, 'On the Remote Drivers of Rainfall Variability in Australia', *Monthly Weather Review*, vol. 137, no. 10, pp. 3233-53, 10.1175/2009mwr2861.1.

Rotstayn, LD, Keywood, MD, Forgan, BW, Gabric, AJ, Galbally, IE, Gras, JL, Luhar, AK, McTainsh, GH, Mitchell, RM & Young, SA 2009, 'Possible impacts of anthropogenic and natural aerosols on Australian climate: a review', *International Journal of Climatology*, vol. 29, no. 4, pp. 461-79, 10.1002/joc.1729.

Rutherford, S, Macintosh, K, Jarvinen, K, McTainsh, G & Chan, A 2003, 'Characterisation and health impacts of the October 2002 dust event in Queensland: a preliminary investigation', in Clean Air Society of Australia and New Zealand: Newcastle: *Proceedings of the Clean Air Society of Australia and New Zealand: Newcastle* Newcastle, NSW.

Shao, Y 2008, *Physics and Modelling of Wind Erosion*, 2. edn, vol. 37, Springer.

Shao, Y & Leslie, LM 1997, 'Wind erosion prediction over the Australian continent', *Journal of Geophysical Research*, vol. 102, no. D25, p. 30091, 10.1029/97jd02298.

Shao, Y, Raupach, M & Leys, J 1996, 'A model for predicting aeolian sand drift and dust entrainment on scales from paddock to region', *Australian Journal of Soil Research*, vol. 34, pp. 309-42.

Shao, Y, McTainsh, G, Leys, J & Raupach, M 1993, 'Efficiencies of sediment samplers for wind erosion measuring', *Australian Journal of Soil Research*, vol. 31, pp. 519-32.

Shao, Y, Leys, J, McTainsh, GH & Tews, K 2007, 'Numerical simulation of the October 2002 dust event in Australia', *Journal of Geophysical Research*, vol. 112, no. D8, 10.1029/2006jd007767.

Shao, Y, Wyrwoll, K-H, Chappell, A, Huang, J, Lin, Z, McTainsh, GH, Mikami, M, Tanaka, TY, Wang, X & Yoon, S 2011, 'Dust cycle: An emerging core theme in Earth system science', *Aeolian Research*, pp. 181–204, 10.1016/j.aeolia.2011.02.001.

Shein, KA 2006, 'State of the Climate 2005', *Bulletin of the American Meteorological Society*, vol. 87, no. S1-S102, p. 102.

Smith, J & Leys, J 2009, *Identification of areas within Australia for reducing soil loss by wind erosion*, 31, The Australian Government Bureau of Rural Sciences.

Sokolik, IN & Toon, OB 1999, 'Incorporation of mineralogical composition into models of the radiative properties of mineral aerosol from UV to IR wavelengths', *Journal of Geophysical Research*, vol. 104, no. D8, pp. 9423-44, 10.1029/1998jd200048.

South Eastern Australian Climate Initiative 2011, *The millennium drough and 2010/11 floods (Factsheet 2 of 4)*, 2, CSIRO, <http://www.seaci.org/publications/documents/SEACI-2Reports/SEACI2_Factsheet2of4_WEB_110714.pdf>.

Sprigg, R 1982, 'Alternating wind cycles of the Quaternary era and their influences on aeolian sedimentation in and around the dune deserts of south eastern Australia', in R Wasson (ed.), *Quaternary dust mantles of China, New Zealand, and Australia*, Australian National University, Canberra, pp. 211-40.

Stewart, JB, Rickards, JE, Bordas, VM, Randall, LA & Thackway, RM 2009, 'Ground cover monitoring for Australia – establishing a coordinated approach to ground cover mapping: Workshop proceedings', ABARES, Canberra, p. 48.

Steyn, D & McKendry, I 1988, 'Quantitative and qualitative evaluation of a three-dimensional mesoscale numerical model simulation of a sea breeze in complex terrain', *Monthly Weather Review*, vol. 116, pp. 1914-26.

Stone, RC, Hammer, G, L. & Marcussen, T 1996, 'Prediction of global rainfall probabilities using phases of the Southern Oscillation Index', *Nature*, vol. 384, pp. 252-5.

Strong, C 2007, 'Effects of soil crusts on the erodibility of a claypan in the Channel Country, South Western Queensland, Australia', *PhD Thesis*, p. 268.

Strong, CL, Parsons, K, McTainsh, GH & Sheehan, A 2011, 'Dust transporting wind systems in the lower Lake Eyre Basin, Australia: A preliminary study', *Aeolian Research*, vol. 2, pp. 205-14, 10.1016/j.aeolia.2010.11.001.

Strong, CL, Bullard, JE, Dubois, C, McTainsh, GH & Baddock, MC 2010, 'Impact of wildfire on interdune ecology and sediments: An example from the Simpson Desert, Australia', *Journal of Arid Environments*, vol. 74, no. 11, pp. 1577-81, 10.1016/j.jaridenv.2010.05.032.

Swanton, EW 1975, *Swanton in Australia - with MCC 1946–1975*, Collins, London, 224.

Tanaka, T & Chiba, M 2006, 'A numerical study of the contributions of dust source regions to the global dust budget', *Global and Planetary Change*, vol. 52, no. 1-4, pp. 88-104, 10.1016/j.gloplacha.2006.02.002.

The Advertiser 1904, 'A Great Storm', News Corp Australia.

The Advertiser 1945, 'Bad Dust-Storm at Broken Hill', News Corp Australia.

The Argus 1896, 'A Record Dust-Storm: The Sun Eclipsed', Argus Melbourne.

The Argus 1922, 'Fierce duststorm: Days of discomfort', Argus Melbourne.

The Canberra Times 1944, 'Dust Storms Envelope Three States', Fairfax Media.

The Canberra Times 1950, 'Dust Storm in Canberra', Fairfax Media.

The Canberra Times 1965, 'Dust pall chokes Queensland - gales NSW', Fairfax Media.

The Queenslander 1928, 'Dust Storms in Queensland', Brisbane Newspaper Company.

The Sydney Morning Herald 1888, 'A Severe Dust-Storm', Fairfax Media.

Thompson, A 2014, *Soils - erosion: Wind erosion, water erosion*, Frank Fenner Foundation, 21 January 2015, <http://www.natsoc.org.au/our-projects/biosensitivefutures/part-4-facts-and-principles/ecological-issues/soils-erosion>.

Timmermann, A, Oberhuber, J, Bacher, A, Esch, M, Latif, M & Roeckner, E 1999, 'Increased El Nino frequency in a climatemodel forced by future greenhousewarming', *Nature*, vol. 398, pp. 694-7.

Tozer, P & Leys, J 2013, 'Dust Storms – What do they really cost?', *The Rangeland Journal*, vol. 35, pp. 131-42.

Trenberth, KE, Caron, JM, Stepaniak, DP & Worley, SJ 2002, 'Evolution of El Niño–Southern Oscillation and global atmospheric surface temperatures', *Journal of Geophysical Research*, vol. 107, no. D8, pp. 1-22.

van Dijk, AIJM, Beck, HE, Crosbie, RS, de Jeu, RAM, Liu, YY, Podger, GM, Timbal, B & Viney, NR 2013, 'The Millennium Drought in southeast Australia (2001-2009): Natural and human causes and implications for water resources, ecosystems, economy, and society', *Water Resources Research*, vol. 49, no. 2, pp. 1040-57, 10.1002/wrcr.20123.

Van Pelt, R, Zobeck, T, Baddock, M & Cox, J 2010, 'Design, construction, and calibration of a portable boundary layer wind tunnel for field use', *American Society of Agricultural and Biological Engineers*, vol. 53, no. 5, pp. 1413-22.

Wagner, L 1996, 'An overview of the wind erosion prediction system', in *Proceedings: International Conference on Air Pollution from Agricultural Operations*, Kansas City, Missouri, pp. 73-5.

Webb, NP 2008, 'Modelling Land Susceptibility to Wind Erosion in Western Queensland, Australia', University of Queensland, unpublished thesis, Brisbane.

Williams, AAJ & Stone, RC 2009, 'An assessment of relationships between the Australian subtropical ridge, rainfall variability, and high-latitude circulation patterns', *International Journal of Climatology*, vol. 29, no. 5, pp. 691-709, 10.1002/joc.1732.

Williams, P & Young, M 1999, *Costing Dust: How much does wind erosion cost the people of South Australia?*, 36, CSIRO Land and Water.

Wilson, AD & Graetz, ED 1979, 'Management of the semi-arid rangelands of Australia', in BH Walker (ed.), *Management of Semi-arid Ecosystems*, Elsevier, Amsterdam.

World Meteorological Organization 1995, *Manual on Codes - International Codes*, Annex II to WMO Technical Regulations Part A — Alphanumeric Codes, Secretariat of the World Meteorological Organization, Geneva, Switzerland.

World Meteorological Organization 2015, *What is Climate?*, 12 November 2015, <http://www.wmo.int/pages/prog/wcp/ccl/faqs.php>.

Wu, W 2014, 'The Generalized Difference Vegetation Index (GDVI) for Dryland Characterization', *Remote Sensing*, vol. 6, no. 2, pp. 1211-33, 10.3390/rs6021211.

Wurzler, S, Reisin, TG & Levin, Z 2000, 'Modification of mineral dust particles by cloud processing and subsequent effects on drop size distributions', *Journal of Geophysical Research*, vol. 105, no. D4, pp. 4501-12, 10.1029/1999jd900980.

Yang, X & Leys, J 2014, 'Mapping wind erosion hazard in Australia using MODIS-derived ground cover, soil moisture and climate data', *IOP Conference Series: Earth and Environmental Science*, vol. 17, p. 012275, 10.1088/1755-1315/17/1/012275.

Zhao, C, Liu, X, Ruby Leung, L & Hagos, S 2011, 'Radiative impact of mineral dust on monsoon precipitation variability over West Africa', *Atmospheric Chemistry and Physics*, vol. 11, no. 5, pp. 1879-93, 10.5194/acp-11-1879-2011.

Zhao, Y & Nigam, S 2015, 'The Indian Ocean Dipole: A Monopole in SST', *Journal of Climate*, vol. 28, pp. 3-19.

Zhou, L, Ramanathan, V, Li, F & Kim, D 2007, 'Dust plumes over the Pacific, Indian, and Atlantic Oceans: climatology and radiative impact', *Journal of Geographical Research*, vol. 112, no. D16208, doi:10.1029/2007JD008427.